This Project has received funding from European Commission by means of Horizon 2020,
the EU Framework Program for Research and Innovation, under Grant Agreement no.727348

Grant Agreement No. 727348

Project Acronym:

SOCRATCES

Project title:

SOlar Calcium-looping integRAtion for Thermo-Chemical Energy Storage.

DELIVERABLE D4.2

Power cycles: schemes, models, analysis

Funding scheme:	Research and Innovation Action (RIA)		
Project Coordinator:	USE		
Start date of the project:	01.01.2018	**Duration of the project:**	36 months
Contractual delivery date:	Month 16		
Actual delivery date:	30.04.2019		
Contributing WP:	WP4		
Dissemination level:	Public		
Authors:	Elisa Guelpa, Umberto Tesio, Vittorio Verda		
Contributors:	TTZ, USE, POLITO, CERTH, Calix		
Corresponding author:	Elisa Guelpa		
Version:	V1		
Document name:	**SOCRATCES_Deliverable_4.2_Final**		

Table of contents:

Nomenclature list

Abbreviation	Parameter	Measurement unit
$\eta_{is,T}$	CaL storage turbine isentropic efficiency	[-]
$\eta_{is,t}$	CaL main turbine isentropic efficiency	[-]
$\eta_{is,C}$	CaL compressor isentropic efficiency	[-]
η_{el}	Electric efficiency	[-]
$\Delta P_{\%,CO2,stoic}$	Stoichiometric CO_2 pressure loss percentage	[-]
$\Delta P_{\%,HP}$	Pressure loss percentage at high pressure	[-]
$\Delta P_{\%,LP}$	Pressure loss percentage at low pressure	[-]
$\dot{W}_{conv,\%}$	Conveying consumptions percentage	[kW/(kg*m)]
$\dot{W}_{rej,\%}$	Rejection consumption percentage	[kW_e/kW_t]
$\Delta L_{stor\text{-}carb}$	Storages-carbonator distance	[m]
$\dot{Q}_{loss\%,carb}$	Carbonator thermal loss percentage	[-]
$\Delta T_{min,pinch}$	Minimum temperature difference	[°C]
$T_{ambient}$	Ambient temperature	[°C]
X	Calcium oxide activity	[-]
T_{carb}	Carbonator temperature	[°C]
P_{carb}	Carbonator pressure	[bar]
β_t	CaL main turbine pressure ratio	[-]
$T_{CO2,in}$	Carbon dioxide carbonator inlet temperature	[°C]
$T_{CaO,in}$	Calcium oxide carbonator inlet temperature	[°C]
CIT	CaL compressor inlet temperature	[°C]
TIT	CaL main turbine inlet temperature	[°C]
n_{CO_2}	CO_2 excess index	[-]
tOT	CaL main turbine outlet temperature	[°C]
COT	CaL compressor outlet temperature	[°C]
TOT	Storage turbine outlet temperature	[°C]
$T_{co2,mix}$	Mixed carbon dioxide temperature	[°C]
$\dot{m}_{CaO}$	Calcium oxide mass flowrate	[kg/s]
$\dot{m}_{CO_2,stoic}$	Stoichiometric carbon dioxide mass flowrate	[kg/s]
$\dot{m}_{CO_2,rec}$	Recirculated carbon dioxide mass flowrate	[kg/s]
$\dot{m}_{CaO,unr}$	Unreacted calcium oxide mass flowrate	[kg/s]
$\dot{m}_{CaCO_3}$	Calcium carbonate mass flowrate	[kg/s]
η_{carb}	Carbonator side efficiency	[-]
$\dot{W}_t$	CaL main turbine shaft power	[kW]
$\dot{W}_C$	CaL compressor shaft power	[kW]
$\dot{W}_T$	Storage turbine shaft power	[kW]
$\dot{W}_{convey}$	Conveying power	[kW_e]
$\dot{W}_{rej}$	Rejection power	[kW_e]
$\dot{W}_{aux}$	Total auxiliaries consumption	[kW_e]
$\dot{W}_{tot,net}$	Total plant net electrical power	[kW_e]
$\dot{Q}_{heat,need}$	CaL external thermal power requirement	[kW_t]
VF	Vapor fraction	[-]
$\dot{W}_{turb}$	Power block turbine shaft power	[kW]
$\dot{W}_{pump}$	Power block pump shaft power	[kW]
$\dot{W}_{comp}$	Power block compressor shaft power	[kW]

ABSTRACT

This deliverable reports the activities developed by the consortium within task 4.2. It is focused on the analysis of several power cycles by taking into account their characteristics, with special focus on the operation in design conditions. For this reason, the effects of temperature, pressure, flow compositions are examined. In a first approximation, possible schemes are proposed in which power production is carried out directly (using an open air or a closed CO2 Brayton power cycle) or indirectly (by means of a steam Rankine cycle or a supercritical CO2 Brayton cycle). Each power cycle integration is modelled at system level considering Matlab and Aspen models. Integration is considered through application of pinch analysis combined with design optimization. For selected cases, a multiscale modelling approach is applied, in order to consider the effects of heat transfer in the reactor on the system design.

The characteristics of the CSP sources considered in this project is taken into account while keeping in mind their integration into the whole system thanks to the definition of the various hot and cold fluid in the process integration. The crucial operational parameters of the system are investigated. Their impact on the overall system performance are assessed leading to the final optimal thermodynamic design of the system.

Simplified thermodynamic cycle models are used in order to provide a general overview of the system performance. These models are steady-state and on-design. The systems are then simulated under different nominal conditions (i.e. the design conditions is modified) while considering different working fluids. The goal of this simulation is to investigate the on-design expected performance of the cycles and determine viable and technically feasible operating conditions, thus excluding impossible ones. Moreover, different design configurations are investigated in order to select those ones that are most favourable. Furthermore, the optimal working fluids and the thermodynamic operation variables are selected. The key operating parameters, such as the loads of the heat exchangers, and the power loads of the compressor and the expander, are calculated in order to guide the selection of proper equipment type to be used in each case.

1. CALCIUM-LOOPING INTEGRATION IN A CSP PLANT

1.1. INTRODUCTION

1.1.1 Case study

The possibility to store energy is a key point in the entire field of the renewable energy sources and especially for those that involve a thermodynamic cycle. In fact, the intrinsic fluctuations which characterise this kind of technologies may lead to some consistent drawbacks, such as a very frequent change of the operating conditions for the components involved in the process and, consequently, a continuous variation of the electrical power production.
One of the most representative cases in this field is constituted by the Concentrated Solar Power technology, whose main discontinuity factors are represented by the daily weather variation due to the presence of clouds, by the alternation of day and night and by the alternation of the seasons.

Therefore, to exploit the highest amount of the energy collected from the solar radiation, to avoid a design oversizing of the plant and to guarantee a power production as continuous as possible, it's requested a thermal energy storage.

At the state of the art there are three main categories of thermal energy storage, in accordance to the different thermophysical property that is exploited: sensible heat storage, latent heat storage and chemical heat storage.

This last one, although not already widely used in the CSP technology, seems to be a very promising alternative; this is due to two main reasons: for first, the energy density of the storage is higher than both the other two categories, which allows to install smaller storages with a consequent saving on the plant investment cost. For second, is possible to keep the vessels containing the reactants/products at a temperature equal to the external environment, fact that eliminates any kind of heat loss related to the storage period.

The thermochemical energy storage chosen for the European project SOCRATCES is based on a reversible reaction of calcination and carbonation.

$$CaCO_{3\,(s)} + HEAT \leftrightarrow CaO_{(s)} + CO_{2\,(g)} \qquad \Delta H_r^0 = \pm 178 \frac{kJ}{mol}$$

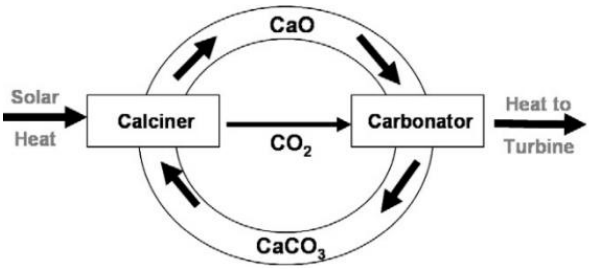

Figure 1 – Conceptual scheme for the CaL integration in a CSP plant [1]

The endothermic reaction takes place in the calciner and the predicted operating temperature is in the range of 700°C÷950°C, while the exothermic process is conducted in the carbonator and the expected reactor temperature is around 700°C÷875°C.

Now, the two different alternatives for the CaL integration in a CSP plant are already well known: direct integration and indirect integration.

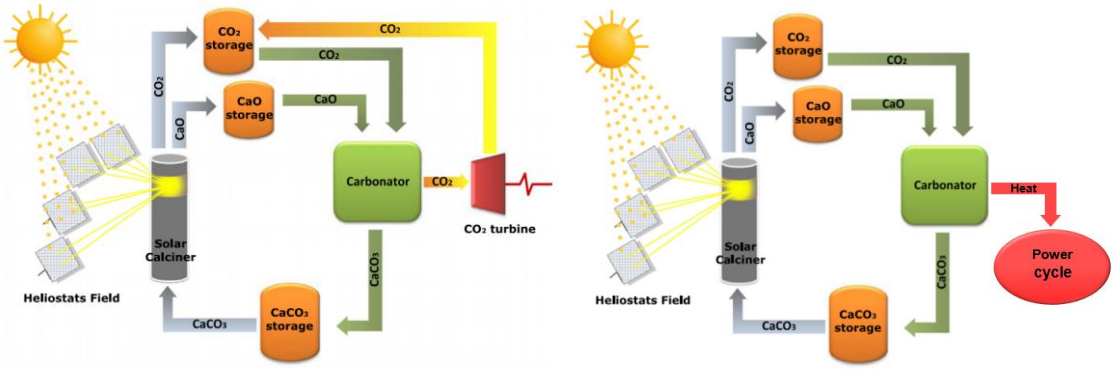

Figure 2 - Simplified scheme for the CaL integration alternatives: direct and indirect [2]

The direct integration generates electrical power through the expansion of a stream of carbon dioxide heated up by the exothermic reaction occurring in the carbonator, while for the indirect integration a thermal flux is provided to a power cycle by means of a heat exchangers network, keeping the power block physically separated from the CaL.

The main features of these two alternatives are summed up in the following table:

DIRECT INTEGRATION	INDIRECT INTEGRATION
• CO_2 is the only working fluid • Easier configuration when compared to the indirect integration • Components performing the Calcuim – Looping are strictly coupled with the components related to the electrical power generation • Carbonator operating pressure can be equal or higher than the atmospheric pressure (with a physical limitation due to the reactor technology) • Heat exchangers involving CO_2 may operate at subatmospheric or superatmospheric pressures (according to the carbonator working conditions)	• Physical distinction between power cycle and CaL • Possibility to adopt nearly any type of thermodynamic cycle and therefore different working fluids • More complex layout in terms of components involved, both regarding the power cycle and the heat exchanger network • CaL operating conditions are less limiting on the electrical power generation compartment, especially concerning the maximum achievable pressures

1.1.2 Work purpose and configuration analysed

The aim of this study has been to recognise the possible CaL integration alternatives in a CSP plant and find the thermodynamic cycles compatible with this technology. Then, in order to make a comparison between them, it has been requested to evaluate their efficiency and to do that has been necessary to find the optimal operating conditions for the selected layouts; this has been done with a genetic algorithm.

For first, it is necessary to establish the plant configuration that will be analysed. Very recently has been payed attention to the possibility of store the solid compounds involved in the Calcium-Looping at high temperatures [3]. The advantages of this technique are that the gas-solid heat exchangers are removed, leading to an easier plant configuration and consequently there is no

more necessity to increase/decrease the temperature of the solid streams entering/exiting the two chemical reactors.
Anyway, it must be recognised that this configuration is not particularly adequate for the long-term energy storage, which was firstly assumed at SOCRATCES.
Therefore, assuming the storages at low temperature (thermal equilibrium with the external environment), a suitable heat recovery system must be developed in order to preheat the reactants and cool down the products of the chemical reactions.
In order to evaluate the different alternatives for the power production, it must be observed that the calciner side layout is actually independent to the type of integration performed and, as a consequence, to the type of thermodynamic cycle adopted in the power block. This is due to the fact that the use of the three storages introduces a decoupling of the two sides that compose the Calcium-Looping. This is a very important aspect because it allows to compare the various options for the electrical generations without perform a complete (and therefore more complex) plant simulation. Therefore, the plant portion simulated in this work consists only in the carbonator side.

Now, before to expose the analysis performed, it's important to define two of the most important parameters for the plant functioning: the first one is the CaO activity and it represents the fraction of the total amount of calcium oxide provided to the carbonator that participates to the exothermic reaction.

$$X = \frac{CaO\ moles\ reacted}{CaO\ moles\ provided}$$

The other parameter is the excess index of carbon dioxide with the whom is fed the carbonator and it represent the effective amount of carbon dioxide provided to the chemical reaction normalised by the stoichiometric flowrate.

$$CO_2\ excess\ index = n_{CO_2} = \frac{\dot{m}_{CO_{2_{eff}}}}{\dot{m}_{CO_{2_{stoich}}}}$$

Furthermore, another assumption made for the purposes of this analysis is that the only heat source exploited by the CSP plant is the solar radiation; in this way the obtained configuration won't release global warming gases in the atmosphere, coherently with the renewable and sustainable principles at the base of the international policies that started up the SOCRATCES project.

Regarding the amount of power generation, it has been chosen the size of a pilot-scale plant whose power block produces a net electrical output equal to 1 MWe.

Finally, as will be exposed further on, has been analysed both the case in which the heat requested by the thermodynamic cycle is provided by the hot products of the carbonation reaction and the case of power block fed directly with an heat exchange in correspondence of the carbonator wall. Anyway, most of the work performed has been referred to the first configuration and this has been done for because of two main reasons: for first, it's possible to imagine that the second layout may have a more complex regulation and therefore its functioning could be affected by some criticalities. For second, all the designs investigated for the indirect integration that can be found in the scientific literature adopt the first layout and therefore it has been chosen to give more attention to this alternative.

1.2. DIRECT INTEGRATION

1.1.3 Simulation modelling and optimization

According to the scientific literature, at the state of the art have been proposed two different type of direct integration: one is the closed CO_2 cycle and the other is the air/CO_2 open cycle. Anyway, being this last one more complex and showing some criticalities in its functioning (due to the particular conditions required at the carbonator) it was chosen to not take it into account in the present work.

So, the closed CO_2 layout has been the indirect integration configuration analysed, but before to explain the optimization process it may be useful to recall the carbonator side functioning: the CO_2 extracted from its storage (75 bar and 20°C) must be expanded in order to reach the carbonator pressure (usually equal to few bars) and to do that it's necessary to heat up the stream, otherwise the temperatures reached at the end of the expansion will be too low. In many works found in literature it's adopted a multistage expansion with about seven inter-heatings fed by a traditional thermal power source; anyway, taking into account the relatively small plant size, it has been decided to perform a single heating before the turbine inlet, in order to simplify both the simulation and the final plant layout.
Leaving the turbine, the CO_2 is mixed with another stream of carbon dioxide and the resulting flow exchange heat to reach the carbonator inlet temperature. At the meantime, the calcium oxide is preheated from its storage conditions (1 bar, 20°C) and enters the chemical reactor.
At the reactor outlet are present the carbon dioxide in excess, the calcium carbonate (product of carbonation) and the unreacted calcium oxide; all these compounds are at the carbonation temperature and it's important to notice that the two solids are intrinsically related, because they are both constituting the same solid grains.
Anyway, the carbonator outlet is sent to a cyclone with the aim of divide the carbon dioxide from the solids, then, the $CaCO_3$ and the unreacted CaO are cooled down and directly sent to their storage (1 bar, 20°C), while the CO_2 in excess is expanded in order to produce electrical power, then it's performed a heat recovery and finally it's compressed and recirculated.

The optimal operating conditions have been obtained performing an optimization of the independent variables based on the genetic algorithm in order to maximise the carbonator side efficiency. At the same time, the external heating need is calculated through the pinch analysis and, if different from zero, the set of independent variables (which is a single element of the population) is discarded because unacceptable, since the plant must avoid the use of fossil fuels. The algorithm continues the research for the optimum until both the convergence tolerance and the thermophysical constraints are satisfied.

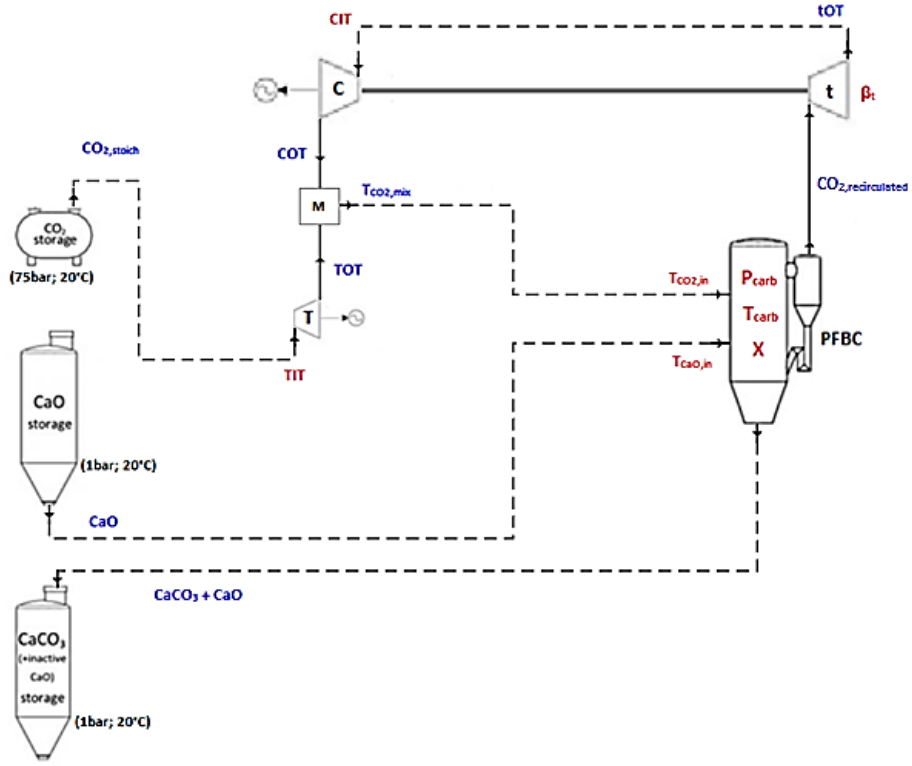

Figure 3 - Plant layout with streams data for the pinch analysis. The fixed parameters are the ones in black, the independent variables in red and the dependent variables in blue

As shown in the tables below, the storages thermophysical states are considered as fixed, while the parameters assumed as independent variables are: the CaO activity, the carbonator operating pressure and temperature, the carbonator feed streams temperatures, the main turbine pressure ratio, the compressor inlet temperature and the CO2 storage turbine inlet temperature. Any other pressure, temperature or flowrate is directly calculated from these parameters and most of the values chosen for the assumptions have been taken from the deliverable D4.1.

Therefore the genetic algorithm return a layout optimised but its heat exchangers network has to be designed separately.

Assumptions	
$\eta_{is,T}$	0,75
$\eta_{is,t}$	0,9
$\eta_{is,C}$	0,87
η_{el}	0,97
$PressureLoss_{\%,CO2,stoic}$	1%
$PressureLoss_{\%,HP}$	6%
$PressureLoss_{\%,LP}$	4%
Conveying consumptions	10 kJ/(kg*100m)
Storages-carbonator distance	100 m
Auxiliaries consumptions	0,8% rejected heat
Carbonator thermal loss	1% carbonation heat
$\Delta T_{min,pinch}$	15°C
$T_{ambient}$	20°C

Independent variables	Lower bound	Upper bound	Handled as
X	0,2	0,5	Discrete
T_{carb}	775°C	875°C	Discrete
P_{carb}	1,5 bar	15 bar	Continuous
β_t	1,2	15	Continuous
$T_{CO2,in}$	$T_{amb} + \Delta T_{pinch}$	$T_{carb} - \Delta T_{pinch}$	Continuous
$T_{CaO,in}$	310°C	$T_{carb} - \Delta T_{pinch}$	Continuous
CIT	$T_{amb} + \Delta T_{pinch}$	250°C	Continuous
TIT	250°C	650°C	Continuous

Constraints			
CIT_{min} and $T_{CO2,in,min}$	35°C	$\dot{Q}_{heat,need}$	0 MW
$P_{CO2,min}$	1 bar	$P_{el(t+c),net}$	1 MW

Tables 1,2,3 - Assumptions, constraints and variation range for the independent variables to optimise ([3], [4], [5])

Concerning the provided constraints, the value imposed for the net electrical power production is only related to the CaL main turbine and compressor (t and C), while the storage turbine (T) doesn't have any size constraint.
Furthermore, the minimum pressure achievable by the recirculated carbon dioxide is set to 1 bar because in this way the heat exchangers utilized at the main turbine outlet will operate under no particularly demanding conditions (pipelines and turbomachinery high dimensions), in accordance to the efforts already justified to avoid, whenever as possible, any not essential complication. Making this assumption leads at the meantime to another benefit, because is consequently eliminated any eventual air infiltration, which could bring negative drawbacks on the efficiency, since the carbonator wouldn't operate with an atmosphere only composed by carbon dioxide.

In order to reduce wherever as possible the internal electricity consumption, when the solid stream exiting from the carbonator ends to exchange their thermal power to heat up the cold fluids, it is directly sent to its storage even if it has not reached the target temperature of 20°C. In fact, cooling down completely this stream is not actually strictly necessary and, on the other hand, it would just determine an increase in the auxiliaries consumptions to feed the dry-coolers.

Obviously, the objective function evaluated by the genetic algorithm is the carbonator side efficiency, which is calculated as the ratio between the net electrical power output and the heat flux developed by the exothermic reaction, as reported by the following formula.

$$\eta_{carbonator\ side} = \frac{\dot{W}_{net,el}}{\dot{Q}_{carb}} = \frac{\dot{W}_{net,el}}{\dot{m}_{CaO_{provided}} \cdot X \cdot \Delta h_r^0}$$

The term Δh^0_r stands for the standard enthalpy of reaction per unit of mass of calcium oxide (3178,6 kJ/kg).
Of course, it could be argued that the two reactants extracted from their storages aren't in standard conditions since both are at 20°C and the carbon dioxide has a pressure of 75bar, so they do not only make available a thermal power during the chemical reaction, but there is also an amount of power in form of pressure of the CO_2.
Anyway the fact that the energy previously consumed to compress this stream is not considered in the definition of the carbonator side efficiency but, on the contrary, the power received by its expansion is taken into account (giving a contribute to the net electrical power) must not mislead: as already explained, this parameter is only referred to a portion of the complete plant. The most important thing is that all the simulations performed (direct and indirect integrations) start from the same storages conditions, which is sufficient to get consistent and comparable results.

At this point, starting from the independent variables, the constant parameters, all the assumptions and constraints, it's possible to simulate completely the carbonator side and therefore to execute the optimization. The carbonator simulation has been executed on Aspen Plus and then the data have been imported on Matlab, where the compounds properties have been evaluated with the COOLPROP library and the genetic algorithm has been performed.

1.1.4 Results, comments and comparison

Here are reported the optimization results, compared each other according to their efficiency in order to make possible the evaluation of the most suitable alternative.

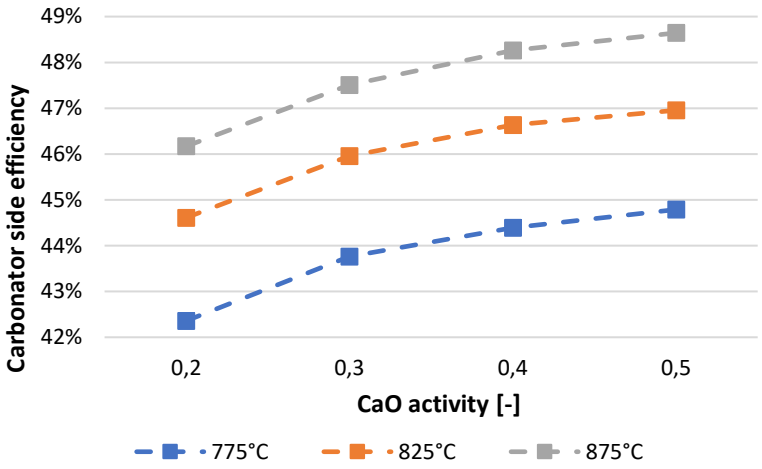

Figure 4 - Carbonator side efficiency for the direct integration

As could be imagined, the higher is the reactor temperature, the higher is the carbonator side efficiency and the same happens for the calcium oxide reactivity, where a smaller amount of inert CaO brings benefits to the integration performance, although the trend seems to have an asymptote.

So, at this point is possible to make some interesting considerations. In fact, for every investigated value of carbonator temperature and CaO reactivity, the algorithm converges to values of carbonator pressure and pressure ratio such that the recirculated carbon dioxide reaches its minimum acceptable pressure, equal to 1 bar, in correspondence of the compressor inlet.
Moreover, operating at lower reaction temperatures makes necessary (in order to satisfy the constraint on the power production) higher flowrates of the recirculated carbon dioxide, which determines an increase of both the compressor and main turbine size, while the storage turbine size, which is mainly dependent on its intel operating temperature, doesn't shows a precise trend.
As could be expected, the compressor inlet temperature always reaches its lower value, in order to minimize the compression power requirement, and, obviously, the calcium oxide flowrate decreases with the increasing of the solid reactivity, although the amount of reactant that participates actively to the chemical reaction has an opposite variation, in accordance to the results obtained for the efficiency.
As a consequence of that, the conveying power decrease with the increase of the calcium oxide activity, while the rejection power is relatively small and its variations are actually negligible (if considered in absolute terms). So, the total auxiliaries consumption (which is the sum of these two components) becomes smaller both for higher values of the carbonator temperature and CaO reactivity.

Independent variables	T_{carb} [°C]	875
	X [-]	0,5
	P_{carb} [bar]	3,43
	β_t [-]	3,3
	$T_{CaO,in}$ [°C]	822
	$T_{CO2,in}$ [°C]	707
	TIT [°C]	339
	CIT [°C]	35,1
Dependent variables	Excess index [-]	17,77
	tOT [°C]	704
	COT [°C]	146
	TOT [°C]	134
	$T_{co2,mix}$ [°C]	145
Flowrates	$\dot{m}_{CaO}$ [kg/s]	1,38
	$\dot{m}_{CO_2,stoic}$ [kg/s]	0,54
	$\dot{m}_{CO_2,rec}$ [kg/s]	9,06
	$\dot{m}_{CaO,unr}$ [kg/s]	0,69
	$\dot{m}_{CaCO_3}$ [kg/s]	1,23
	η_{carb} [%]	48,64

Shaft and electrical powers	
Main turbine power [kW]	1931
Compressor power [kW]	900
Storage turbine power [kW]	105
Conveying power [kWe]	32,9
Rejection power [kWe]	6,2
Total auxiliaries consumption [kWe]	39,1
Total plant net power [kWe]	1063

Table 4, 5 – Optimisation results for the direct integration with X=0,5 and T_{carb}=875°C

All the results obtained for the other configurations investigated are presented in the Appendix 2.

Now, it is interesting to observe both the grand composite curve and the hot and cold fluids composite curves for the case with the highest efficiency value (between the ones analysed), that is when the calcium oxide activity is equal to 0,5 and the carbonator temperature reaches 875°C.

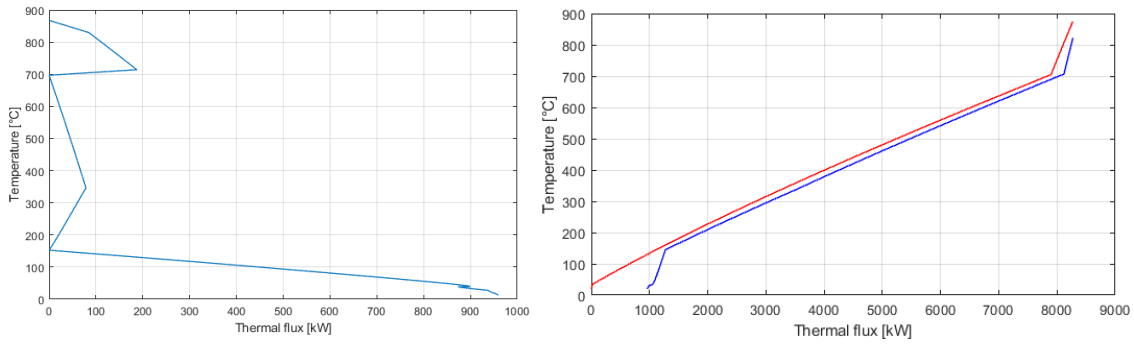

Figure 5 - Grand composite curve and hot and cold composite curves for the optimised direct integration with X=0,5 and T_{carb}=875°C

All the graphs obtained for the other configurations investigated are presented in the Appendix 1.

Concerning the grand composite curve, it reaches a null thermal flux in correspondence of three different temperatures: in the case of the highest value it simply means that the external heat requirement is equal to zero, as imposed to the pinch analysis outcomes; instead, in the case of the mid and lower value it means that the hot and cold fluids reach the minimum temperature difference and therefore the final layout will have two different pinch points.
Concerning the hot and cold composites graph, the genetic algorithm converges to values of the independent variables such that the two curves manage to approach each others very well, except when the plant temperatures are at their minimum or maximum.

Finally, for the same optimized configuration has been developed a possible heat exchanger network. As is possible to find in [4], there are two advices regarding the heat exchanger network design that, if followed, help to obtain a relatively easier to manage plant configuration: the first one is that splitting a solid stream should be avoided because, in practical terms, it is much more complex with respect to the split of a fluid stream. The second one is that it would be better also to avoid heat exchange between solid streams because, if compared to the case of gas-solid or gas-gas heat exchange, it shows lower performances and adopts a less mature technology.
Now, regarding the first advice, no particular difficulties have been encountered in order to respect it and therefore all the stream splitting appearing in the layout have been only performed on the carbon dioxide. However, it hasn't been possible to satisfy the second advice because prohibiting the coupling between the two solid streams brings to an increment of the external heat requirement, which, as imposed during the optimization process, must be null in order to avoid the use of fossil fuels.
Anyway, this drawback shouldn't constitute a strong disadvantage because it has been obtained only one heat exchanger performing this kind of thermal recovery and moreover its size is relatively small when compared to the total power involved in the process.

Stream	Flowrate [kg/s]	T_{in} [°C]	T_{out} [°C]	Thermal power [kW_t]
$CaCO_3 + CaO_{un}$	1,92	875	20	1764
$CO_{2,rec}$	9,06	704	35,1	6553
CaO	1,38	20	822	996
$CO_{2,mix}$	9,60	145	707	6024
$CO_{2,stoic}$	0,540	20	339	287

Branch	%
A	85,5
B	12,4
C	2,1
D	86,8
E	13,2
F	18,9
G	81,1

Table 6, 7 – Hot and cold streams participating to the heat exchange and branches split percentages for the optimised layout with X=0,5 and T_{carb}=875°C

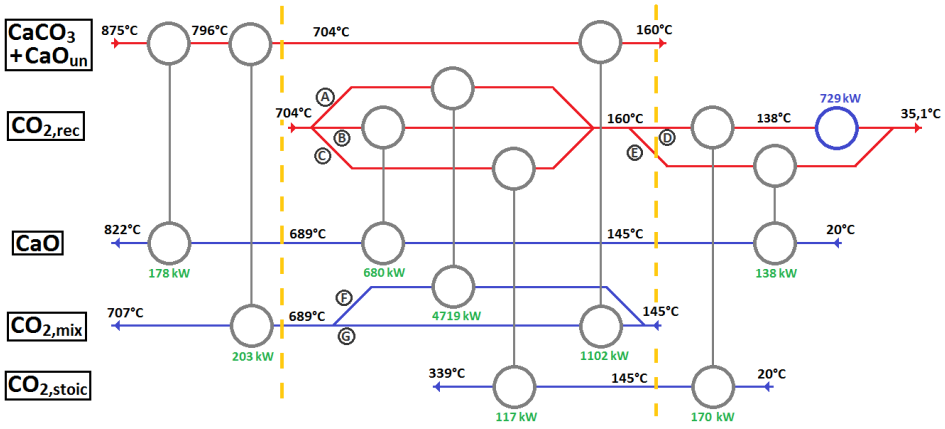

Figure 6 - Heat exchangers network obtained for the optimised direct integration with X=0,5 and T_{carb}=875°C

1.3. INDIRECT INTEGRATION

1.1.5 Power cycles alternatives

Thanks to the high temperatures reached by the carbonation reaction there are many different thermodynamic cycles that could be integrated with the Calcium-Looping:

- Organic Rankine cycles
- Steam Rankine cycles
- Brayton-Joule cycles
- Combined cycles
- Kalina cycles
- Stirling cycles

For the purposes of this work, taking into account the plant size analysed, the layout complexities that could be encountered and the state of development of every one of these technologies, it has been chosen to investigate only the first three of the alternatives listed above.

1.1.6 Simulation modelling and optimization

The main difference from the previously analysed integration type is that it has been chosen to **divide** the optimization process **in two parts**: in the first one it's optimized only the thermodynamic cycle while in the second one it's optimized the carbonator side configuration. Anyway, the objective function is not changed: the carbonator side efficiency, always defined as for the direct integration.

Before to explain the optimization process, it may be useful to point out some aspects of the carbonator side functioning in case of indirect integration. Broadly speaking, the operating principle is the same already discussed for the direct integration, but there are some fundamental differences: the first one is that both the carbonator outlet streams are now only acting as heat transfer fluids, since the power generation is left to the power block. The second one is that, as a consequence, the carbonator it's not any more pressurized and the carbon dioxide recirculated is affected by small pressure losses (in absolute terms); therefore the compressor size will be much smaller than in the previous case.

Anyway, also for this configuration it has been imposed an external heating requirement equal to zero, in order to avoid any use of fossil fuels.

Concerning the optimisation structure, the process adopted has been the following: in a first step, once that both the power cycle design and the working fluid are chosen, it's possible to perform a specific optimization in order to maximise the thermodynamic cycle efficiency in accordance to any technical constraints. In this case, all the power block components have been modelled on Aspen with the REFPROP method. The optimization strategies assumed for this step are the quadratic approximation method and the conjugate directions method, respectively in case of a single or double variable problem. In any case, the power unit size must be sufficient to provide a net electrical power output of 1 MW.

Moreover, once that the thermodynamic cycle optimization is terminated, all the data of the streams passing through the heater/boiler and cooler/condenser are exported and provided to the second and last step of the optimization procedure.
So, in this following part, as already done for the integration previously investigated, the first distinction to do is between the constant and variable parameters, and then the dependencies between these last ones. Obviously, since the carbonator pressure is not any more assumed as a variable parameter, only the temperatures and mass flowrates can be varied in the carbonator side.
Regarding the involved streams, also in this case the carbon dioxide extracted from its storage will be equal to the required stoichiometric amount but now the calcium oxide flowrate is assumed as an independent variable and its value is established imposing the constraint of null external heating need.
For the optimization purposes, the others independent variables assumed are: the carbonator temperature, the CaO reactivity, the temperature of the two streams entering the reactor and finally, the inlet temperature of the compressor and turbine belonging to the carbonator side.

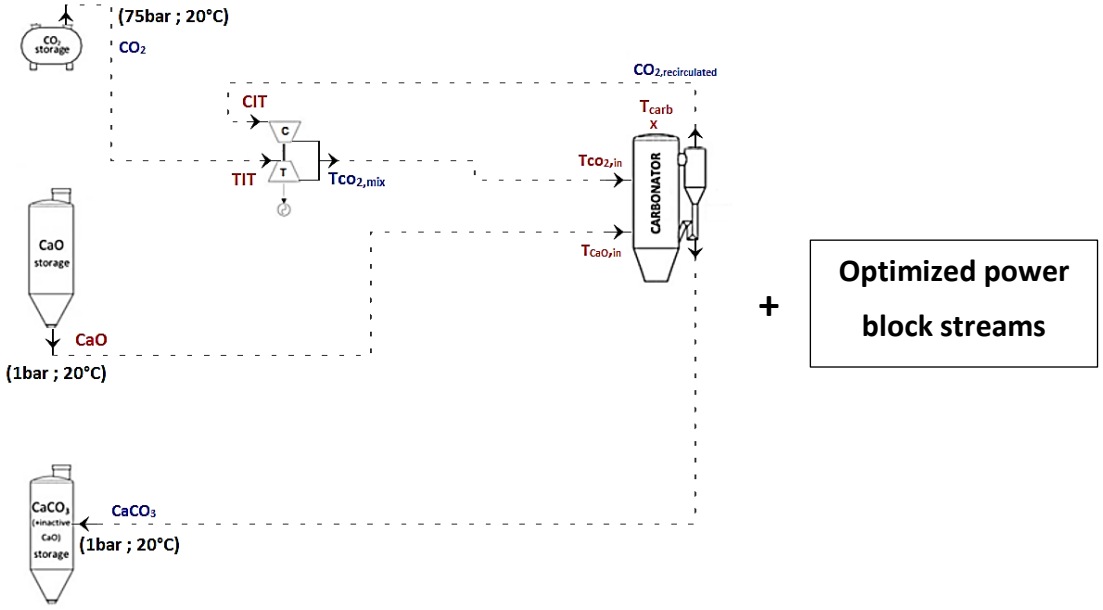

Figure 7 - Indirect integration layout adopted for the second step of the optimisation process

Assumptions	
$\eta_{is,T}$	0,75
$\eta_{is,C}$	0,65
η_{el}	0,97
P_{carb}	1 bar
ΔP_{comp}	10% P_{carb}
Conveying consumptions	10 MJ/(ton*100m)
Storages-carbonator distance	100 m
Auxiliaries consumptions	0,8% rejected heat
$\Delta T_{min,pinch}$	15°C
$T_{ambient}$	20°C

Independent variables	Lower bound	Upper bound	Handled as
X	0,2	0,5	Discrete
T_{carb}	775°C	875°C	Discrete
$T_{CO2,in}$	$T_{amb} + \Delta T_{pinch}$	$T_{carb} - \Delta T_{pinch}$	Continuous
$T_{CaO,in}$	310°C	$T_{carb} - \Delta T_{pinch}$	Continuous
CIT	$T_{amb} + \Delta T_{pinch}$	250°C	Continuous
TIT	250°C	650°C	Continuous
$\dot{n}_{CaO}$	-	-	Continuous

Constraints	
CIT_{min} and $T_{CO2,in,min}$	35°C
$\dot{Q}_{heat,need}$	0 MW
P_{el,net_power_block}	1 MW

Table 8, 9, 10 – Assumptions, constraints and independent variables for the carbonator side ([5], [6], [3], [4])

The optimisation method for this second step is again the genetic algorithm based on the pinch analysis outcomes for the streams belonging to both the carbonator side and the power block. The single components have been modelled in the same way already done for the direct integration and any other assumption made in this previous case is still valid for the layout now investigated.

1.1.7 Organic Rankine cycles

Layouts investigated

Despite the common operating field of these thermodynamic cycles is quite different from the case analyzed in this work, it could be interesting to investigate their integration because of the good thermal properties of these power fluids and the consistent performance advantages at reduced power loads given by the machineries.
Furthermore, despite most of the constructed power plants operate at **subcritical** conditions, it has been considered as interesting to perform the integration of **supercritical** cycles in order to evaluate the possible benefits related to the absence of an isothermal step determined by the evaporation, in addition to the higher pressures that can be reached.

For all the different ORC fluids investigated and for both the subcritical and supercritical operating conditions have been assumed one single power block layout, which is actually the simplest as possible: one turbine and one condenser divided by one heating and one cooling stage. This essential design has been chosen according to the common trend (at least in the ORC field) in searching to adopt the most basic configuration as possible.

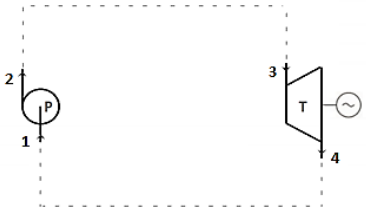

Figure 8 - ORCs layout

Machinery data and assumptions	
P_{min}	0,1bar
P_{max}	110 bar
T_{max}	510°C
η_{el}	0,97
$\eta_{is,turb}$	0,85
$\eta_{is,pump}$	0,75
$\Delta P_{cooling}$	2%
$\Delta P_{heating}$	2%

Constraints	
$T_{condenser,min}$	$T_{amb} + \Delta T_{pinch}$ = 35°C
$P_{el,net}$	1 MW
$\dot{Q}_{heat,need}$	0 MW
Minimum vapor fraction during expansion	0,85

Table 11, 12 – Assumptions and constraints for the ORCs operating conditions ([7], [8], [9], [10], [11])

For the analysis performed have been considered two different values for the condensing pressure. In fact, since most of the ORC fluids are compounds quite unstable and inflammable, it wouldn't be a bad decision to avoid pressures lower than the **atmospheric** value at the condenser, in order to avoid air infiltration. However, it's very common to find cases in literature where the condenser works under **vacuum** conditions, obviously allowing to reach higher thermodynamic efficiencies. So, trying to make an assessment as complete as possible, both the configurations have been considered.

ORC fluid	Saturation curve type	P_{crit} [bar]	T_{crit} [°C]	T_{max} [°C]
Benzene	Isentropic	48,94	289	452
Cyclohexane	Dry	40,82	280,5	427
Cyclopentane	Isentropic	45,71	238,6	277
Ethanol	Wet	62,68	242	377
Toluene	Dry	41,26	318,6	427

Table 13 – Organic Rankine fluids analysed and some of their physical properties (COOLPROP library)

Integration results

From the first step of the optimization process are obtained the results exposed in the following table; it must be remembered that it hasn't been performed a heat recovery between the turbine outlet and the evaporator inlet because any heat exchange is executed in the second step through the pinch analysis.

From the sensitivity analysis performed for the subcritical cycles it's possible to observe that higher pressures always determine a performance improvement, except for the case of the benzene, which presents a non-monotonic trend. Furthermore, the toluene, cyclopentane and benzene pressures must be limited to avoid excessively low value of vapor fraction at the beginning of the expansion.
Regarding the supercritical cycles, the cyclopentane is the only case in which the thermodynamic efficiency presents a non-monotonic behavior when the turbine inlet pressure is increased. The performances dependence on the turbine inlet temperature is instead a little bit more complex, since its trend changes with the pressure achieved.

Furthermore the passage from counter pressure condensation to vacuum condensation is always convenient, with an efficiency relative gain up to 43%; of course the practical feasibility must be carefully evaluated for the reasons already explained. A smaller improvement (up to +11%) is encountered when the cycle changes from subcritical to supercritical operating conditions, except for the case of the Toluene, which reaches its best performance when it operates below the critical pressure.
Anyway, the effective benefits of these configuration must be evaluated when the power block is integrated in the Calcium-Looping.

		1		2		3		4		$\dot{m}_{ORC}$ [kg/s]	η_{cycle} [-]	$\dot{W}_{turb}$ [kW]	$\dot{W}_{pump}$ [kW]
		P [Bar]	T [°C]	P [Bar]	T [°C]	P [Bar]	T [°C]	P [Bar]	T [°C]				
SUBCRITICAL + COUNTERPRESSURE CONDENSATION	Benzene	1,1	82,8	46,75	85,2	45,82	283,4	1,12	133,1	8,785	0,1963	1097	65,9
	Cyclohexane	1,1	83,5	39,8	85,6	39	276,9	1,12	168,6	9,200	0,1758	1097	66,2
	Cyclopentane	1,1	51,8	41,84	54,1	41	230,6	1,12	93,8	9,056	0,1964	1100	69,0
	Ethanol	1,1	80,5	62,24	82,8	61	370	1,12	203,2	3,368	0,2149	1068	37,4
	Toluene	1,1	113,5	37,72	115,5	36,96	309,7	1,12	189,3	9,918	0,1711	1093	62,4
SUBCRITICAL + VACUUM CONDENSATION	Benzene	0,198	35	46,71	37,2	45,78	283,3	0,202	91,4	5,944	0,2518	1074	42,7
	Cyclohexane	0,201	35	39	36,9	38,22	275,3	0,205	138	6,034	0,2303	1072	40,8
	Cyclopentane	0,619	35	41,84	37,3	41	230,6	0,631	79,9	7,732	0,2177	1089	58,2
	Ethanol	0,138	35	62,2	37,1	61	370	0,14	134,4	2,372	0,2799	1056	25,3
	Toluene	0,1	45,25	37,72	47	36,96	309,7	0,102	141	5,653	0,2462	1065	33,6
SUPERCRITICAL + COUNTERPRESSURE CONDENSATION	Benzene	1,1	82,76	112,25	88,6	110	420	1,12	256,1	5,297	0,2182	1128	96,8
	Cyclohexane	1,1	83,47	112,25	89,42	110	370	1,12	239,9	6,516	0,188	1166	134,7
	Cyclopentane	1,1	51,78	57	55	55,86	270	1,12	134,4	7,384	0,2067	1108	77,2
	Ethanol	1,1	80,52	112,25	84,62	110	370	1,12	165,2	3,293	0,2312	1097	66,5
	Toluene	1,1	113,5	112,25	119,4	110	420	1,12	264,8	6,864	0,1778	1162	131
SUPERCRITICAL + VACUUM CONDENSATION	Benzene	0,198	35	112,25	40,2	110	428	0,202	223,8	3,724	0,2746	1095	64,5
	Cyclohexane	0,2009	35	112,25	40,93	110	365	0,205	201,4	4,614	0,2419	1121	90,2
	Cyclopentane	0,619	35	59	38,23	57,82	270	0,631	116,6	6,466	0,2281	1100	68,9
	Ethanol	0,138	35	112,25	38,9	110	370	0,14	98,8	2,404	0,2891	1077	46,3
	Toluene	0,1	45,25	112,25	50,39	110	420	0,102	216,2	4,268	0,2586	1107	75,6

Table 14 – First step optimisation results for the Organic Rankine thermodynamic cycles

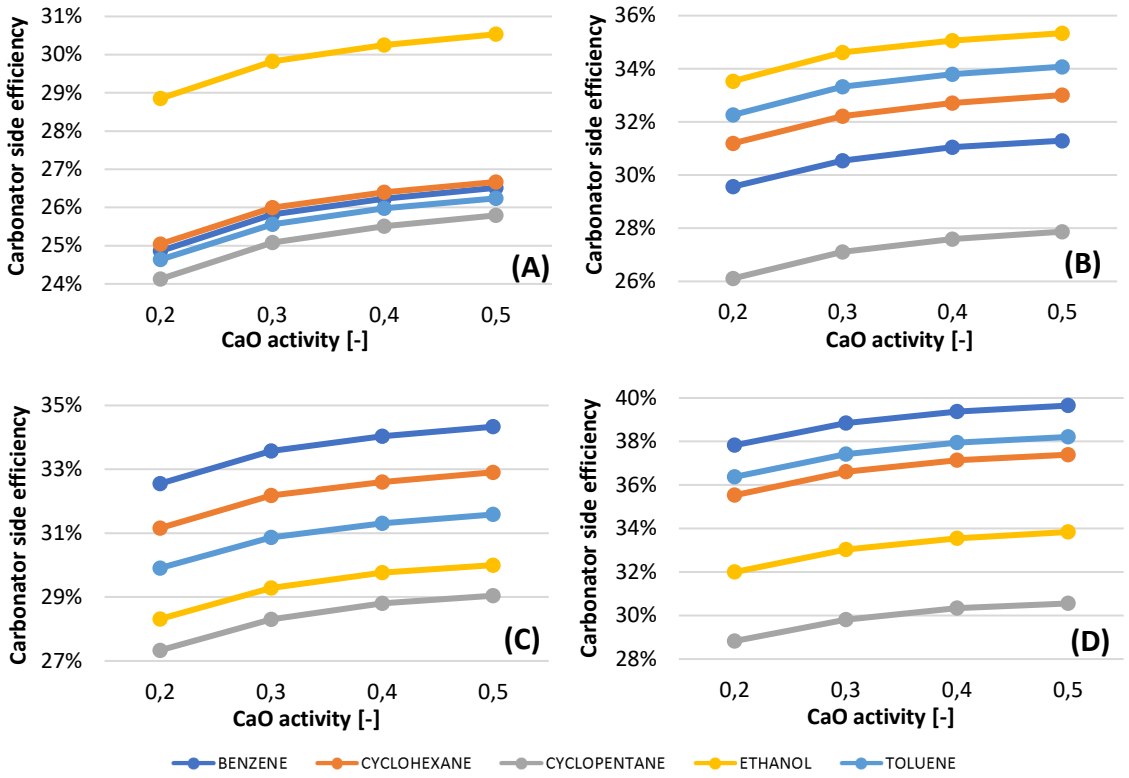

Figure 9 – Carbonator side efficiencies for the indirect integration with ORCs: (A) Subcritical with counterpressure condensation, (B) Subcritical with vacuum condensation, (C) Supercritical with counterpressure condensation, (D) Supercritical with vacuum condensation

The results obtained from the indirect integration optimization are very interesting because they show an important concept related to the power block integration in the carbonator side: a higher thermodynamic efficiency of the power cycle doesn't mean necessary a higher integration efficiency. In fact, the best alternative between the optimized thermodynamic cycles is not always the best alternative when the power block is integrated in the carbonator side.

	Organic Rankine fluid	Storage turbine power [kW]	Compressor power [kW]	Conveying power [kW_e]	Rejection power [kW_e]	Total auxiliaries consumption [kW_e]	Total plant net power [kW_e]
SUBCRITICAL + COUNTERPRESSURE CONDENSATION	Benzene	411	17,71	62	21	83	1298
	Cyclohexane	384	17,77	58	18,9	77	1278
	Cyclopentane	480	20,91	73	25	98	1347
	Ethanol	352	16,53	53	16,9	70	1255
	Toluene	373	18,44	57	7,1	64	1280
SUBCRITICAL + VACUUM CONDENSATION	Benzene	411	17,71	62	21	83	1298
	Cyclohexane	384	17,77	58	18,9	77	1278
	Cyclopentane	480	20,91	73	25	98	1347
	Ethanol	352	16,53	53	16,9	70	1255
	Toluene	373	18,44	57	7,1	64	1280
SUPERCRITICAL + COUNTERPRESSURE CONDENSATION	Benzene	365	21,12	55	15,9	71	1262
	Cyclohexane	384	22,38	58	18,4	77	1274
	Cyclopentane	453	21,94	69	23,2	92	1326
	Ethanol	433	23,11	66	21	87	1311
	Toluene	411	27,41	62	5,1	62	1310
SUPERCRITICAL + VACUUM CONDENSATION	Benzene	305	16,48	46	12,6	59	1221
	Cyclohexane	328	16,61	50	14,5	64	1238
	Cyclopentane	424	18,5	64	21,1	85	1308
	Ethanol	373	16,72	57	17,8	74	1271
	Toluene	320	17,09	49	13,8	62	1231

	Organic Rankine fluid	Independent variables					Dependent variables				Flowrates					
		T_{carb} [°C]	$T_{CaO,in}$ [°C]	$T_{CO2,in}$ [°C]	TIT [°C]	CIT [°C]	COT [°C]	TOT [°C]	$T_{co2,mix}$ [°C]	Excess index [-]	$\dot{m}_{CaO}$ [kg/s]	$\dot{m}_{CO_2,stoic}$ [kg/s]	$\dot{m}_{CO_2,rec}$ [kg/s]	$\dot{m}_{CaO,unr}$ [kg/s]	$\dot{m}_{CaCO_3}$ [kg/s]	η_{carb} [%]
SUBCRITICAL + COUNTERPRESSURE CONDENSATION	Benzene	875	310	52	650	52	63	294	148	2,722	2,61	1,03	1,764	1,3	2,33	31,3
	Cyclohexane	875	312	51	650	75	87	294	163	2,725	2,44	0,96	1,651	1,22	2,18	33,01
	Cyclopentane	875	312	54	650	54	66	294	149	2,732	3,04	1,2	2,07	1,52	2,72	27,87
	Ethanol	875	313	52	650	80	92	294	166	2,728	2,23	0,88	1,515	1,11	1,99	35,34
	Toluene	875	310	75	650	87	99	294	169	2,785	2,36	0,93	1,658	1,18	2,11	34,08
SUBCRITICAL + VACUUM CONDENSATION	Benzene	875	310	52	650	52	63	294	148	2,722	2,61	1,03	1,764	1,3	2,33	31,3
	Cyclohexane	875	312	51	650	75	87	294	163	2,725	2,44	0,96	1,651	1,22	2,18	33,01
	Cyclopentane	875	312	54	650	54	66	294	149	2,732	3,04	1,2	2,07	1,52	2,72	27,87
	Ethanol	875	313	52	650	80	92	294	166	2,728	2,23	0,88	1,515	1,11	1,99	35,34
	Toluene	875	310	75	650	87	99	294	169	2,785	2,36	0,93	1,658	1,18	2,11	34,08
SUPERCRITICAL + COUNTERPRESSURE CONDENSATION	Benzene	875	310	143	650	104	116	294	176	2,995	2,31	0,91	1,814	1,16	2,07	34,33
	Cyclohexane	875	310	145	650	104	117	294	176	3,004	2,44	0,96	1,918	1,22	2,18	32,91
	Cyclopentane	875	310	74	650	80	92	294	165	2,783	2,87	1,13	2,012	1,43	2,56	29,04
	Ethanol	875	311	100	650	100	112	294	176	2,859	2,75	1,08	2,007	1,37	2,45	30
	Toluene	875	310	178	650	134	148	294	194	3,122	2,61	1,03	2,177	1,3	2,33	31,59
SUPERCRITICAL + VACUUM CONDENSATION	Benzene	875	310	81	650	116	129	294	188	2,803	1,94	0,76	1,371	0,97	1,73	39,65
	Cyclohexane	875	310	98	650	82	94	294	164	2,851	2,08	0,82	1,514	1,04	1,86	37,39
	Cyclopentane	875	310	53	650	55	67	294	150	2,726	2,69	1,06	1,825	1,34	2,4	30,55
	Ethanol	875	311	47	650	67	79	294	158	2,712	2,36	0,93	1,591	1,18	2,11	33,84
	Toluene	875	310	118	650	90	102	294	168	2,912	2,03	0,8	1,523	1,01	1,81	38,21

Tables 15, 16 - Optimisation results for the indirect integration of Organic Rankine cycles with X=0,5 and T_{carb}=875°C

All the results obtained for the other configurations investigated are presented in the Appendix 1.

Concerning the carbonator side efficiency, the highest values in case of integration of a subcritical cycle (A and B of figure 9) are reached when the ethanol is chosen as working fluid; this is due to the fact that, being the only substance with a wet saturation curve, the thermodynamic cycle reaches the highest temperature, determining an high temperature heat recovery and therefore exploiting in the best way the high-quality power flux provided by the carbonation products.
Things are different when the supercritical operating conditions are adopted (C and D of figure 9): in fact, the most important aspect in this case are the working fluids thermophysical properties and the way in which they affect the heat recovery simulated through the pinch analysis. So, for this configuration, the most performing alternative is constituted by the benzene.

Concerning the results of the other parameters obtained for the various configurations have some interesting aspects in common. One of those is the fact that the optimization algorithm converges always to the highest achievable value of the carbonator operating temperature, such that the thermal power recovery is performed on a source of high-quality heat.

Another thing that is very easy to notice is the fact that also the heating temperature of the stoichiometric carbon dioxide extracted from the pressurized storage (TIT) reaches always its acceptable maximum. This can be explained considering the temperatures achieved by the other cold fluids, which are quite small if compared to the temperature at which are available the two hot streams exiting the carbonator. So, heating the stoichiometric CO_2 up to a relatively high temperature allows both to make the two composite curves to approach each others (at least at their ends) and to obtain a very effective expansion, producing a consistent amount of electrical power from a fluid that is at high pressure (75 bar).

Concerning the shaft and electrical powers involved in the process, the storage turbine power production slightly decreases when the CaO reactivity increases because an higher carbonator efficiency means a lower CaO and CO_2 consumption, so the stoichiometric flowrate of carbon dioxide becomes smaller.
On the opposite, the compressor power increases with X and this is due to the fact that a higher value of the CO_2 excess (requested to control the carbonator temperature) determines a higher flowrate for the recirculated carbon dioxide with the consequent need of more shaft power to compensate the pressure losses that take place in the CO_2 circuit.
Finally, as already noticed in the direct integration analysis, the rejection power is quite small and, in absolute terms, its variations are considerable as negligible, while the conveying power is inversely proportional to the CaO activity because lowering the amount of inert matter obviously determines a reduction of the total solid mass that must be transported.

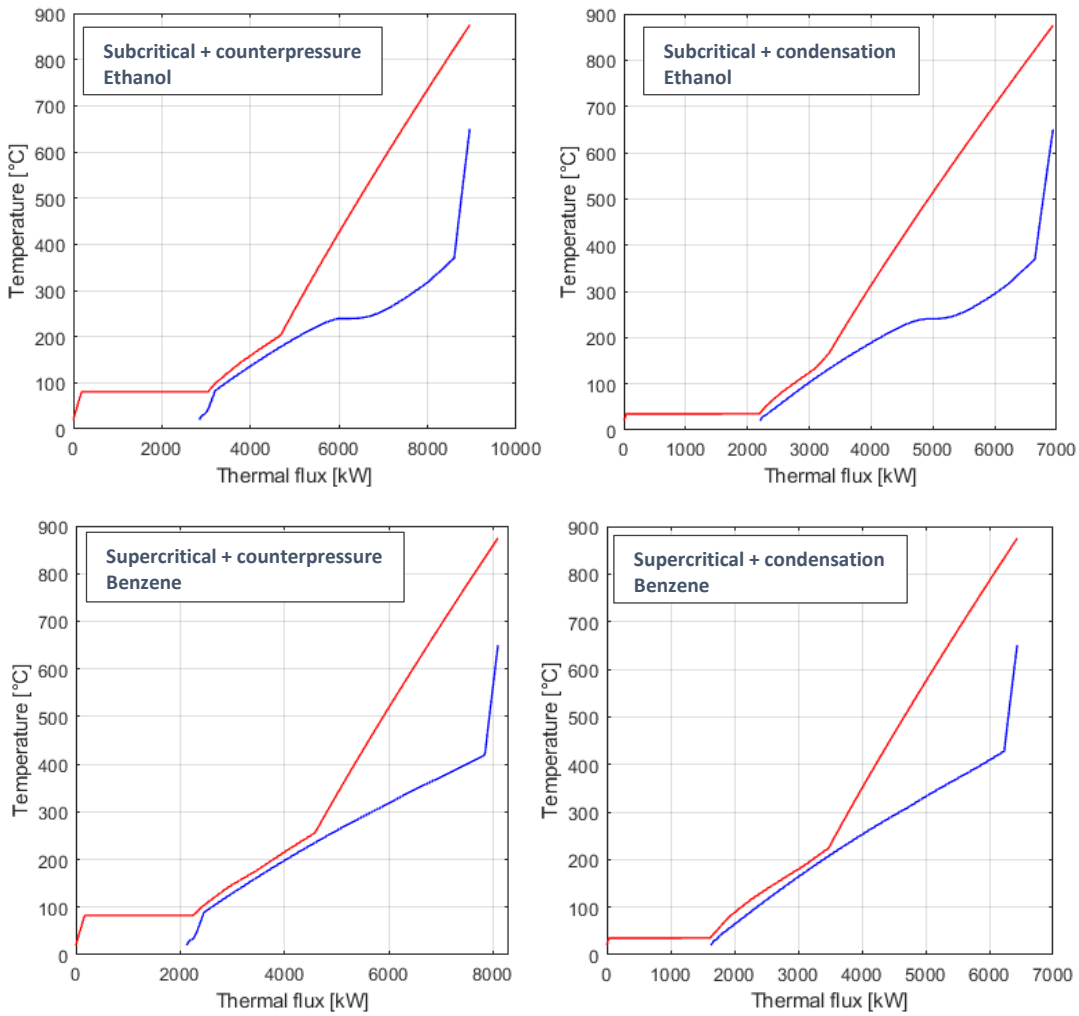

Figure 10 - Hot and cold composite curves for the ORC fluid that provides the best efficiency in the four configurations investigated (X=0,5)

The graphs above obtained with the pinch analysis show the differences between the configurations analyzed, especially concerning the cold fluids composite curve. In fact the absence of an isothermal step in correspondence of the evaporation seems to make the two curves closer each other, determining an improvement in the thermal exchange. The main consequence of the condensation under vacuum conditions is instead to decrease the total amount of heat flux transferred by the streams, since the power block itself requires a lower amount of thermal power.

All the graphs obtained for the other configurations investigated are presented in the Appendix 2.

1.1.8 Steam Rankine cycles

Layouts investigated

The second investigated typology of power cycle consist in the classic water steam Rankine cycle (SRC).

In general terms the cycles operating conditions are strictly related to the power plant size and, strictly speaking, the bigger are the machineries the higher are the sustainable temperatures and pressure. Therefore, taking into account the relatively small plant size analyzed, it hasn't

been investigated the case of a supercritical water steam cycle and all the simulated power blocks operate in subcritical conditions.

Furthermore, unlike already done for the ORCs, when the power block is integrated in the carbonator side and it's executed the pinch analysis, the condensing water isn't considered between the hot fluids and therefore all the latent heat is rejected in the atmosphere with dry-coolers. This choice has been made because the gain in terms of carbonator efficiency aren't enough consistent to justify the related layout complications introduced if this stream had been taken into account.

Steam turbine data and assumptions					
One-step expansion		Double-step expansion		$\eta_{is,turb}$	0,85
TIP_{max}	110 bar	TIP_{max}	101 bar	$\eta_{is,pump}$	0,75
TIT_{max}	510°C	TIT_{max}	500°C	η_{el}	0,97
TOP_{min}	0,1 bar	TOP_{min}	0,1 bar	$\Delta P_{cooling}$	$2\% \cdot TOP$
TOP_{max}	15 bar	TOP_{max}	11 bar	$\Delta P_{heating}$	$2\% \cdot POP$

Constraints	
$T_{cond,min}$	$T_{amb} + \Delta T_{pinch} = 35°C$
$P_{el,net}$	1 MW
$\dot{Q}_{heat,need}$	0 MW
Minimum vapor fraction at turbine outlet	0,85

Table 17, 18 – Assumptions and constraints for the SRCs operating conditions ([9], [10], [11], [12])

The layouts investigated are shown below with their optimized operating conditions. The thermodynamic cycles independent variables assumed for the optimization purposes are the bleeding pressure and the reheating pressure. Finally, it has been imposed the saturated conditions at the mixer outlet.

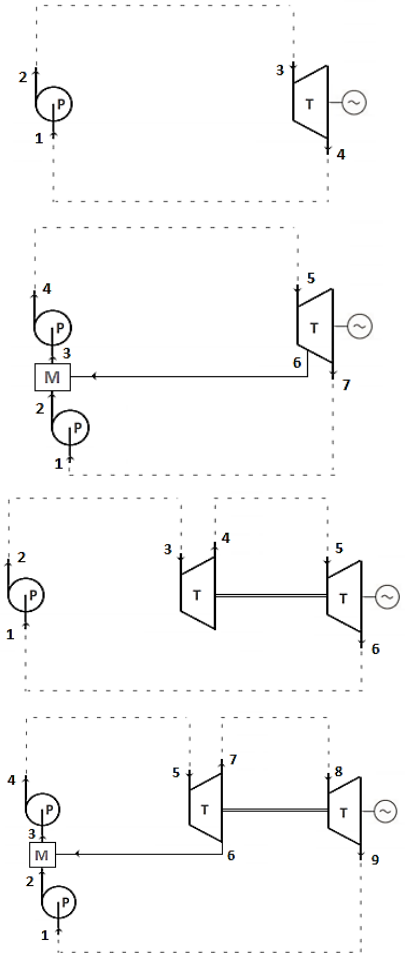

Figure 11 - SRC configurations investigated

		Basic	Single bleeding	Single reheat	Regeneration + Reheat
1	P [Bar]	0,1	0,1	0,1	0,1
	T [°C]	45,8	45,8	45,8	45,8
2	P [Bar]	112,24	12,5	103,1	11
	T [°C]	47,1	46	47	46
3	P [Bar]	110	12,5	101	11
	T [°C]	510	189,8	500	184,1
4	P [Bar]	0,102	112,24	11	103,1
	T [°C]	46,2	192,2	226,5	186,2
5	P [Bar]	-	110	10,78	101
	T [°C]	-	510	500	500
6	P [Bar]	-	12,5	0,102	11
	T [°C]	-	236,9	57,6	226,5
7	P [Bar]	-	0,102	-	11
	T [°C]	-	45,8	-	226,5
8	P [Bar]	-	-	-	10,78
	T [°C]	-	-	-	500
9	P [Bar]	-	-	-	0,102
	T [°C]	-	-	-	57,6
VF [-]		0,87 [4]	0,87 [7]	1 [4,6]	1 [7,9]
$\dot{m}_{water}$ [kg/s]		0,943	1,062	0,766	0,893
$\dot{W}_{turb,1}$ [kW]		1045	1048,4	373,8	435,8
$\dot{W}_{turb,2}$ [kW]		-	-	667,8	608,6
$\dot{W}_{pumps}$ [kW]		14,2	17,5	10,6	13,4
Bleeding		-	22,63%	-	21,83%
η_{cycle}		33,33%	36,69%	34,71%	36,81%

Table 19 - First step optimisation results for the Steam Rankine thermodynamic cycles

Figure 11 shows the analyzed steam Rankine cycles: Basic layout, Single bleeding layout, Single reheat layout, Regeneration and reheat layout (from the top to the bottom).

It's interesting to notice that although the regeneration and reheat layout has the higher efficiency (in absolute terms), its performance is very close to the one achieved with a single bleeding. In fact both the cases of single reheat and regeneration with reheat have a double-step expansion, which means that must be used two smaller turbines whose rated functioning conditions are less competitive than the ones achieved with a single turbine: this fact penalizes their efficiency.

Integration results

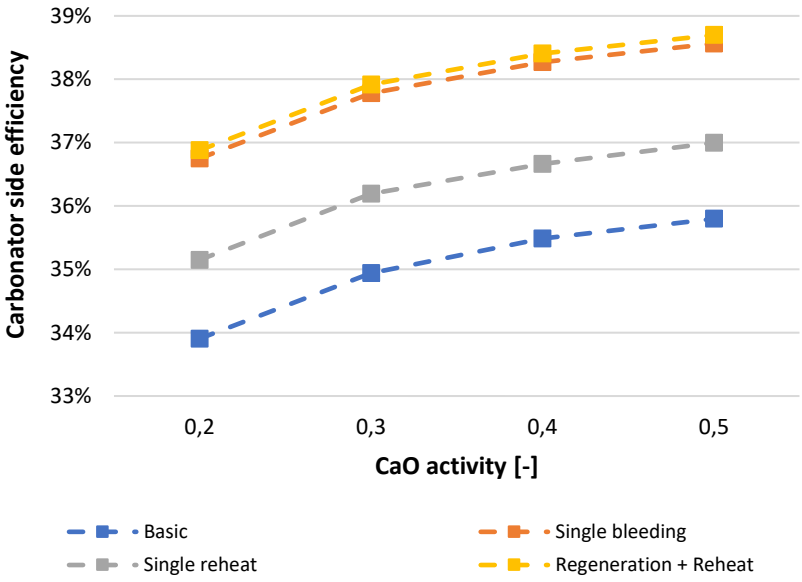

Figure 12 - Carbonator side efficiencies for the indirect integration with SRCs

The results obtained by the integration optimization show a trend very similar to the ones exposed in the optimization of the single power blocks.

	Basic	Simple bleeding	Simple reheat	Regeneration + Reheat
Storage turbine power [kW]	348	314	333	313
Compressor power [kW]	14,41	21,92	16,04	21,27
Conveying power [kW_e]	53	48	51	48
Rejection power [kW_e]	15,7	13,6	14,7	13,5
Total auxiliaries consumption [kW_e]	69	61	65	61
Total plant net power [kW_e]	1255	1222	1242	1222

		Basic	Simple bleeding	Simple reheat	Regeneration + Reheat
Independent variables	T_{carb} [°C]	875	875	875	875
	$T_{CaO,in}$ [°C]	310	310	310	310
	$T_{CO2,in}$ [°C]	36	197	52	192
	TIT [°C]	650	650	650	650
	CIT [°C]	47	139	90	132
Dependent variables	COT [°C]	58	152	102	145
	TOT [°C]	294	294	294	294
	$T_{CO2,mix}$ [°C]	146	197	173	192
	Excess index [-]	2,682	3,196	2,723	3,178
Flowrates	$\dot{m}_{CaO}$ [kg/s]	2,21	1,99	2,11	1,99
	$\dot{m}_{CO_2,stoic}$ [kg/s]	0,87	0,78	0,83	0,78
	$\dot{m}_{CO_2,rec}$ [kg/s]	1,46	1,72	1,43	1,7
	$\dot{m}_{CaO,unr}$ [kg/s]	1,10	1,00	1,06	0,99
	$\dot{m}_{CaCO_3}$ [kg/s]	1,97	1,78	1,89	1,77
	η_{carb} [%]	35,80	38,56	37,00	38,70

Table 20, 21 - Optimisation results for the indirect integration of Steam Rankine cycles with X=0,5 and Tcarb=875°C

All the results obtained for the other configurations investigated are presented in the Appendix 1.

Concerning the values of the independent variables to whom the optimization converged and the obtained turbomachinery powers, all the comments and considerations already made for the indirect integration of the organic Rankine cycles are still valid, as could be expected since the two thermodynamic cycles are actually quite similar.

The following graphs show the pinch analysis results obtained for the single bleeding layout; although it doesn't have the highest carbonator efficiency (the regeneration + reheating layout is actually performing a little bit better) it can be considered as the most interesting alternative between the SRC because, in terms of components involved in the cycle, its layout is quite simple and its performance is overall good.

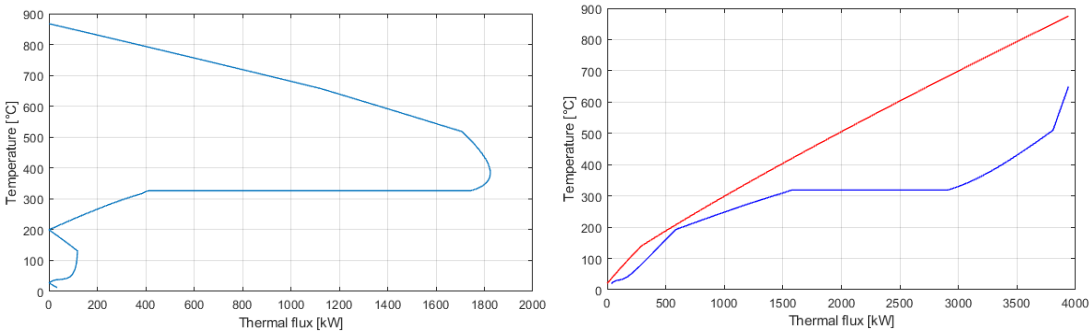

Figure 13 - Grand composite curve and hot and cold composite curves for the SRC with the single bleeding layout (X=0,5)

All the graphs obtained for the other configurations investigated are presented in the Appendix 2.

1.1.9 Brayton-Joule cycles - Supercritical CO_2

Another typology of power block to integrate in the carbonator side consists in the Brayton-Joule cycle.
Also in this case there are many alternatives for the power fluid choice; anyway, according to the scientific literature, the most interesting substance at the state of the art seems to be the carbon dioxide, which is the alternative chosen for this analysis.

Layouts investigated

The turbine operating conditions assumed have been taken from the 1 MW prototype of the turbine that General Electrics is building for the U.S. Department of Energy's SunShot Initiative.

Machinery data and assumptions			
TIP_{max}	250 bar	ΔT_{hex}	15°C
TIT_{max}	715°C	$\eta_{is,turb}$	0,9
ΔP_{LP}	$1\% \cdot P_{in}$	$\eta_{is,comp}$	0,87
ΔP_{HP}	$0{,}5\% \cdot P_{in}$	η_{el}	0,97

Constraints	
$P_{el,net}$	1 MW
$\dot{Q}_{heat,need}$	0 MW
$T_{cooler,min}$	$T_{amb} + \Delta T_{pinch}$ = 35°C
$P_{min,abs}$	74 bar

Table 22, 23 - Assumptions and constraints for the SCO2 cycles operating conditions ([5], [13], [14])

The investigated configurations are two: the former is the single inter-cooling layout, while the latter is the recompression layout.
Regarding the first configuration, the parameters assumed as independent variables are the turbine inlet pressure, the turbine pressure ratio and the intercooling pressure.
Instead, for the second layout the variables to optimize are the turbine inlet pressure, the turbine pressure ratio and the split fraction of the hot stream exiting from the low-temperature heat exchanger.

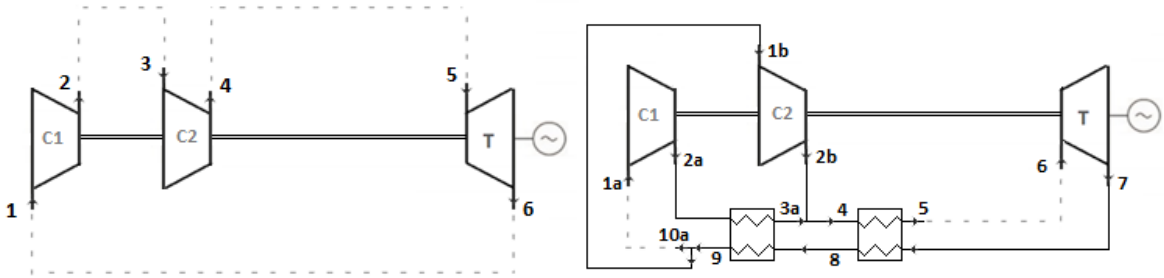

Figure 14 – SCO2 cycles configurations investigated: intercooling layout and recompression layout

	Single intercooling		Recompression	
	P [Bar]	T [°C]	P [Bar]	T [°C]
1/1a	74	35	82,7	35
1b	-	-	83,7	89,7
2/2a	80,3	40,7	253,8	74,7
2b	-	-	252,5	199,2
3/3a	79,5	35	252,5	197,5
4	251,3	97,6	252,5	198,1
5	250	715	251,3	522
6	74,7	555,1	250	715
7	-	-	85,4	571
8	-	-	84,6	213
9	-	-	83,7	89,7
10a	-	-	83,7	89,7
$\dot{m}_{CO_2,tot}$ [kg/s]	6,93		8,32	
$\dot{m}_{10a}/\dot{m}_9$	-		0,649	
$\dot{W}_{turb}$ [kW]	1313		1419	
$\dot{W}_{comp,1}$ [kW]	18,8		159,8	
$\dot{W}_{comp,2}$ [kW]	263,6		228,8	
η_{cycle}	17,13%		49,25%	

Concerning the single intercooling layout optimization, the resulting cycle efficiency could seem quite low (17,13%) but this is due to the fact that, differently from the recompression configuration, at the turbine outlet is **not performed any heat recovery** (since it is left to the second step of the optimization process).

Table 24 - First step optimisation results for the Supercritical CO2 thermodynamic cycles

Integration results

From the integration results is interesting to observe not only the differences on the performances but also the variation of the relative convenience of a layout with respect to the other one.

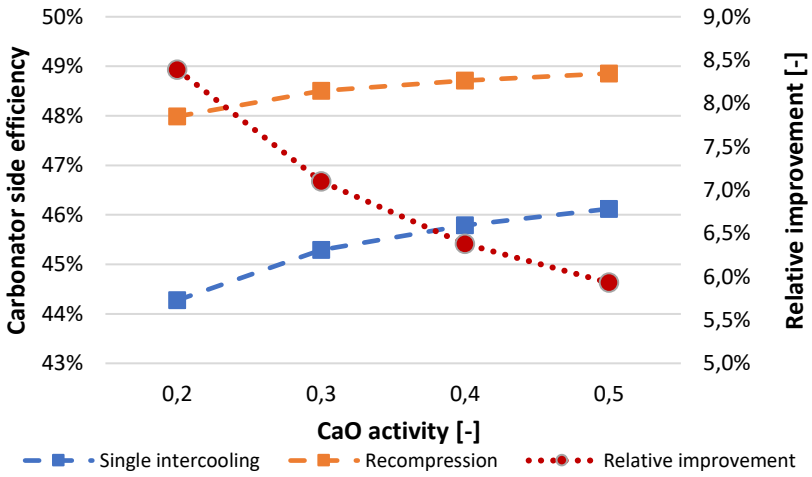

Figure 15 - Carbonator side efficiencies for the indirect integration with SCO2 cycles

Inside the variation range of the parameters analyzed, the recompression layout is always better performing, although its relative improvement (with respect to the single intercooling layout) decreases with the increase of the calcium oxide reactivity. This fact can be explained considering that this is the only thermodynamic cycle (between the ones investigated) in which a partial heat recovery is already performed before the pinch analysis-based optimization and therefore the effectiveness of this second optimization step is reduced.

	Single intercooling	Recompression
Storage turbine power [kW_s]	252	204
Compressor power [kW_s]	24,6	73,9
Conveying power [kW_e]	38	33
Rejection power [kW_e]	8,9	7,3
Total auxiliaries consumption [kW_e]	47	41
Total plant net power [kW_e]	1174	1085

		Single intercooling	Recompression
Independent variables	T_{carb} [°C]	875	875
	$T_{CaO,in}$ [°C]	493	511
	$T_{CO2,in}$ [°C]	291	518
	TIT [°C]	650	589
	CIT [°C]	114	472
Dependent variables	COT [°C]	127	492
	TOT [°C]	294	251
	$T_{CO2,mix}$ [°C]	166	457
	Excess index [-]	4,269	6,847
Flowrates	$\dot{m}_{CaO}$ [kg/s]	1,6	1,4
	$\dot{m}_{CO_2,stoic}$ [kg/s]	0,63	0,55
	$\dot{m}_{CO_2,rec}$ [kg/s]	2,057	3,211
	$\dot{m}_{CaO,unr}$ [kg/s]	0,8	0,7
	$\dot{m}_{CaCO_3}$ [kg/s]	1,43	1,25
	η_{carb} [%]	46,12	48,86

Table 25, 26 - Optimisation results for the indirect integration of SCO2 cycles with X=0,5

All the results obtained for the other configurations investigated are presented in the Appendix 1.

Another thing that is important to notice is that the carbonator feed stream temperatures are much high if compared to the results obtained for the ORC and SRC simulations (especially for the recompression layout), determining the necessity of consistent CO2 excesses and therefore increasing the compressor power consumption.
Furthermore, for the recompression layout are reported some cases where the storage turbine inlet temperature (TIT) doesn't converge to its maximum achievable value (650°C), which had never happened before.
There are actually many reasonable explanations to justify these phenomenon, and one of these consists in the fact that, being the carbon dioxide both the working fluid (in the power block) and one of the carbonator outlet streams, providing heat to the thermodynamic cycle with a CO_2 flowrate as high as possible (with respect to the $CaCO_3$ and the unreacted CaO flowrates) can improve the thermal recovery.
Another reason for that can be related to the fact that the cold fluid of the power block (exiting the high-temperature exchanger and entering the turbine) requires only heat at high temperature (522°C – 715°C) and therefore heating up the two carbonator inlet streams allows to recover the thermal power at mid-low temperature. Moreover, this last consideration can also justify the fact that the storage turbine inlet temperature (TIT) doesn't always reach its acceptable maximum.

Always concerning the recompression layout, another very uncommon aspect that can be observed is related to the particularly high value obtained for the compressor inlet temperature (CIT). The possible explanation for that could be again related to the fact that, since the power block requires heat at high temperature, there are no reasons to completely cool down the recirculated CO_2, also considering that the compression power won't excessively increase in absolute terms because it's only requested a pressure increase equal to 0,1 bar.

Also in this case the hot and cold composite curves are helpful to understand the optimal configuration obtained: the consistent differences between the graphs below can be referred, as already explained, to the different temperatures at which the power block must be fed. As a consequence, the genetic algorithm converges to values of independent variables that allows the two curves to approach each other as much as possible. Furthermore, the fact that the carbon dioxide is present both in the carbonator side and in the power block is another aspect that improves the thermal exchange, since there are hot and cold streams with equal thermophysical properties.

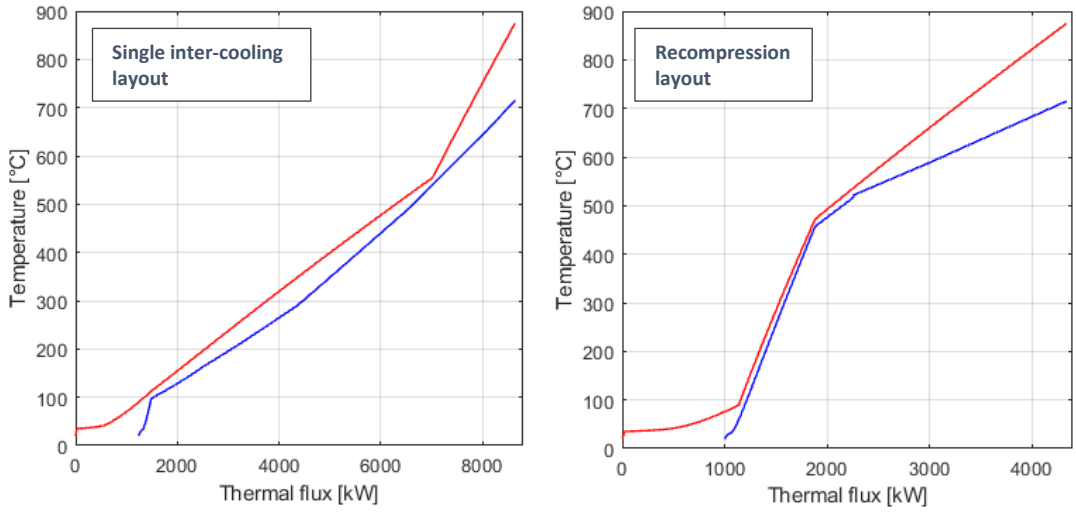

Figure 16 - Hot and cold composite curves for the SCO2 layouts investigated (X=0,5)

All the graphs obtained for the other configurations investigated are presented in the Appendix 2.

1.4. SENSITIVITY ANALYSIS AND BEST ALTERNATIVES COMPARISON

One important aspect related to the CaL integration is the plant performance variation that can occur when one of its main parameters change with respect to its nominal value. As already exposed, in the present work it has been tried to investigate this phenomenon performing different simulation in correspondence of different values of calcium oxide reactivity and carbonator temperature. Anyway, regarding this last independent variable, the schemes reported in the indirect integration analysis doesn't show this aspect because, in order to perform a more compact optimization, the simulations executed were able to return the optimal value of T_{carb} and therefore it hasn't been necessary to run different scripts for different carbonator temperature.

In any case, the influence of this parameter has been separately evaluated performing a sensitivity analysis in which the optimal operating conditions are found in dependence of the carbonator temperature, but this has been done only for the two indirect integration

alternatives that appeared as the most interesting: one is the supercritical Organic Rankine Cycle with vacuum condensation and benzene as working fluid, while the other is the Brayton-Joule cycle with supercritical CO_2 with the recompression layout.

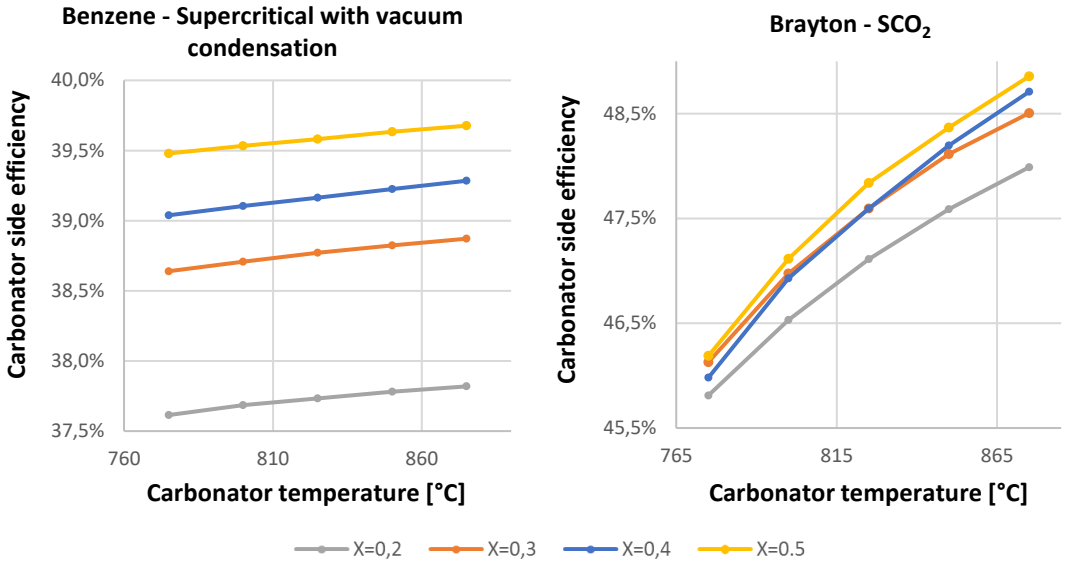

Figure 17 - Sensitivity analysis on the carbonator operating temperature for the two most interesting indirect integration alternatives

So, this sensitivity analysis confirms what already observed from the indirect integration optimizations: the highest performances are reached when the carbonator temperature is at its maximum. Anyway is interesting to notice that the trends encountered for the two alternatives investigated present some differences: for the ORC case, the carbonator side efficiency variation is nearly linear with the reactor temperature and, both in absolute and relative terms, the performance decrease is very poor (about -1%). This means that, although the carbonation products are available at lower temperatures, it's possible to realize an heat exchanger network able to feed the thermodynamic cycle without consistent penalties.
For the SCO_2 case it can be observed a sublinear trend with higher efficiency decreases with respect to the optimal configuration; it seems reasonable to explain this phenomenon considering the higher temperature range at which the power block operates, making the entire plant more sensible to the heat source temperature with the whom the thermodynamic cycle is fed.

So, once that all the simulations have been executed, it's possible to make some comparisons and considerations from the obtained results.

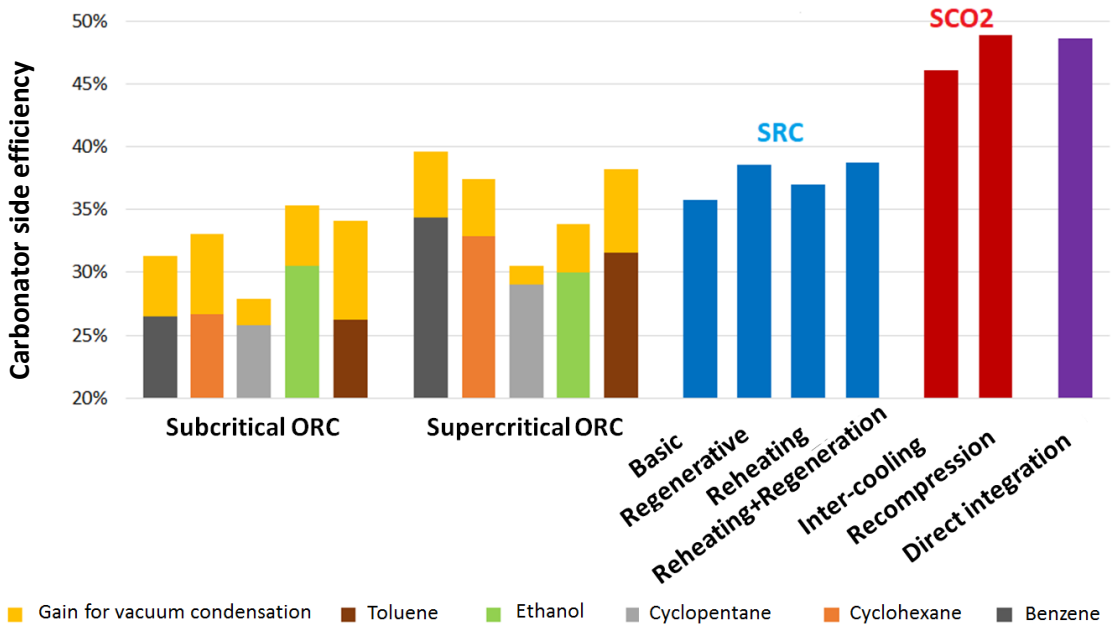

Table 27 – Integration alternatives comparison in terms of carbonator side efficiency (for X=0,5 and T_{carb}=875°C)

As could be expected, the ORC and the SRC are the less convenient alternatives and this can be explained considering both their thermodynamic cycle efficiencies and the intrinsic penalties in the heat exchange process due to the evaporation and condensation steps.
Therefore form this comparison emerged that the most performing typologies are the indirect integration with a supercritical carbon dioxide cycle and the direct integration.
Now, it is actually non-trivial to establish in absolute terms which of these two is the best choice, because there are many other features not considered in this analysis (such as the economic aspect and the plant regulation) that may consistently influence the decision. Anyway, regarding the only thermodynamic point of view, the present study provides some useful elements that can help for the choice of a proper Calcium-Looping integration in a CSP plant.

1.5. INDIRECT INTEGRATION WITH DIRECT HEAT EXCHANGE ON THE CARBONATOR

One last case that it is worth to analyze is represented by the indirect integration with the power block directly fed with a heat exchange on the carbonator wall. Anyway, for the reasons previously explained, the study executed for this configuration hasn't been as detailed as for the case of indirect integration with a thermodynamic cycle whose heating need is satisfied by a thermal recovery on the carbonation products. So the alternatives investigated are the same two for the whom has been done the sensitivity analysis: one is the supercritical Organic Rankine Cycle with vacuum condensation and benzene as working fluid, while the other is the Brayton-Joule cycle with supercritical CO2 with the recompression layout.

The optimization structure is basically equal to the previous case; the first step remains unchanged, while the second step has been modified in order to take into account the thermal flux in correspondence of the chemical reactor and consequently the cold stream of the thermodynamic cycle has been removed from the pinch analysis. The constant parameters and both the dependent and independent variables are the same as before.

Assumptions	
$\eta_{is,T}$	0,75
$\eta_{is,C}$	0,65
η_{el}	0,97
P_{carb}	1 bar
ΔP_{comp}	10% P_{carb}
Conveying consumptions	10 kJ/(kg*100m)
Storages-carbonator distance	100 m
Auxiliaries consumptions	0,8% rejected heat
Carbonator thermal loss	1% carbonation heat
$\Delta T_{min,pinch}$	15°C
$T_{ambient}$	20°C

Independent variables	Lower bound	Upper bound	Handled as
X	0,2	0,5	Discrete
T_{carb}	650°C	875°C	Discrete
$T_{CO2,in}$	$T_{amb} + \Delta T_{pinch}$	$T_{carb} - \Delta T_{pinch}$	Continuous
$T_{CaO,in}$	310°C	$T_{carb} - \Delta T_{pinch}$	Continuous
CIT	$T_{amb} + \Delta T_{pinch}$	250°C	Continuous
TIT	250°C	650°C	Continuous
$\dot{n}_{CaO}$	-	-	Continuous

Constraints	
CIT_{min} and $T_{CO2,in,min}$	35°C
$\dot{Q}_{heat,need}$	0 MW
P_{el,net_power_block}	1 MW

Tables 28, 29, 30 - Assumptions, constraints and independent variables for the carbonator side ([3], [4], [5], [6])

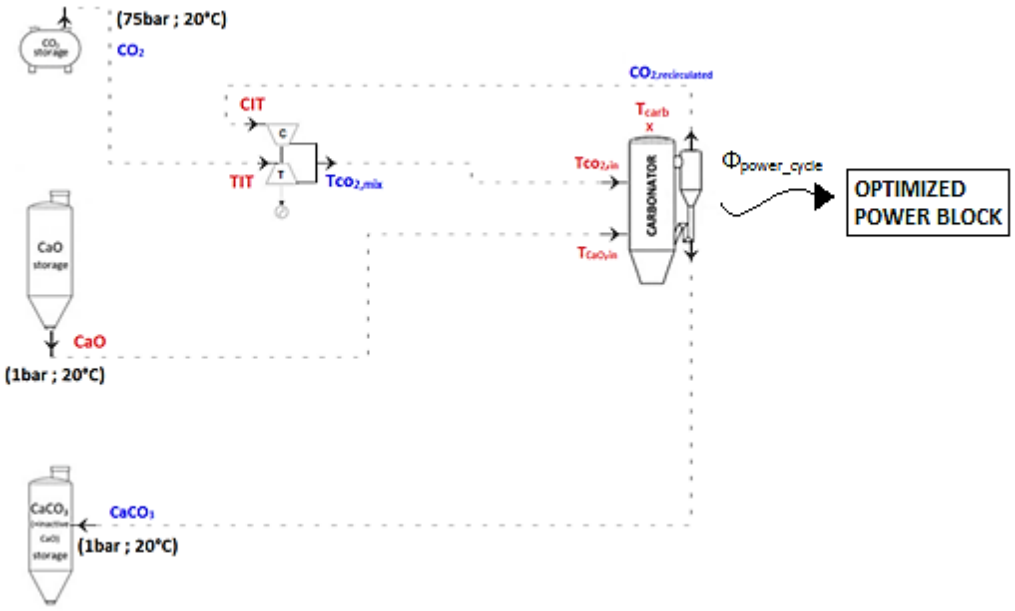

Figure 18 - Plant layout with streams data for the pinch analysis. The fixed parameters are the ones in black, the independent variables in red and the dependent variables in blue

In the graphs below are exposed the optimization process results in terms of carbonator side efficiency for the two alternatives studied.

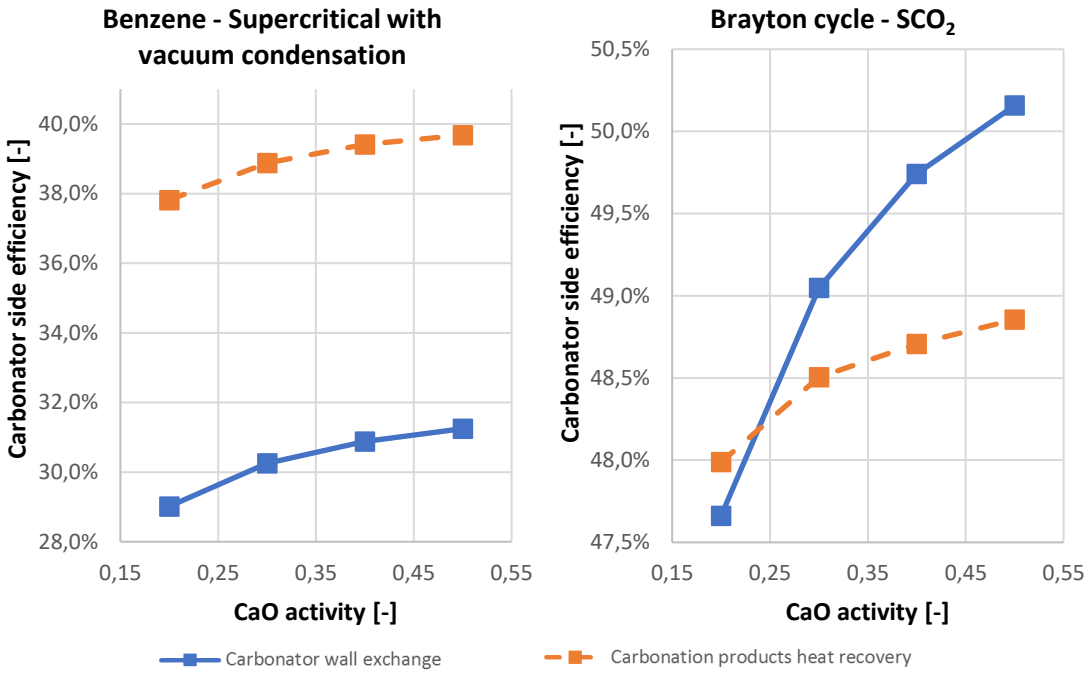

Figure 19 - Carbonator side efficiency obtained from the optimization process for the case of power block directly fed with a heat exchange on the reactor wall

These last results are actually quite interesting because they demonstrate the different behavior in terms of carbonator side efficiency that the power blocks can present when the indirect integration configuration is changed in accordance to the way with the whom the thermodynamic cycle receive the thermal power needed. So, for the case of supercritical benzene with vacuum condensation, feeding the power cycle with a direct heat exchange on the carbonator wall is actually inconvenient because the relative performance reduction is nearly equal to 21%. Things are different for the supercritical carbon dioxide thermodynamic cycle, where the improvement is dependent on the calcium oxide activity and, in any case, is much smaller with respect to the ORC case considered.

It's therefore clear that any consideration about the convenience of one specific layout can be done only after a detailed analysis and the simulations of all the investigated alternatives.

	Benzene	SCO_2
Storage turbine power [kW]	420	234
Compressor power [kW]	2,8E-5	2,2E-04
Conveying power [kW_e]	64	36
Rejection power [kW_e]	32,5	14,1
Total auxiliaries consumption [kW_e]	96	50
Total plant net power [kW_e]	1324	1185

		Benzene	SCO_2
Independent variables	T_{carb} [°C]	700	850
	$T_{CaO,in}$ [°C]	627	794
	$T_{CO2,in}$ [°C]	560	731
	TIT [°C]	650	650
	CIT [°C]	249	323
Dependent variables	COT [°C]	265	340
	TOT [°C]	294	294
	$T_{CO2,mix}$ [°C]	294	294
	Excess index [-]	1	1
Flowrates	$\dot{m}_{CaO}$ [kg/s]	2,67	1,49
	$\dot{m}_{CO_2,stoic}$ [kg/s]	1,05	0,584
	$\dot{m}_{CO_2,rec}$ [kg/s]	1,7E-06	1,2E-05
	$\dot{m}_{CaO,unr}$ [kg/s]	1,33	0,743
	$\dot{m}_{CaCO_3}$ [kg/s]	2,38	1,33
	η_{carb} [%]	31,25	50,16

Tables 31, 32 - Optimisation results for the indirect integration for the case of power block directly fed with a heat exchange on the reactor wall (X=0,5)

The most important thing to notice about the values of the dependent and independent variables to the whom the genetic algorithm converges is the fact that the optimal operating conditions are reached when the recirculated mass stream of carbon dioxide becomes practically equal to zero. This means that the maximum efficiency is reached in correspondence of stoichiometric operating conditions for the two reactants participating the exothermic reaction and therefore all the carbon dioxide provided to the chemical reactor interacts with the calcium oxide to produce the calcium carbonate.

So, on the practical point of view, the compressor present in the carbonator side that recirculates the CO_2 in excess can be removed since there isn't any more a mass flowrate.

1.6. APPENDIX I

Direct integration complete optimization results

	X [-]	Main turbine power [kW]	Compressor power [kW]	Storage turbine power [kW]	Conveying power [kW_e]	Rejection power [kW_e]	Total auxiliaries consumption [kW_e]	Total plant net power [kW_e]
T_{carb} = 775°C	0,2	2087	1056	122	82,5	6,7	89,1	1029
	0,3	2087	1056	112	56,0	7,1	63,1	1046
	0,4	2087	1056	114	43,5	7,4	50,9	1060
	0,5	2087	1056	111	35,8	7,6	43,4	1065
T_{carb} = 825°C	0,2	1981	950	115	78,2	6,0	84,2	1027
	0,3	1981	950	114	53,6	6,5	60,1	1051
	0,4	1981	950	112	41,4	6,7	48,1	1061
	0,5	1981	950	117	34,4	6,9	41,3	1072
T_{carb} = 875°C	0,2	1931	900	108	75,3	5,3	80,6	1024
	0,3	1931	900	111	51,8	5,8	57,6	1050
	0,4	1931	900	106	39,9	6,0	45,9	1057
	0,5	1931	900	105	32,9	6,2	39,1	1063

		Tcarb = 775°C				Tcarb = 825°C				Tcarb = 875°C			
	X [-]	0,2	0,3	0,4	0,5	0,2	0,3	0,4	0,5	0,2	0,3	0,4	0,5
INDEPENDENT VARIABLES	P_{carb} [bar]	3,1	3,1	3,1	3,1	2,92	2,92	2,92	2,92	3,43	3,43	3,43	3,43
	β_t [-]	2,98	2,98	2,98	2,98	2,81	2,81	2,81	2,81	3,3	3,3	3,3	3,3
	$T_{CaO,in}$ [°C]	746	688	737	682	807	728	706	763	842	839	837	822
	$T_{CO2,in}$ [°C]	625	635	626	631	676	689	688	679	708	706	706	707
	TIT [°C]	348	315	322	313	338	337	332	349	345	359	340	339
	CIT [°C]	35,1	35,1	35,1	35,1	35,1	35,1	35,1	35,1	35,1	35,1	35,1	35,1
DEPENDENT VARIABLES	Excess index [-]	20,4	20,7	20,7	20,8	20,5	20,7	20,8	20,7	17,5	17,6	17,7	17,8
	tOT [°C]	629	629	629	629	681	681	681	681	704	704	704	704
	COT [°C]	136	136	136	136	131	131	131	131	146	146	146	146
	TOT [°C]	137	110	116	108	125	125	121	134	139	150	135	134
	$T_{CO2,mix}$ [°C]	136	135	135	135	131	131	130	131	145	146	145	145
FLOWRATES	$\dot{m}_{CaO}$ [kg/s]	3,82	2,51	1,88	1,5	3,62	2,4	1,79	1,44	3,49	2,32	1,72	1,38
	$\dot{m}_{CO_2,stoic}$ [kg/s]	0,601	0,591	0,59	0,588	0,569	0,565	0,562	0,564	0,548	0,546	0,541	0,54
	$\dot{m}_{CO_2,rec}$ [kg/s]	11,6	11,6	11,6	11,6	11,1	11,1	11,1	11,1	9,06	9,06	9,06	9,06
	$\dot{m}_{CaO,unr}$ [kg/s]	3,06	1,75	1,13	0,75	2,9	1,68	1,07	0,72	2,79	1,62	1,03	0,69
	$\dot{m}_{CaCO_3}$ [kg/s]	1,37	1,34	1,34	1,34	1,29	1,28	1,28	1,28	1,25	1,24	1,23	1,23
	η_{carb} [%]	42,36	43,76	44,39	44,79	44,61	45,96	46,63	46,96	46,17	47,51	48,26	48,64

Indirect integration complete optimization results

- **Organic Rankine cycles**

	X [-]	Storage turbine power [kW]	Compressor power [kW]	Conveying power [kW_e]	Rejection power [kW_e]	Total auxiliaries consumption [kW_e]	Total plant net power [kW_e]
BENZENE	0,2	519	0,26	178	24,4	202	1301
	0,3	515	12,53	122	25,5	147	1340
	0,4	514	21,72	94	26,0	120	1357
	0,5	511	27,81	77	26,8	104	1364
CYCLOHEXANE	0,2	514	0,2	176	23,8	200	1299
	0,3	511	12,29	121	24,7	145	1338
	0,4	509	21,68	94	24,6	118	1355
	0,5	506	29,65	77	25,0	102	1360
CYCLOPENTANE	0,2	538	0,16	184	27,9	212	1310
	0,3	535	10,93	127	27,9	154	1354
	0,4	534	19,63	98	28,0	126	1373
	0,5	531	25,11	81	27,9	109	1382
ETHANOL	0,2	429	0,68	147	19,9	167	1249
	0,3	426	10,14	101	20,7	121	1282
	0,4	424	19,2	78	21,0	99	1294
	0,5	422	25,39	64	21,5	86	1299
TOLUENE	0,2	526	0,3	180	23,7	204	1306
	0,3	521	14,49	123	25,2	148	1343
	0,4	519	25,87	95	26,4	122	1357
	0,5	516	33	78	26,2	105	1364

Subcritical cycle with counterpressure condensation

	X [-]	Storage turbine power [kW]	Compressor power [kW]	Conveying power [kW_e]	Rejection power [kW_e]	Total auxiliaries consumption [kW_e]	Total plant net power [kW_e]
BENZENE	0,2	416	0,23	142	20,2	163	1241
	0,3	414	8,57	98	21,0	119	1274
	0,4	413	14,53	76	20,7	97	1290
	0,5	411	17,71	62	21,0	83	1298
CYCLOHEXANE	0,2	389	0,17	133	19,2	152	1225
	0,3	387	8,83	91	18,9	110	1256
	0,4	386	13,89	71	19,3	90	1271
	0,5	384	17,77	58	18,9	77	1278
CYCLOPENTANE	0,2	486	0,26	166	24,8	191	1280
	0,3	483	9,99	114	25,4	139	1319
	0,4	482	16,37	89	25,4	114	1338
	0,5	480	20,91	73	25,0	98	1347
ETHANOL	0,2	357	0,22	122	16,9	139	1207
	0,3	353	9,56	84	16,9	100	1233
	0,4	354	12,97	65	17,7	83	1248
	0,5	352	16,53	53	16,9	70	1255
TOLUENE	0,2	378	1,3	129	6,8	136	1229
	0,3	375	8,86	89	6,5	95	1260
	0,4	375	13,95	69	6,5	75	1275
	0,5	373	18,44	57	7,1	64	1280

Subcritical cycle with vacuum condensation

	X [-]	Storage turbine power [kW]	Compressor power [kW]	Conveying power [kW_e]	Rejection power [kW_e]	Total auxiliaries consumption [kW_e]	Total plant net power [kW_e]
BENZENE	0,2	371	0,08	127	14,8	142	1218
	0,3	368	9,17	87	15,1	102	1246
	0,4	367	16,66	67	15,5	83	1257
	0,5	365	21,12	55	15,9	71	1262
CYCLOHEXANE	0,2	391	0,09	134	17,1	151	1228
	0,3	388	9,48	92	17,2	109	1258
	0,4	387	17,42	71	18,1	89	1269
	0,5	384	22,38	58	18,4	77	1274
CYCLOPENTANE	0,2	459	0,1	157	22,2	179	1266
	0,3	456	9,52	108	22,4	130	1303
	0,4	456	16,68	84	23,2	107	1319
	0,5	453	21,94	69	23,2	92	1326
ETHANOL	0,2	440	0,1	151	19,1	170	1257
	0,3	437	10,44	103	20,4	124	1290
	0,4	436	18,35	80	20,9	101	1304
	0,5	433	23,11	66	21,0	87	1311
TOLUENE	0,2	419	0,1	144	4,8	142	1265
	0,3	416	11,73	98	4,5	98	1294
	0,4	414	21,59	76	4,5	76	1305
	0,5	411	27,41	62	5,1	62	1310

Supercritical cycle with counterpressure condensation

	X [-]	Storage turbine power [kW]	Compressor power [kW]	Conveying power [kW_e]	Rejection power [kW_e]	Total auxiliaries consumption [kW_e]	Total plant net power [kW_e]
BENZENE	0,2	309	0,45	106	12,8	119	1181
	0,3	308	7,51	73	13,3	86	1205
	0,4	307	12,61	56	13,2	70	1216
	0,5	305	16,48	46	12,6	59	1221
CYCLOHEXANE	0,2	333	0,08	114	15,0	129	1194
	0,3	331	7,86	78	14,9	93	1220
	0,4	330	13,81	61	15,1	76	1231
	0,5	328	16,61	50	14,5	64	1238
CYCLOPENTANE	0,2	430	0,12	147	20,6	168	1249
	0,3	427	9,09	101	21,3	122	1283
	0,4	427	14,52	78	21,4	100	1300
	0,5	424	18,5	64	21,1	85	1308
ETHANOL	0,2	378	0,1	129	17,2	147	1220
	0,3	375	8,43	89	18,0	107	1249
	0,4	375	13,76	69	17,4	86	1264
	0,5	373	16,72	57	17,8	74	1271
TOLUENE	0,2	325	0,08	111	13,7	125	1190
	0,3	322	7,88	76	13,6	90	1215
	0,4	321	13,91	59	13,2	72	1226
	0,5	320	17,09	49	13,8	62	1231

Supercritical cycle with vacuum condensation

	INDEPENDENT VARIABLES						DEPENDENT VARIABLES				FLOWRATES					
	X [-]	T_{carb} [°C]	$T_{CaO,in}$ [°C]	$T_{CO2,in}$ [°C]	TIT [°C]	CIT [°C]	COT [°C]	TOT [°C]	$T_{co2,mix}$ [°C]	Excess index [-]	$\dot{m}_{CaO}$ [kg/s]	$\dot{m}_{CO_2,stoic}$ [kg/s]	$\dot{m}_{CO_2,rec}$ [kg/s]	$\dot{m}_{CaO,unr}$ [kg/s]	$\dot{m}_{CaCO_3}$ [kg/s]	η_{carb} [%]
BENZENE	0,2	875	368	178	650	163	177	294	292	1,015	8,23	1,29	0,019	6,59	2,94	24,86
	0,3	875	311	101	650	106	118	294	214	1,834	5,44	1,28	1,071	3,81	2,92	25,82
	0,4	875	312	102	650	100	113	294	186	2,470	4,07	1,28	1,883	2,44	2,91	26,23
	0,5	875	311	106	650	104	116	294	178	2,877	3,24	1,27	2,389	1,62	2,89	26,52
CYCLOHEXANE	0,2	875	368	179	650	128	141	294	292	1,012	8,16	1,28	0,016	6,53	2,91	25,04
	0,3	875	310	101	650	103	116	294	213	1,831	5,40	1,27	1,057	3,78	2,89	25,99
	0,4	875	311	105	650	102	115	294	187	2,473	4,04	1,27	1,871	2,42	2,89	26,40
	0,5	875	323	112	650	122	135	294	189	2,928	3,21	1,26	2,431	1,60	2,86	26,67
CYCLOPENTANE	0,2	875	368	177	650	118	131	294	292	1,010	8,54	1,34	0,013	6,83	3,05	24,13
	0,3	875	311	70	650	69	81	294	201	1,775	5,66	1,33	1,034	3,96	3,03	25,08
	0,4	875	312	69	650	71	82	294	171	2,389	4,23	1,33	1,850	2,54	3,03	25,51
	0,5	875	313	72	650	71	83	294	159	2,783	3,37	1,32	2,360	1,69	3,01	25,79
ETHANOL	0,2	875	368	206	650	156	170	294	288	1,048	6,81	1,07	0,051	5,45	2,43	28,85
	0,3	875	310	98	650	101	113	293	212	1,826	4,51	1,06	0,877	3,15	2,41	29,82
	0,4	875	310	99	649	130	143	293	204	2,458	3,37	1,06	1,544	2,02	2,41	30,25
	0,5	875	318	100	650	143	156	294	204	2,879	2,68	1,05	1,976	1,34	2,39	30,53
TOLUENE	0,2	875	368	179	650	132	145	294	291	1,018	8,34	1,31	0,024	6,67	2,98	24,64
	0,3	875	311	131	650	131	144	294	223	1,894	5,51	1,30	1,162	3,86	2,95	25,56
	0,4	875	310	133	650	144	158	294	211	2,549	4,12	1,29	2,006	2,47	2,94	25,98
	0,5	875	310	156	650	134	147	294	195	3,042	3,28	1,28	2,627	1,64	2,92	26,24

Subcritical cycle with counterpressure condensation

	INDEPENDENT VARIABLES						DEPENDENT VARIABLES				FLOWRATES					
	X [-]	T_{carb} [°C]	$T_{CaO,in}$ [°C]	$T_{CO2,in}$ [°C]	TIT [°C]	CIT [°C]	COT [°C]	TOT [°C]	$T_{co2,mix}$ [°C]	Excess index [-]	$\dot{m}_{CaO}$ [kg/s]	$\dot{m}_{CO_2,stoic}$ [kg/s]	$\dot{m}_{CO_2,rec}$ [kg/s]	$\dot{m}_{CaO,unr}$ [kg/s]	$\dot{m}_{CaCO_3}$ [kg/s]	η_{carb} [%]
BENZENE	0,2	875	339	343	650	144	157	294	291	1,017	6,60	1,04	0,018	5,28	2,36	29,57
	0,3	875	310	51	650	90	102	294	212	1,742	4,37	1,03	0,765	3,06	2,34	30,55
	0,4	875	311	51	650	66	78	294	170	2,346	3,28	1,03	1,386	1,97	2,34	31,05
	0,5	875	310	52	650	52	63	294	148	2,722	2,61	1,03	1,764	1,30	2,33	31,30
CYCLOHEXANE	0,2	875	368	179	650	168	182	294	292	1,012	6,18	0,97	0,012	4,94	2,21	31,20
	0,3	875	313	51	650	121	134	294	225	1,753	4,09	0,96	0,726	2,86	2,19	32,22
	0,4	875	315	49	650	72	84	294	173	2,353	3,06	0,96	1,303	1,84	2,19	32,71
	0,5	875	312	51	650	75	87	294	163	2,725	2,44	0,96	1,651	1,22	2,18	33,01
CYCLOPENTANE	0,2	875	339	343	650	135	148	294	291	1,017	7,71	1,21	0,021	6,17	2,75	26,11
	0,3	875	312	49	650	88	100	294	211	1,745	5,10	1,20	0,896	3,57	2,73	27,11
	0,4	875	312	51	650	54	66	294	163	2,346	3,82	1,20	1,619	2,30	2,73	27,59
	0,5	875	312	54	650	54	66	294	149	2,732	3,04	1,20	2,070	1,52	2,72	27,87
ETHANOL	0,2	875	368	184	650	138	151	294	291	1,019	5,66	0,89	0,017	4,53	2,02	33,54
	0,3	875	313	53	650	190	204	294	255	1,758	3,74	0,88	0,668	2,62	2,00	34,62
	0,4	875	315	47	650	80	92	294	178	2,348	2,81	0,88	1,189	1,69	2,00	35,07
	0,5	875	313	52	650	80	92	294	166	2,728	2,23	0,88	1,515	1,11	1,99	35,34
TOLUENE	0,2	875	399	69	650	172	186	294	284	1,100	5,99	0,94	0,095	4,79	2,14	32,26
	0,3	875	311	63	650	129	142	294	228	1,764	3,96	0,93	0,714	2,78	2,12	33,33
	0,4	875	310	62	650	80	92	294	177	2,368	2,97	0,93	1,279	1,79	2,12	33,80
	0,5	875	310	75	650	87	99	294	169	2,785	2,36	0,93	1,658	1,18	2,11	34,08

Subcritical cycle with vacuum condensation

	INDEPENDENT VARIABLES						DEPENDENT VARIABLES				FLOWRATES					
	X [-]	T_{carb} [°C]	$T_{CaO,in}$ [°C]	$T_{CO2,in}$ [°C]	TIT [°C]	CIT [°C]	COT [°C]	TOT [°C]	$T_{co2,mix}$ [°C]	Excess index [-]	$\dot{m}_{CaO}$ [kg/s]	$\dot{m}_{CO_2,stoic}$ [kg/s]	$\dot{m}_{CO_2,rec}$ [kg/s]	$\dot{m}_{CaO,unr}$ [kg/s]	$\dot{m}_{CaCO_3}$ [kg/s]	η_{carb} [%]
BENZENE	0,2	875	368	174	650	168	182	294	293	1,007	5,89	0,92	0,006	4,71	2,1	32,55
	0,3	875	310	104	650	114	127	294	218	1,836	3,89	0,92	0,767	2,73	2,09	33,57
	0,4	875	310	125	650	113	126	294	192	2,526	2,91	0,92	1,397	1,75	2,08	34,03
	0,5	875	310	143	650	104	116	294	176	2,995	2,31	0,91	1,814	1,16	2,07	34,33
CYCLOHEXANE	0,2	875	368	174	650	156	170	294	293	1,007	6,20	0,97	0,007	4,96	2,21	31,16
	0,3	875	310	104	650	106	119	294	214	1,837	4,10	0,97	0,809	2,87	2,2	32,18
	0,4	875	310	132	650	105	117	294	187	2,548	3,07	0,96	1,492	1,84	2,19	32,60
	0,5	875	310	145	650	104	117	294	176	3,004	2,44	0,96	1,918	1,22	2,18	32,91
CYCLOPENTANE	0,2	875	368	175	650	136	149	294	293	1,007	7,29	1,14	0,008	5,83	2,6	27,33
	0,3	875	310	70	650	77	89	294	205	1,773	4,83	1,14	0,880	3,38	2,59	28,31
	0,4	875	310	70	650	70	82	294	171	2,385	3,61	1,14	1,573	2,17	2,58	28,80
	0,5	875	310	74	650	80	92	294	165	2,783	2,87	1,13	2,012	1,43	2,56	29,04
ETHANOL	0,2	875	368	174	650	180	194	294	293	1,007	6,98	1,10	0,007	5,58	2,49	28,32
	0,3	875	311	100	650	100	112	294	211	1,832	4,62	1,09	0,906	3,23	2,47	29,28
	0,4	875	311	100	650	101	114	294	187	2,462	3,46	1,09	1,588	2,07	2,47	29,76
	0,5	875	311	100	650	100	112	294	176	2,859	2,75	1,08	2,007	1,37	2,45	30,00
TOLUENE	0,2	875	368	174	650	169	183	294	293	1,007	6,65	1,05	0,007	5,32	2,38	29,91
	0,3	875	310	134	650	134	148	294	225	1,899	4,40	1,04	0,931	3,08	2,36	30,87
	0,4	875	310	170	650	135	148	294	203	2,660	3,29	1,03	1,715	1,97	2,35	31,30
	0,5	875	310	178	650	134	148	294	194	3,122	2,61	1,03	2,177	1,30	2,33	31,59

Supercritical cycle with counterpressure condensation

	INDEPENDENT VARIABLES						DEPENDENT VARIABLES				FLOWRATES					
	X [-]	T_{carb} [°C]	$T_{CaO,in}$ [°C]	$T_{CO2,in}$ [°C]	TIT [°C]	CIT [°C]	COT [°C]	TOT [°C]	$T_{co2,mix}$ [°C]	Excess index [-]	$\dot{m}_{CaO}$ [kg/s]	$\dot{m}_{CO_2,stoic}$ [kg/s]	$\dot{m}_{CO_2,rec}$ [kg/s]	$\dot{m}_{CaO,unr}$ [kg/s]	$\dot{m}_{CaCO_3}$ [kg/s]	η_{carb} [%]
BENZENE	0,2	875	397	44	649	47	58	293	280	1,059	4,91	0,77	0,046	3,93	1,75	37,83
	0,3	875	310	47	650	158	172	294	242	1,735	3,25	0,77	0,564	2,28	1,74	38,84
	0,4	875	310	49	650	126	139	294	205	2,338	2,44	0,77	1,024	1,46	1,74	39,37
	0,5	875	310	81	650	116	129	294	188	2,803	1,94	0,76	1,371	0,97	1,73	39,65
CYCLOHEXANE	0,2	875	368	174	650	183	197	294	293	1,007	5,29	0,83	0,006	4,23	1,89	35,53
	0,3	875	310	57	650	138	151	294	233	1,751	3,49	0,82	0,619	2,45	1,87	36,61
	0,4	875	310	62	650	125	138	294	204	2,367	2,62	0,82	1,124	1,57	1,87	37,13
	0,5	875	310	98	650	82	94	294	164	2,851	2,08	0,82	1,514	1,04	1,86	37,39
CYCLOPENTANE	0,2	875	368	176	650	146	159	294	293	1,009	6,82	1,07	0,009	5,45	2,43	28,83
	0,3	875	311	51	650	99	112	294	216	1,743	4,51	1,06	0,791	3,16	2,42	29,81
	0,4	875	311	51	650	56	68	294	164	2,344	3,38	1,06	1,429	2,03	2,42	30,34
	0,5	875	310	53	650	55	67	294	150	2,726	2,69	1,06	1,825	1,34	2,4	30,55
ETHANOL	0,2	875	368	176	650	137	150	294	292	1,009	6,00	0,94	0,008	4,80	2,14	32,00
	0,3	875	311	47	650	122	135	294	226	1,738	3,96	0,94	0,690	2,78	2,13	33,04
	0,4	875	311	47	650	84	96	294	181	2,336	2,97	0,93	1,248	1,79	2,12	33,54
	0,5	875	311	47	650	67	79	294	158	2,712	2,36	0,93	1,591	1,18	2,11	33,84
TOLUENE	0,2	875	368	174	650	184	199	294	293	1,007	5,15	0,81	0,005	4,12	1,84	36,37
	0,3	875	310	65	650	142	156	294	234	1,765	3,40	0,80	0,614	2,39	1,82	37,42
	0,4	875	310	97	650	114	127	294	195	2,452	2,55	0,80	1,163	1,53	1,82	37,95
	0,5	875	310	118	650	90	102	294	168	2,912	2,03	0,80	1,523	1,01	1,81	38,21

Supercritical cycle with vacuum condensation

- **Steam Rankine cycle**

	X [-]	Storage turbine power [kW]	Compressor power [kW]	Conveying power [kW_e]	Rejection power [kW_e]	Total auxiliaries consumption [kW_e]	Total plant net power [kW_e]
BASIC	0,2	353	0,17	121	15,7	136	1205
	0,3	350	8,24	83	15,7	98	1233
	0,4	350	11,32	64	15,7	80	1246
	0,5	348	14,41	53	15,7	69	1255
SIMPLE BLEEDING	0,2	320	0,12	110	13,6	123	1187
	0,3	317	10,29	75	13,6	89	1209
	0,4	316	18,38	58	13,6	72	1217
	0,5	314	21,92	48	13,6	61	1222
SIMPLE REHEAT	0,2	338	0,09	116	14,7	130	1197
	0,3	335	7,80	79	14,7	94	1224
	0,4	335	10,81	61	14,7	76	1238
	0,5	333	16,04	51	14,7	65	1242
REGENERATION + REHEAT	0,2	319	0,09	109	13,5	123	1187
	0,3	316	9,94	75	13,5	88	1209
	0,4	315	17,52	58	13,5	71	1217
	0,5	313	21,27	48	13,5	61	1222

	INDEPENDENT VARIABLES						DEPENDENT VARIABLES				FLOWRATES					
	X [-]	T_{carb} [°C]	$T_{CaO,in}$ [°C]	$T_{CO2,in}$ [°C]	TIT [°C]	CIT [°C]	COT [°C]	TOT [°C]	$T_{co2,mix}$ [°C]	Excess index [-]	$\dot{m}_{CaO}$ [kg/s]	$\dot{m}_{CO_2,stoic}$ [kg/s]	$\dot{m}_{CO_2,rec}$ [kg/s]	$\dot{m}_{CaO,unr}$ [kg/s]	$\dot{m}_{CaCO_3}$ [kg/s]	η_{carb} [%]
BASIC	0,2	875	368	177	650	114	127	294	291	1,016	5,59	0,88	0,014	4,47	2,00	33,91
	0,3	875	312	52	650	134	148	294	231	1,751	3,70	0,87	0,655	2,59	1,98	34,94
	0,4	875	310	38	650	47	58	294	160	2,314	2,77	0,87	1,145	1,66	1,98	35,48
	0,5	875	310	36	650	47	58	294	146	2,682	2,21	0,87	1,458	1,10	1,97	35,80
SIMPLE BLEEDING	0,2	875	368	175	650	213	228	294	293	1,010	5,08	0,80	0,008	4,07	1,82	36,75
	0,3	875	312	145	650	179	193	294	245	1,932	3,36	0,79	0,737	2,35	1,80	37,78
	0,4	875	312	170	650	179	193	294	231	2,668	2,51	0,79	1,315	1,51	1,79	38,27
	0,5	875	310	197	650	139	152	294	197	3,196	1,99	0,78	1,721	1,00	1,78	38,56
SIMPLE REHEAT	0,2	875	368	176	650	144	158	294	293	1,008	5,36	0,84	0,007	4,29	1,91	35,15
	0,3	875	311	35	650	148	162	294	239	1,717	3,55	0,84	0,599	2,48	1,90	36,19
	0,4	875	310	36	650	47	58	294	160	2,310	2,66	0,83	1,093	1,59	1,90	36,66
	0,5	875	310	52	650	90	102	294	173	2,723	2,11	0,83	1,430	1,06	1,89	37,00
REGENERATION + REHEAT	0,2	875	368	175	650	250	266	294	293	1,007	5,06	0,80	0,006	4,05	1,81	36,88
	0,3	875	310	132	650	183	197	294	248	1,895	3,34	0,79	0,706	2,34	1,79	37,91
	0,4	875	310	172	650	159	172	294	218	2,671	2,50	0,79	1,313	1,50	1,79	38,41
	0,5	875	310	192	650	132	145	294	192	3,178	1,99	0,78	1,700	0,99	1,77	38,70

- **Brayton-Joule cycle: SCO_2**

	X [-]	Storage turbine power [kW]	Compressor power [kW]	Conveying power [kW_e]	Rejection power [kW_e]	Total auxiliaries consumption [kW_e]	Total plant net power [kW_e]
SINGLE INTERCOOLING	0,2	258	1,5	88	8,3	97	1152
	0,3	255	14,7	60	8,6	69	1164
	0,4	254	20,6	47	8,8	55	1171
	0,5	252	24,6	38	8,9	47	1174
RECOMPRESSION	0,2	228	32,4	78	6,8	85	1105
	0,3	215	54,7	53	7,1	60	1095
	0,4	212	67,6	41	7,2	48	1092
	0,5	204	73,9	33	7,3	41	1085

	INDEPENDENT VARIABLES						DEPENDENT VARIABLES				FLOWRATES					
	X [-]	T_{carb} [°C]	$T_{CaO,in}$ [°C]	$T_{CO2,in}$ [°C]	TIT [°C]	CIT [°C]	COT [°C]	TOT [°C]	$T_{co2,mix}$ [°C]	Excess index [-]	$\dot{m}_{CaO}$ [kg/s]	$\dot{m}_{CO_2,stoic}$ [kg/s]	$\dot{m}_{CO_2,rec}$ [kg/s]	$\dot{m}_{CaO,unr}$ [kg/s]	$\dot{m}_{CaCO_3}$ [kg/s]	η_{carb} [%]
SINGLE INTERCOOLING	0,2	875	387	179	650	215	230	294	285	1,157	4,09	0,64	0,101	3,28	1,46	44,27
	0,3	875	446	241	650	125	138	294	192	2,886	2,70	0,64	1,198	1,89	1,44	45,29
	0,4	875	433	303	650	113	126	294	171	3,725	2,02	0,63	1,728	1,21	1,44	45,79
	0,5	875	493	291	650	114	127	294	166	4,269	1,60	0,63	2,057	0,80	1,43	46,12
RECOMPRESSION	0,2	875	516	504	650	401	419	293	386	3,731	3,62	0,57	1,554	2,90	1,29	47,99
	0,3	875	514	514	616	438	458	270	424	5,458	2,37	0,56	2,488	1,66	1,27	48,50
	0,4	875	506	521	612	468	488	267	453	6,308	1,77	0,56	2,950	1,06	1,26	48,71
	0,5	875	511	518	589	472	492	251	457	6,847	1,40	0,55	3,211	0,70	1,25	48,86

- **Indirect integration with heat exchange directly performed on the carbonator wall**

	X [-]	Storage turbine power [kW]	Compressor power [kW]	Conveying power [kW_e]	Rejection power [kW_e]	Total auxiliaries consumption [kW_e]	Total plant net power [kW_e]
SUPERCRITICAL BENZENE WITH VACUUM CONDENSATION	0,2	426	1,6E-03	146	32,7	179	1248
	0,3	423	2,7E-04	100	32,6	133	1290
	0,4	421	1,7E-03	77	32,5	110	1311
	0,5	420	2,8E-05	64	32,5	96	1324
SUPERCRITICAL CO_2 RECOMPRESSION	0,2	238	5,4E-05	81	13,8	95	1143
	0,3	236	2,1E-06	56	14,0	70	1166
	0,4	235	3,6E-04	43	14,0	57	1178
	0,5	234	2,2E-04	36	14,1	50	1185

	INDEPENDENT VARIABLES						DEPENDENT VARIABLES				FLOWRATES					
	X [-]	T_{carb} [°C]	$T_{CaO,in}$ [°C]	$T_{CO2,in}$ [°C]	TIT [°C]	CIT [°C]	COT [°C]	TOT [°C]	$T_{co2,mix}$ [°C]	Excess index [-]	$\dot{m}_{CaO}$ [kg/s]	$\dot{m}_{CO_2,stoic}$ [kg/s]	$\dot{m}_{CO_2,rec}$ [kg/s]	$\dot{m}_{CaO,unr}$ [kg/s]	$\dot{m}_{CaCO_3}$ [kg/s]	η_{carb} [%]
SUPERCRITICAL BENZENE WITH VACUUM CONDENSATION	0,2	675	638	524	650	326	343	294	294	1	6,76	1,06	8,7E-05	5,41	2,42	29,02%
	0,3	725	674	600	650	297	314	294	294	1	4,47	1,05	1,5E-05	3,13	2,40	30,26%
	0,4	700	654	520	650	315	332	294	294	1	3,34	1,05	9,3E-05	2,00	2,39	30,88%
	0,5	700	627	560	650	249	265	294	294	1	2,67	1,05	1,7E-06	1,33	2,38	31,25%
SUPERCRITICAL CO_2 RECOMPRESSION	0,2	775	753	585	650	335	352	294	294	1	3,77	0,593	2,9E-06	3,02	1,35	47,66%
	0,3	800	773	620	650	331	348	294	294	1	2,49	0,588	1,1E-07	1,75	1,34	49,05%
	0,4	825	773	708	650	346	364	294	294	1	1,86	0,585	1,9E-05	1,12	1,33	49,74%
	0,5	850	794	731	650	323	340	294	294	1	1,49	0,584	1,2E-05	0,74	1,33	50,16%

1.7. APPENDIX II: PINCH ANALYSIS

Direct integration

T_{carb} = 775°C

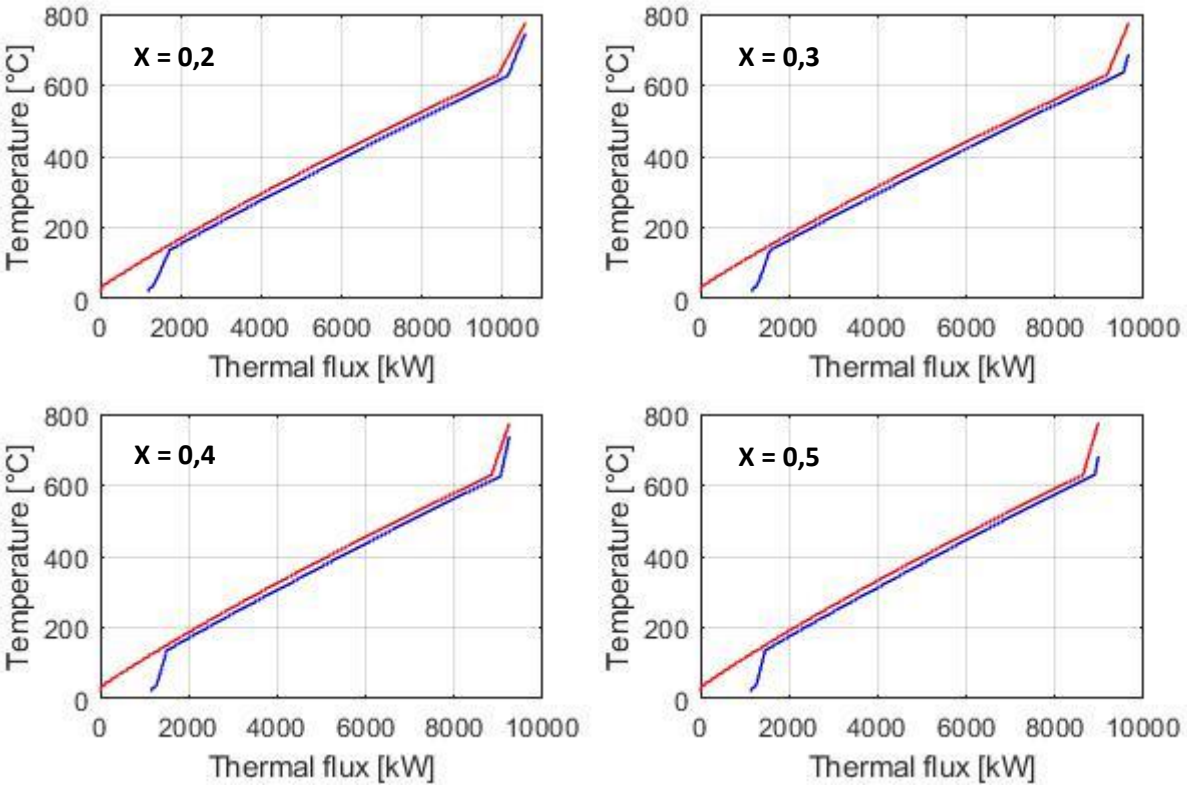

T_{carb} = 825°C

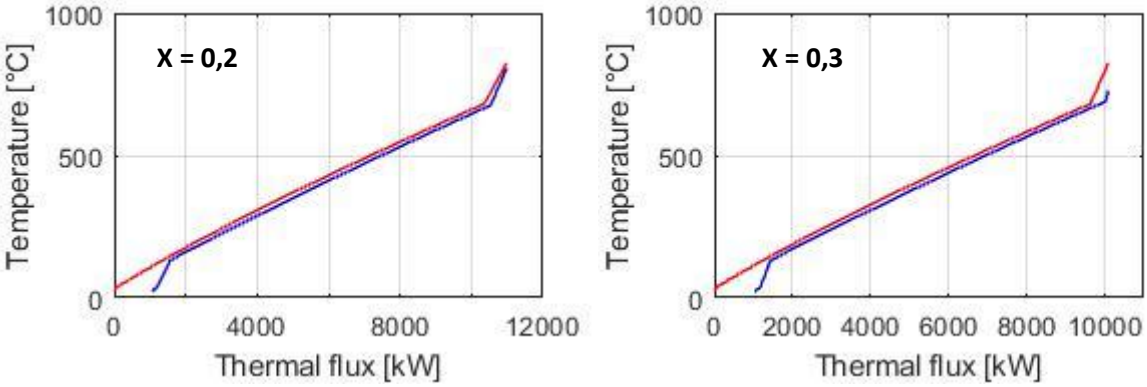

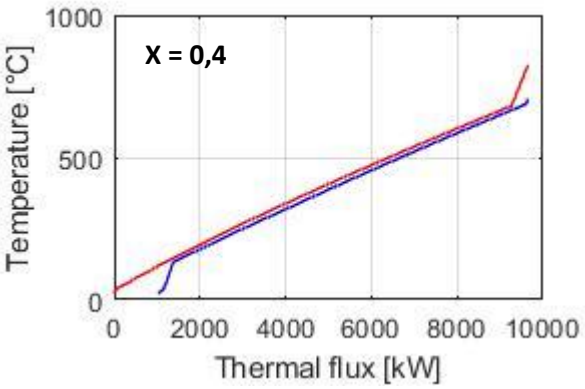

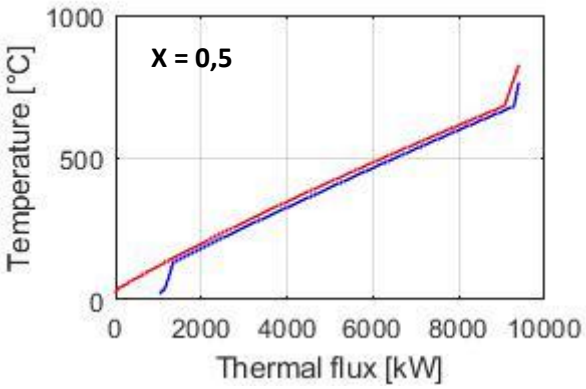

T_{carb} = 875°C

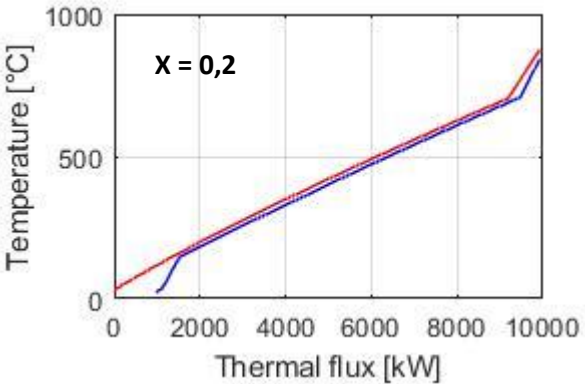

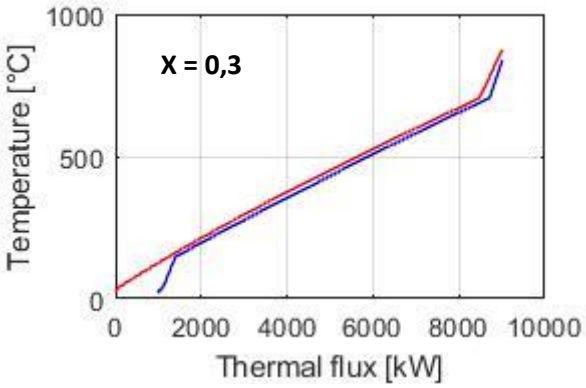

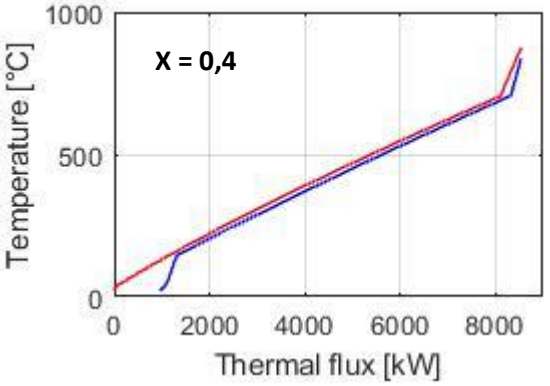

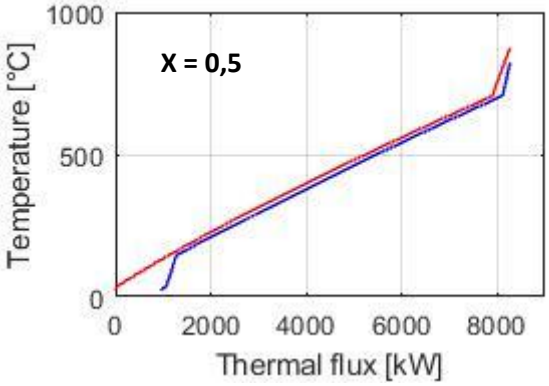

<u>Indirect integration</u>

- **ORC – Subcritical cycles with counterpressure condensation**

Benzene

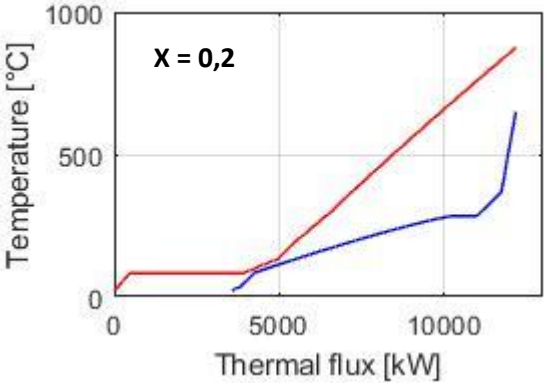

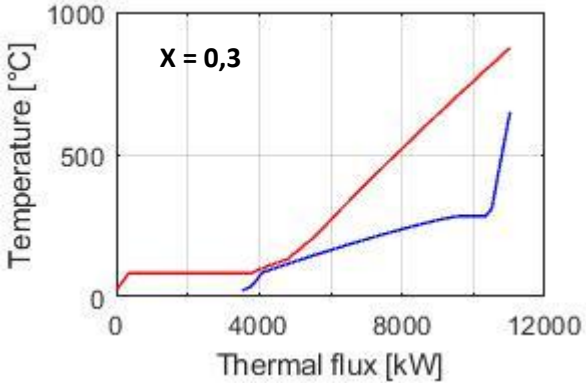

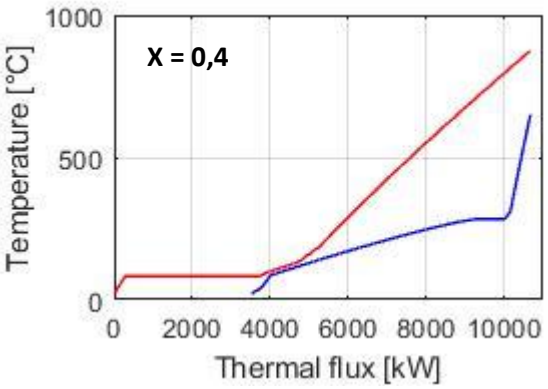

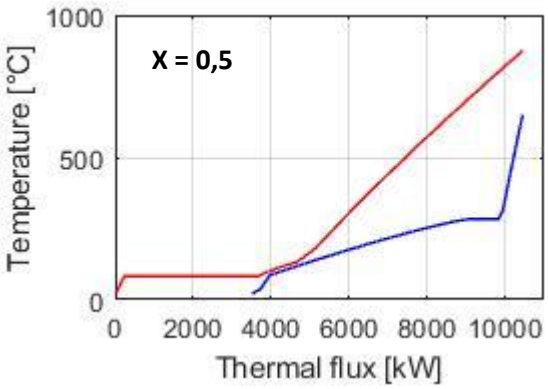

Cyclohexane

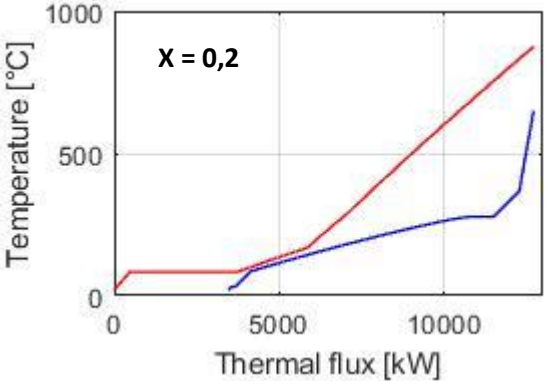

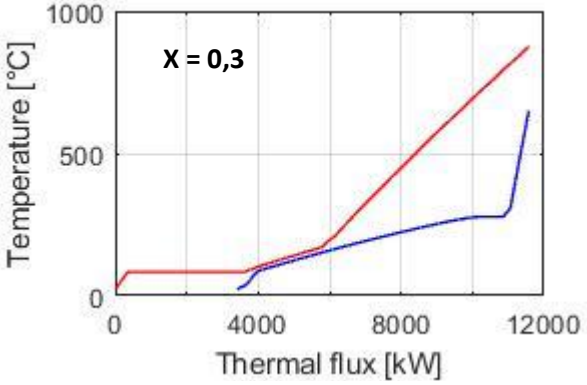

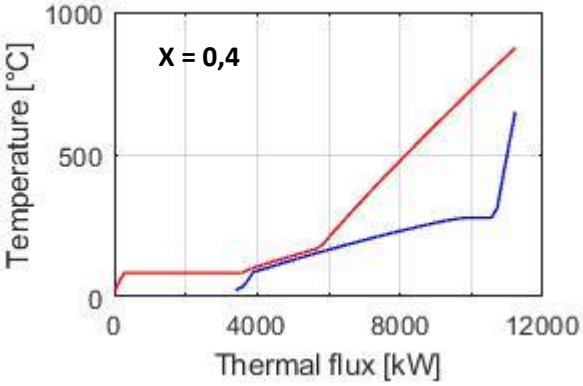

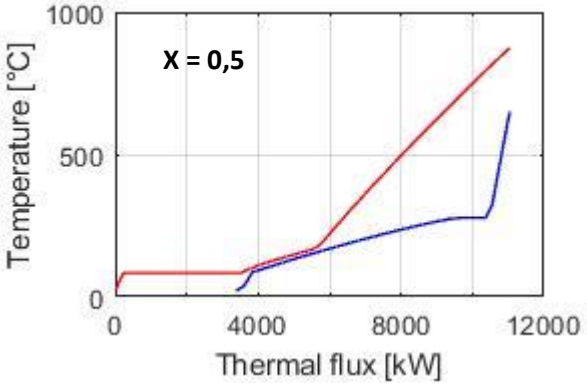

Cyclopenthane

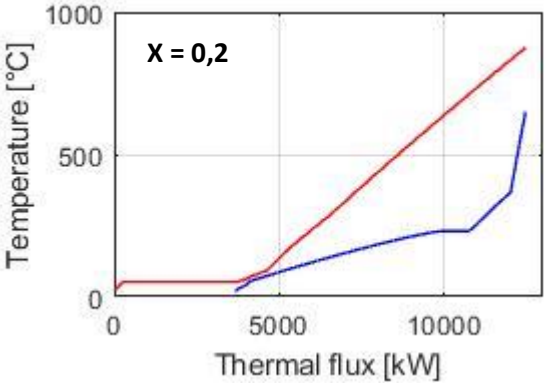

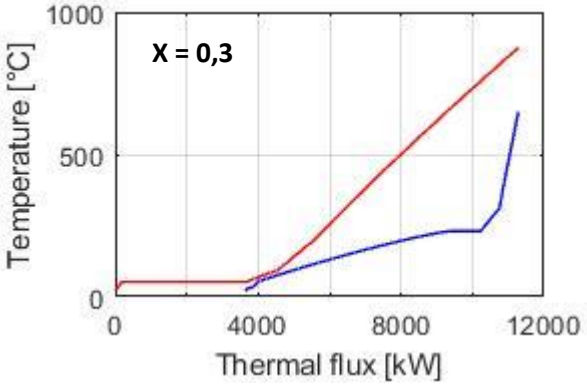

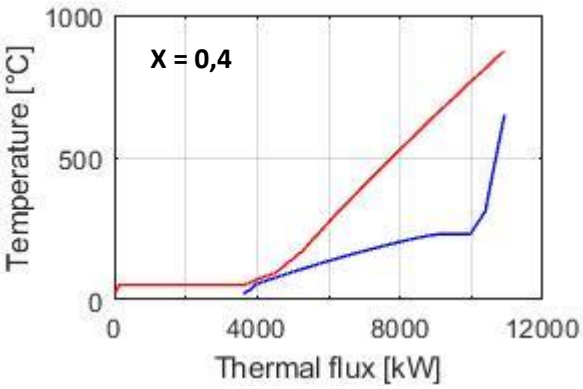

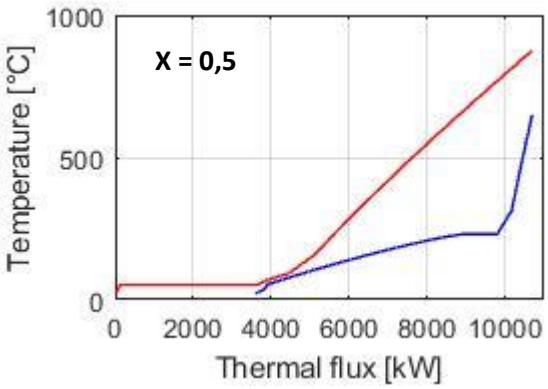

Ethanol

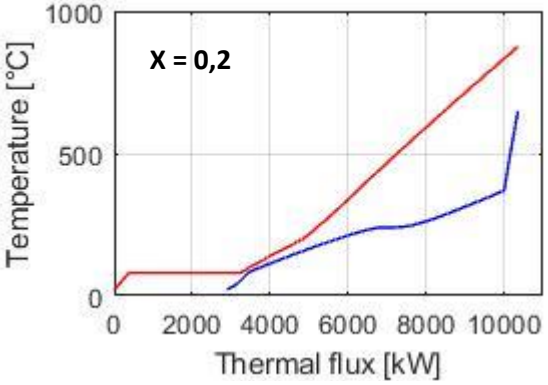

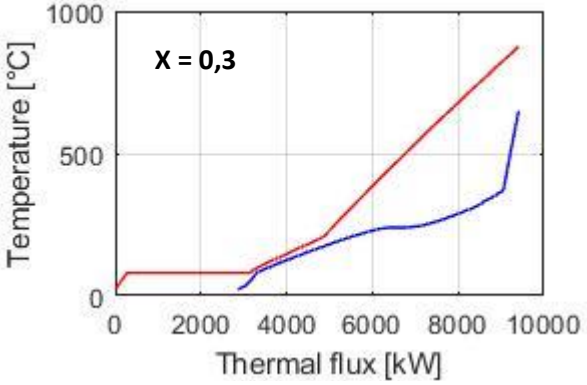

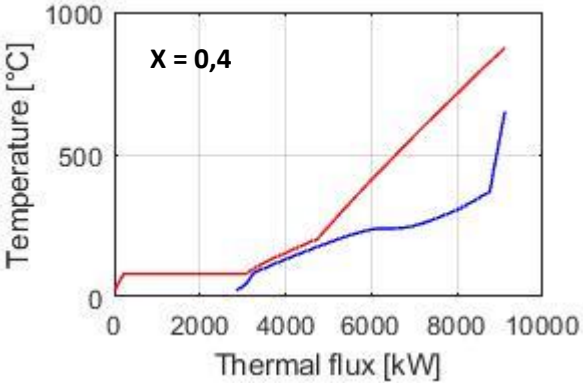

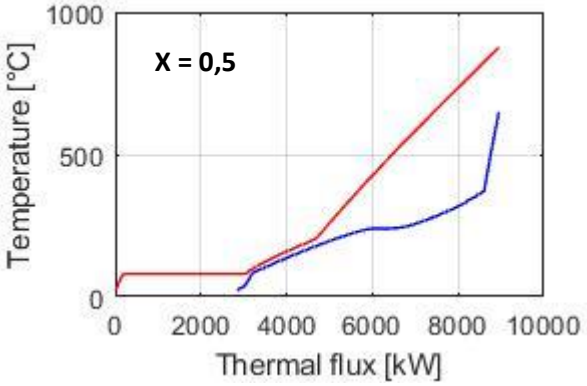

Toluene

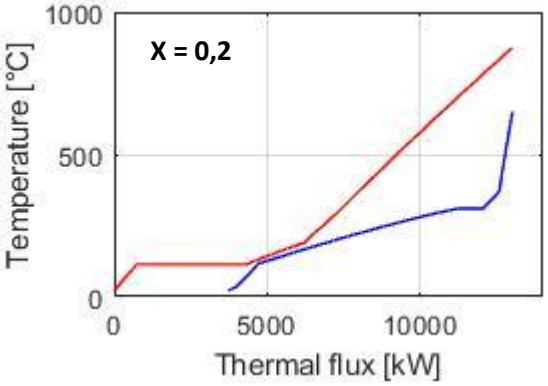

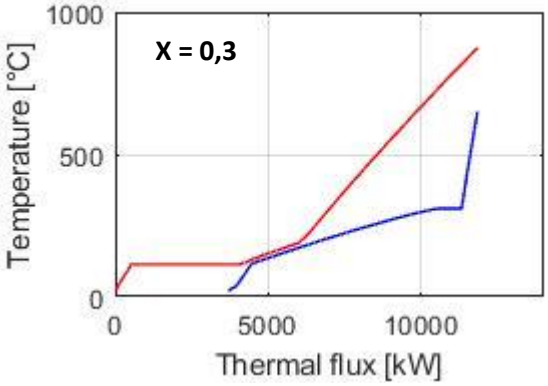

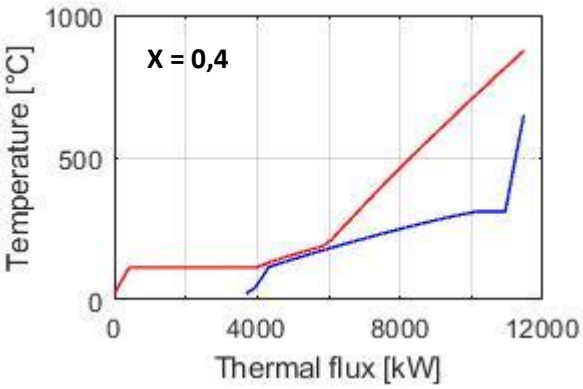

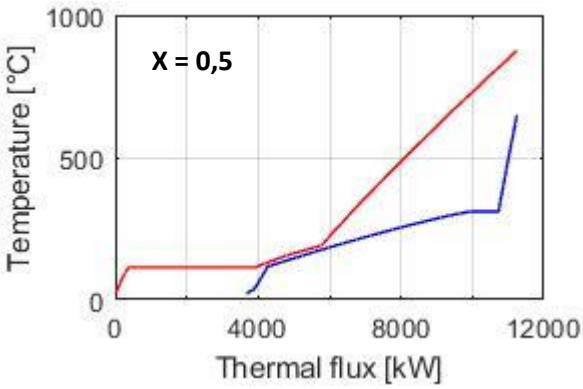

- **ORC – Subcritical cycles with vacuum condensation**

Benzene

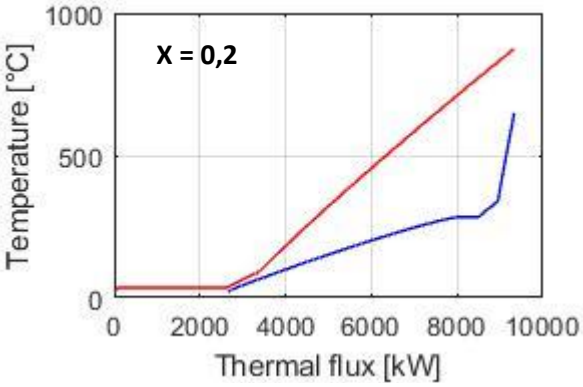

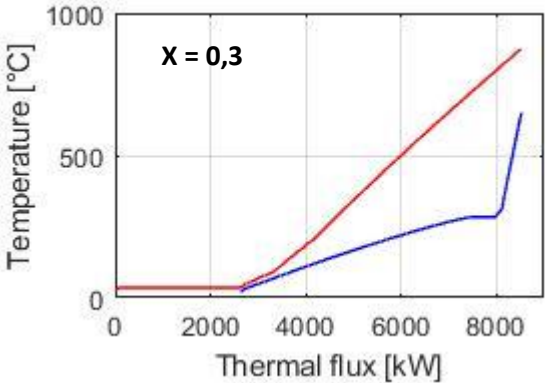

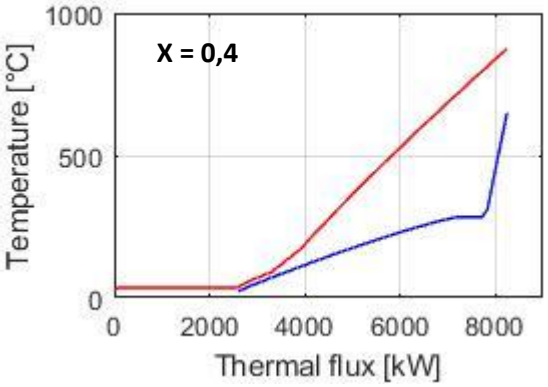

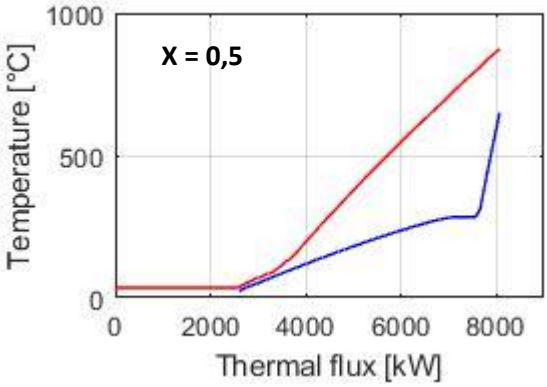

Cyclohexane

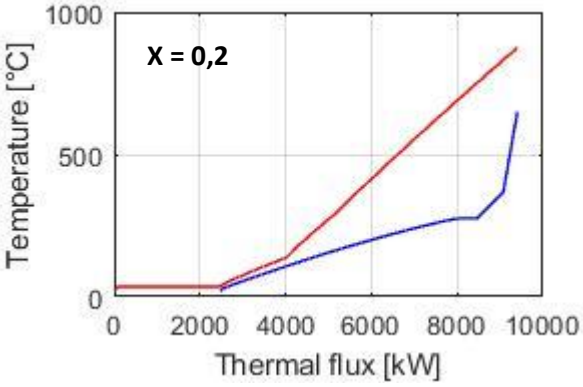

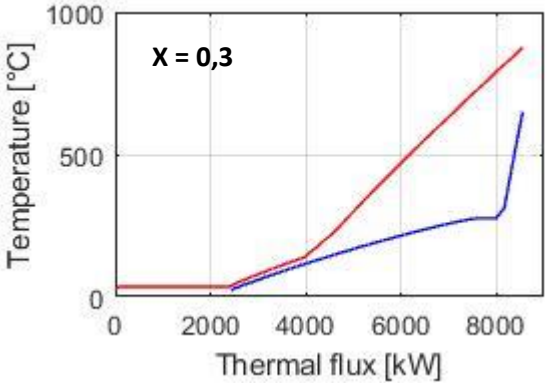

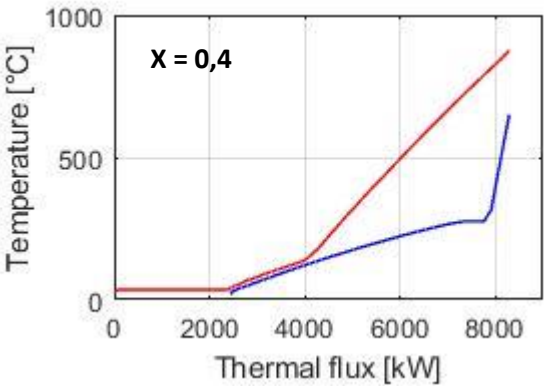

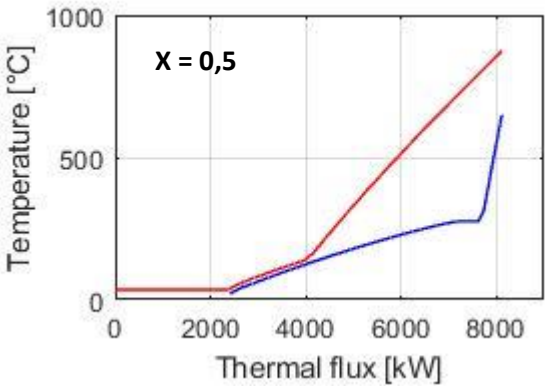

Cyclopentane

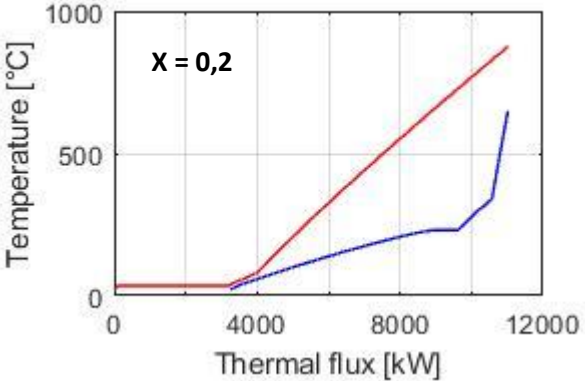

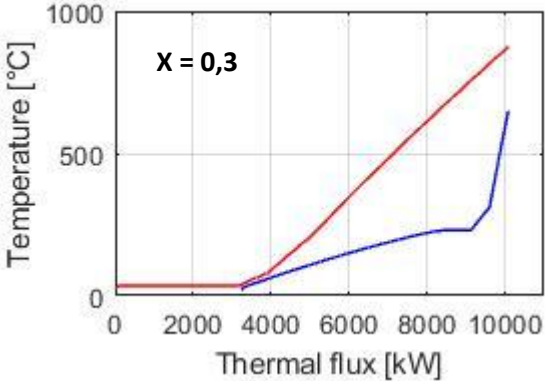

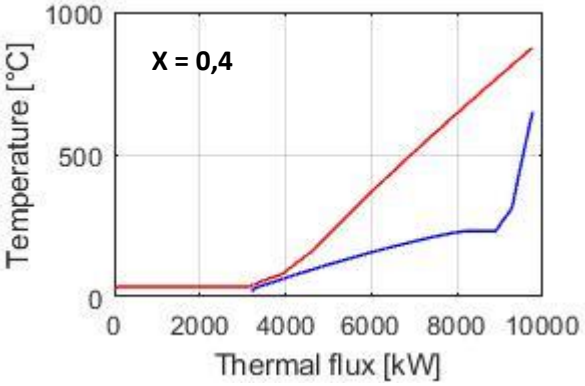

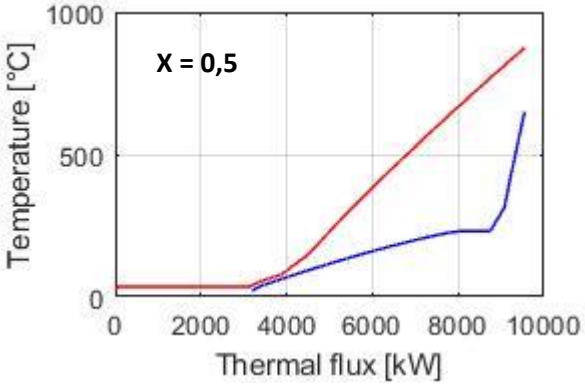

Ethanol

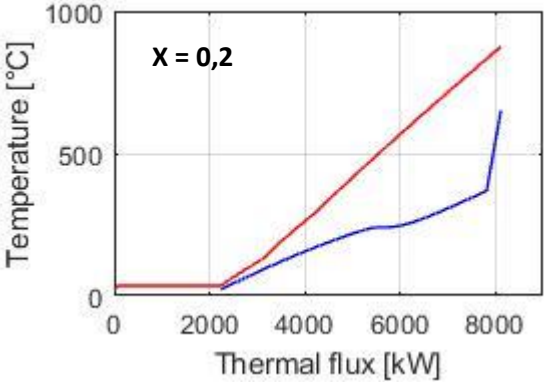

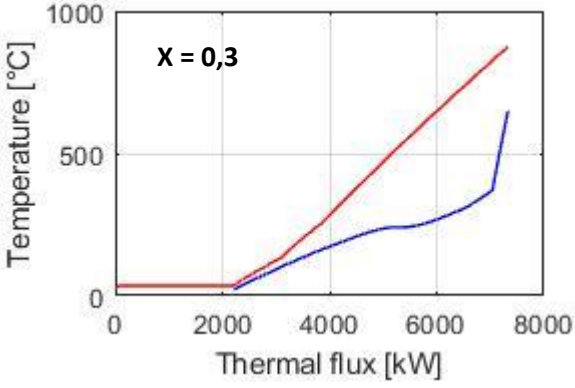

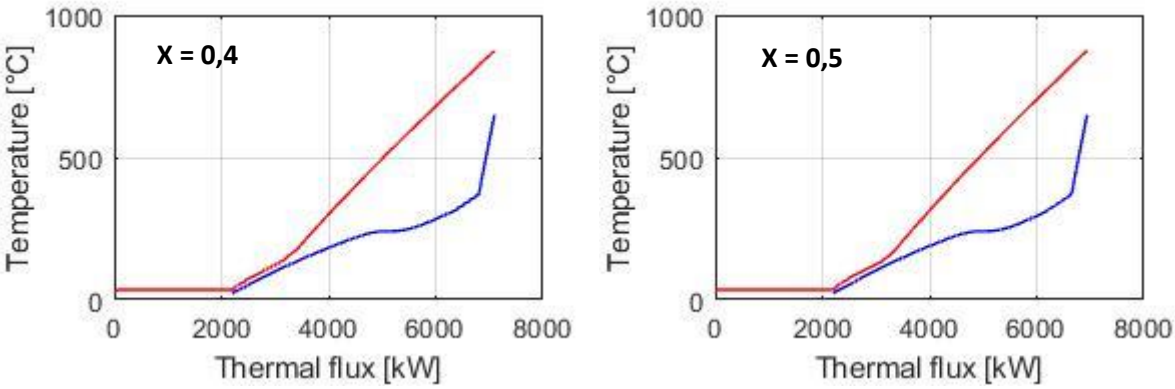

Toluene

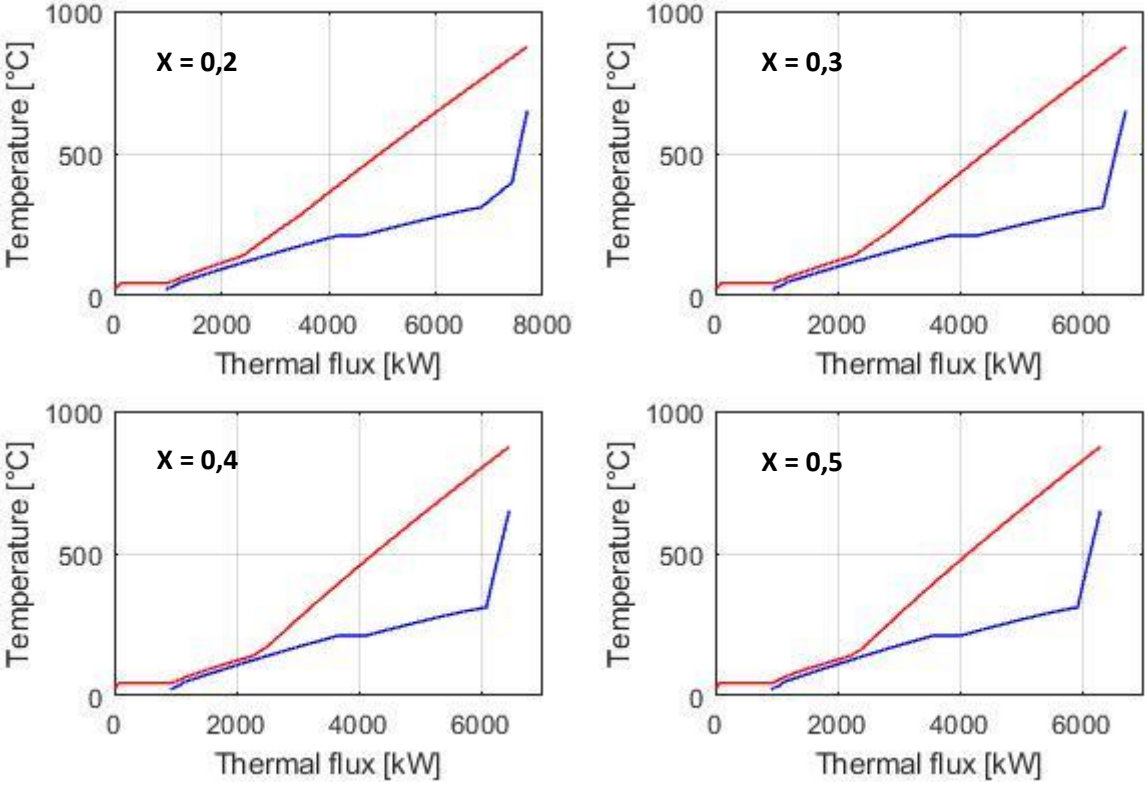

- **ORC – Supercritical cycles with counterpressure condensation**

Benzene

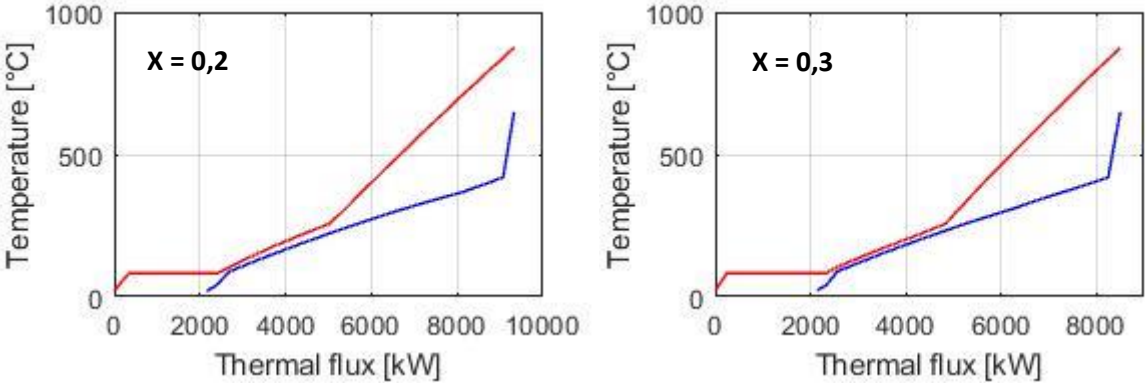

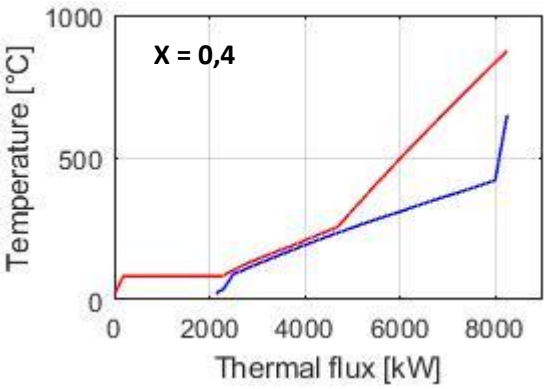

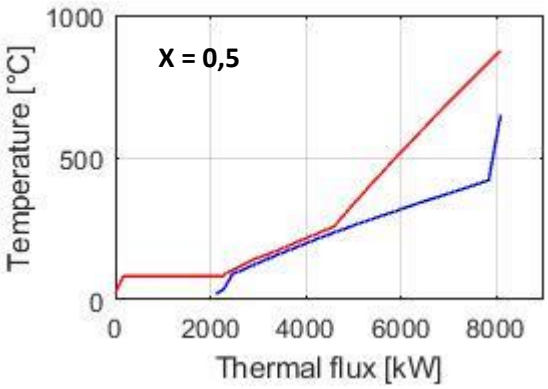

Cyclohexane

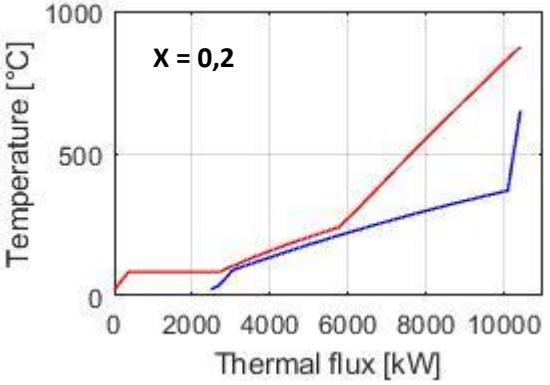

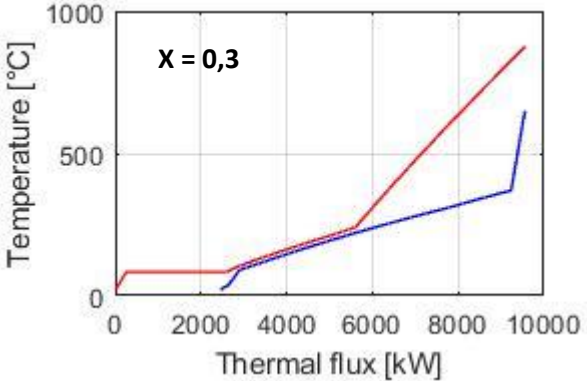

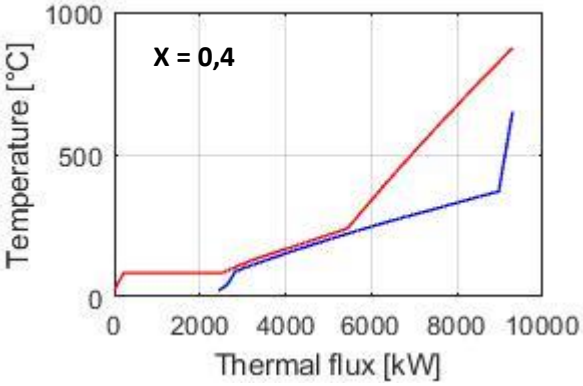

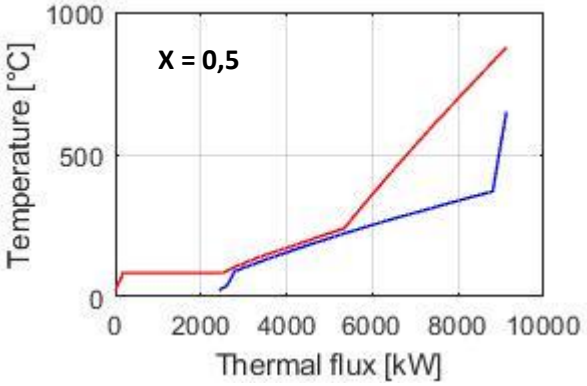

Cyclopentane

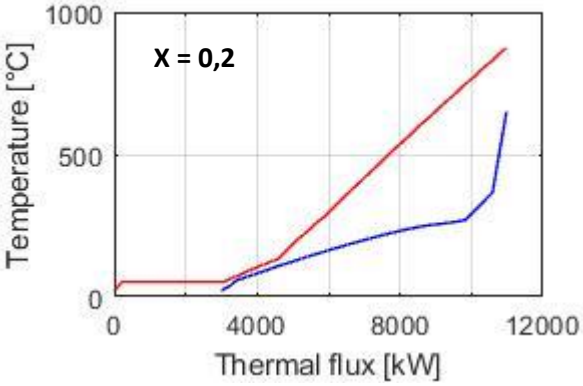

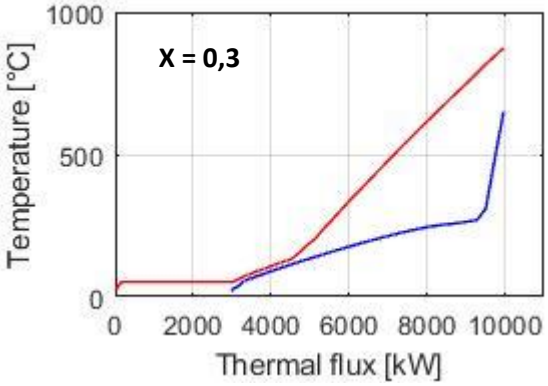

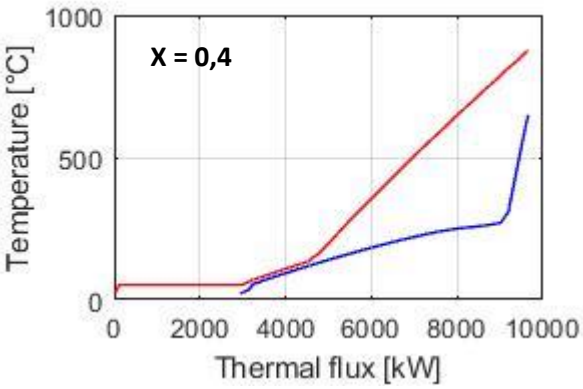

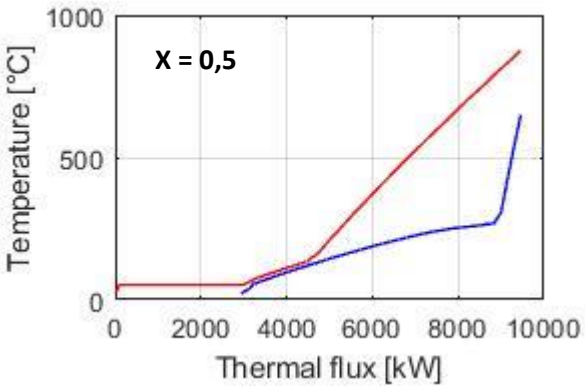

Ethanol

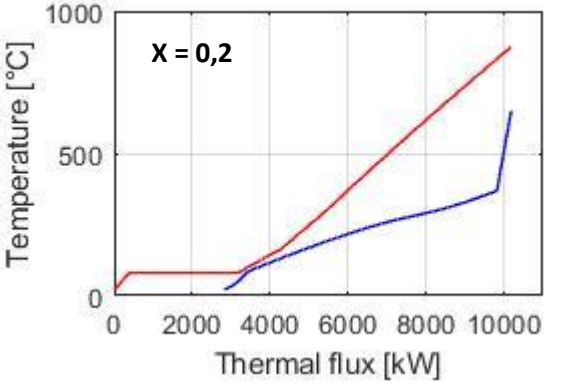

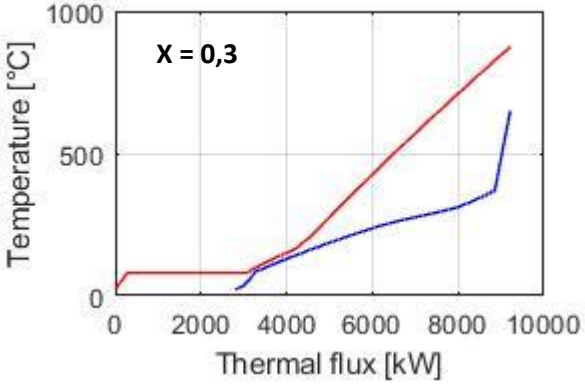

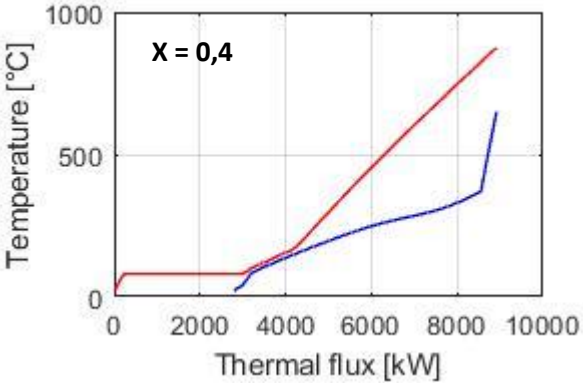

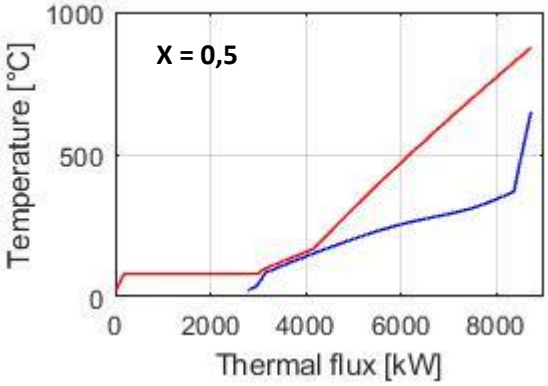

Toluene

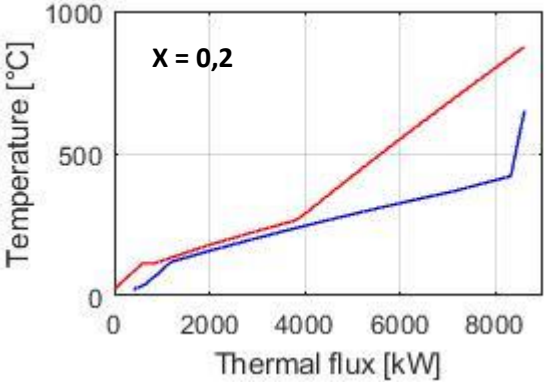

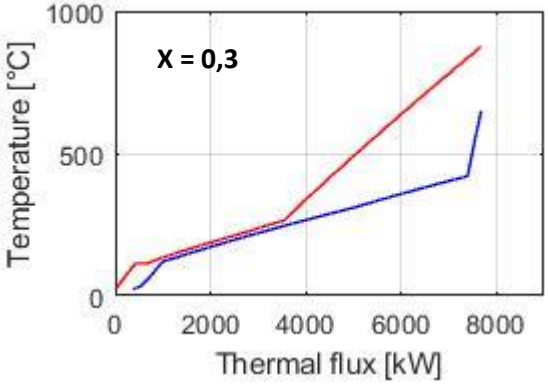

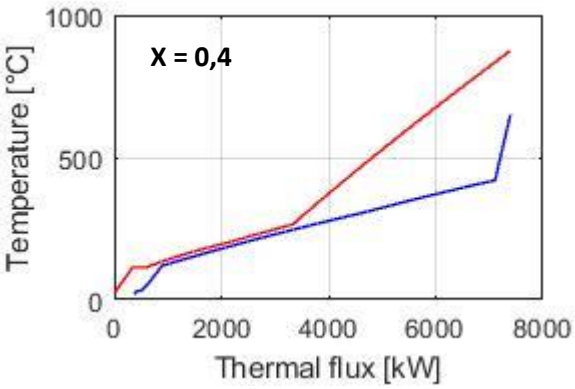

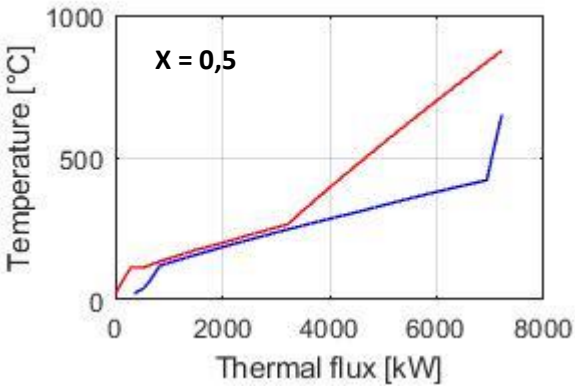

- **ORC – Supercritical cycles with vacuum condensation**

Benzene

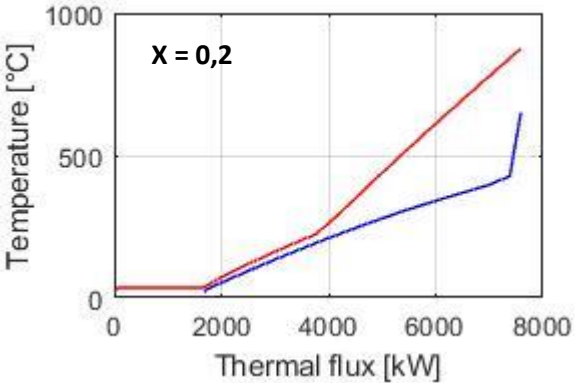

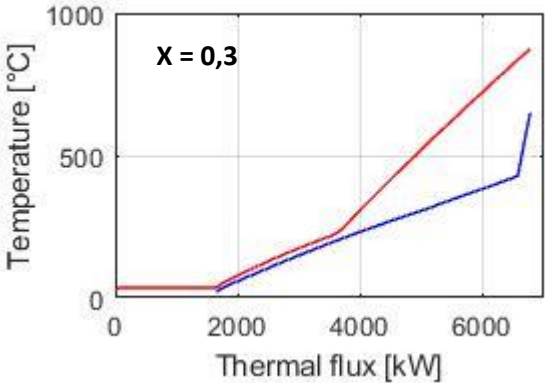

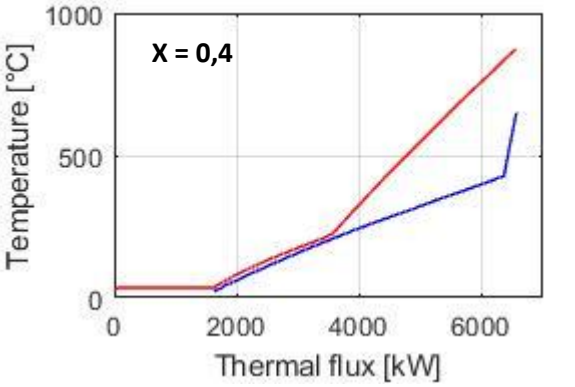

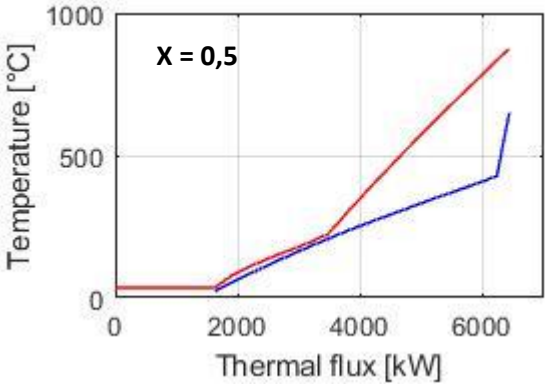

Cyclohexane

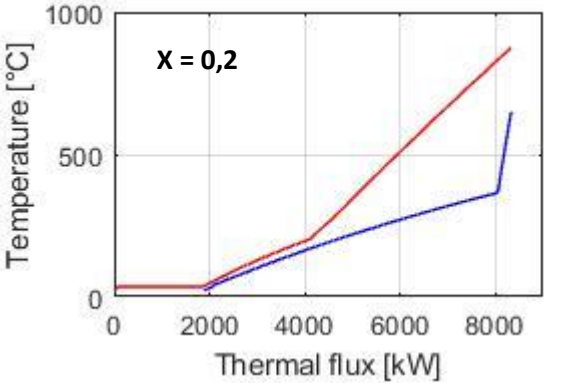

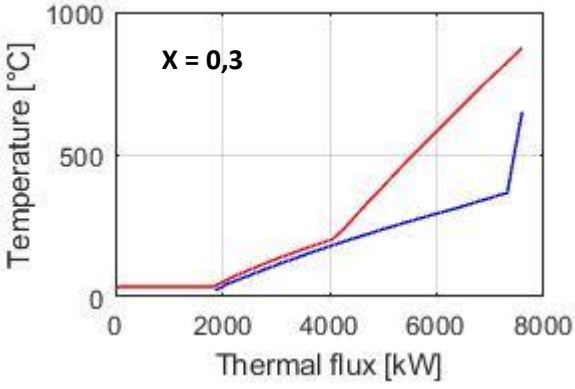

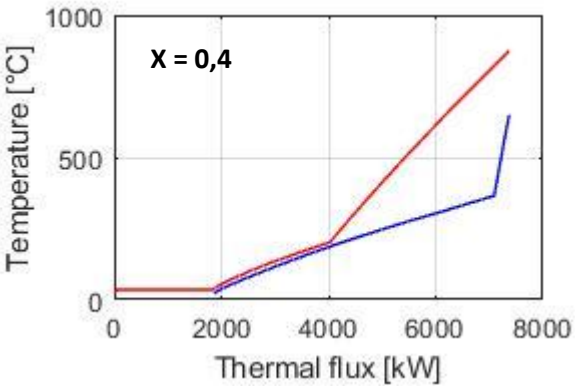

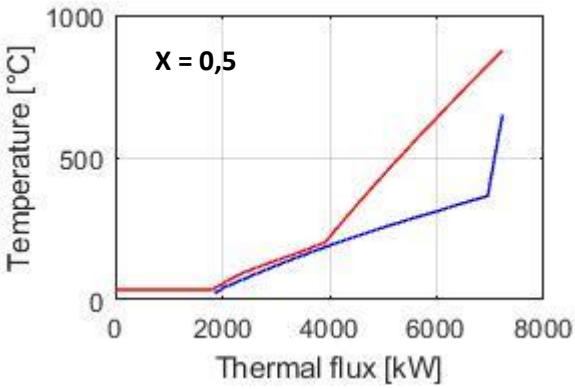

Cyclopentane

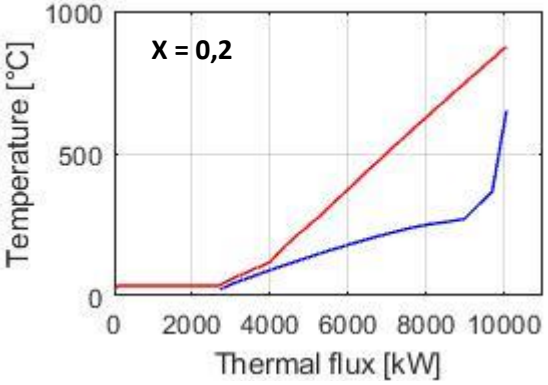

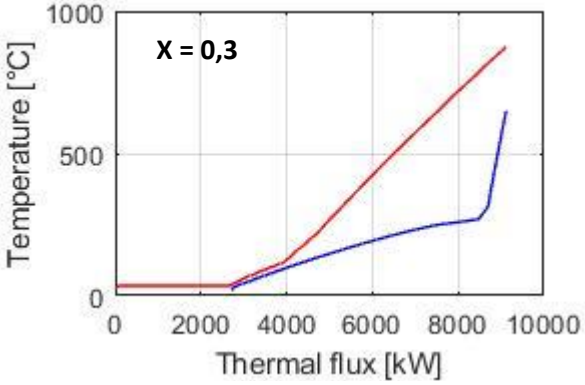

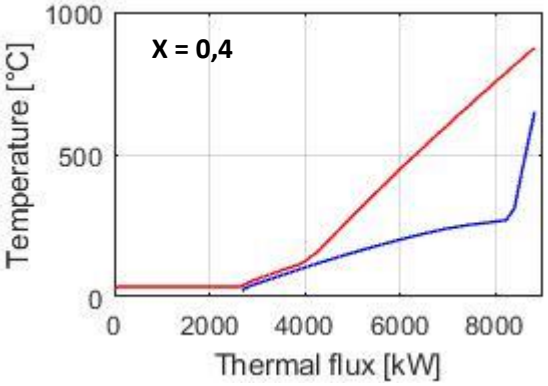

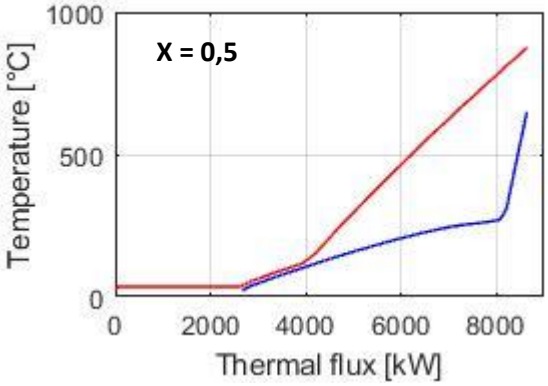

Ethanol

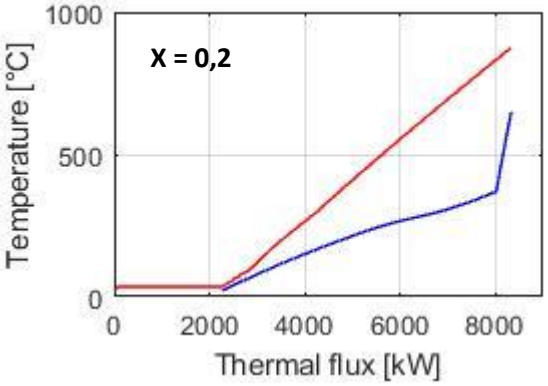

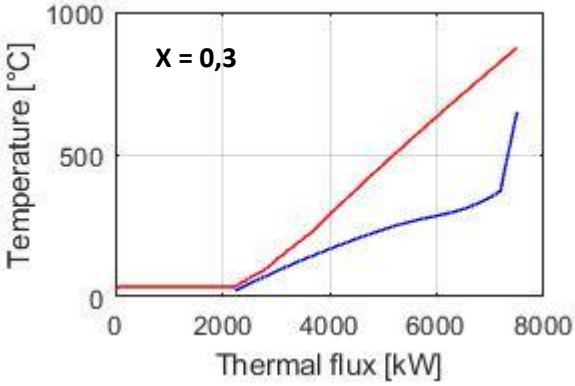

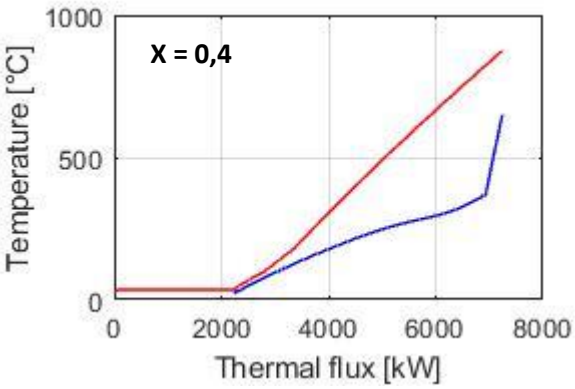

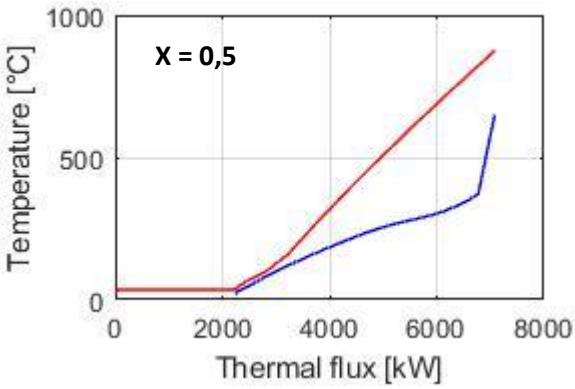

Toluene

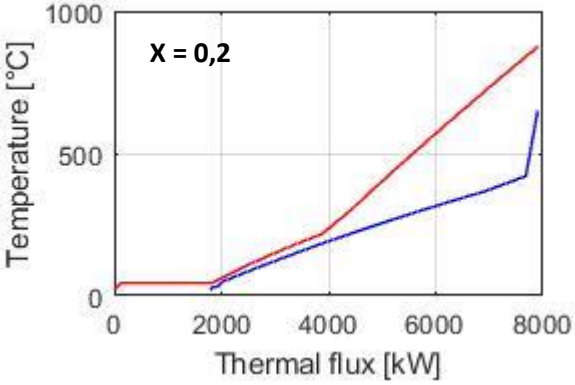

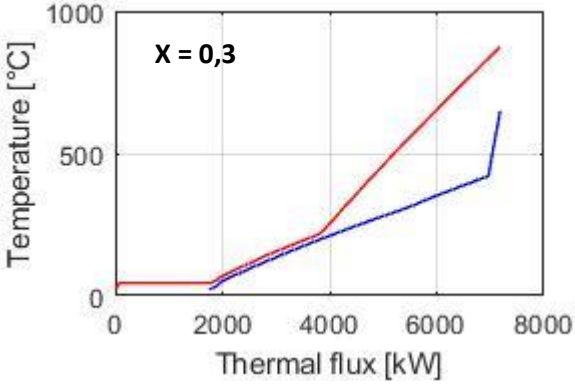

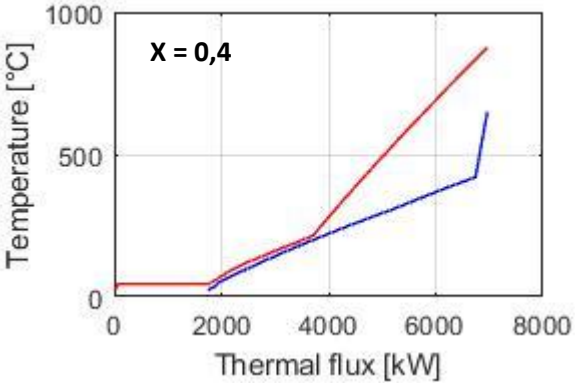

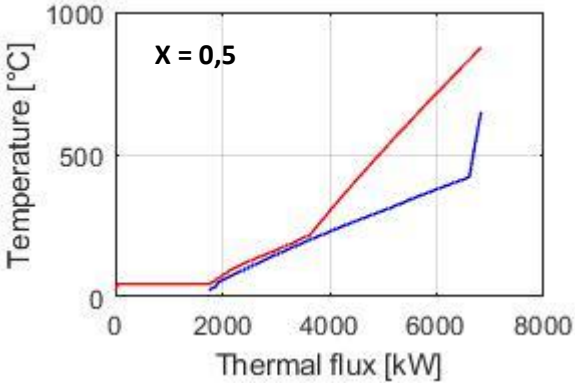

- **Steam Rankine cycles**

Basic layout

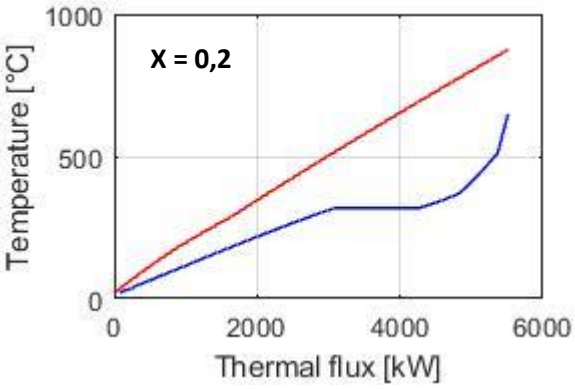

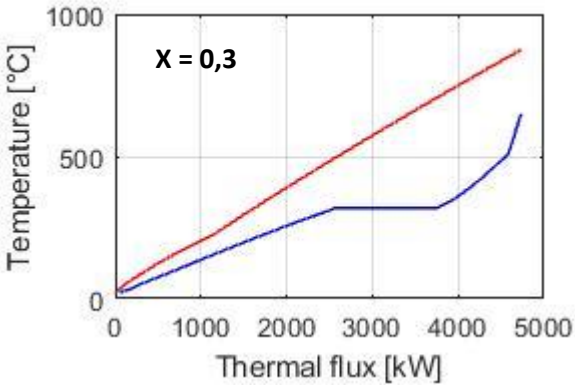

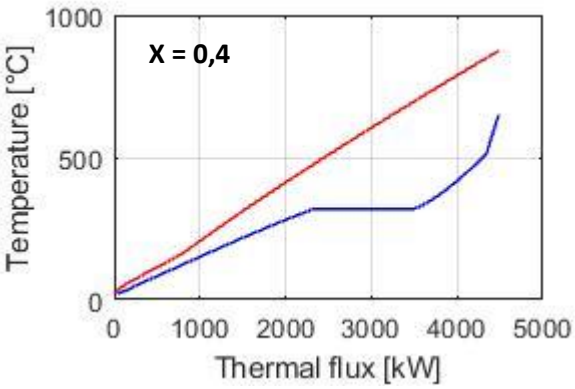

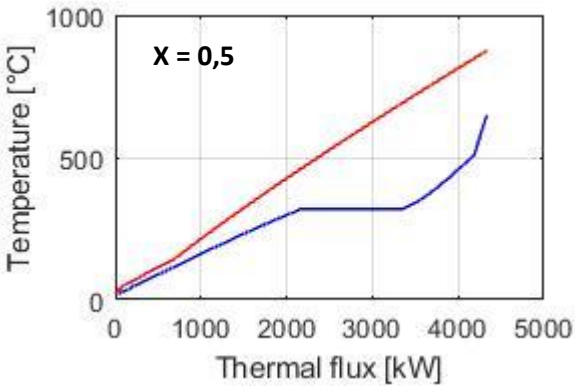

Single bleeding layout

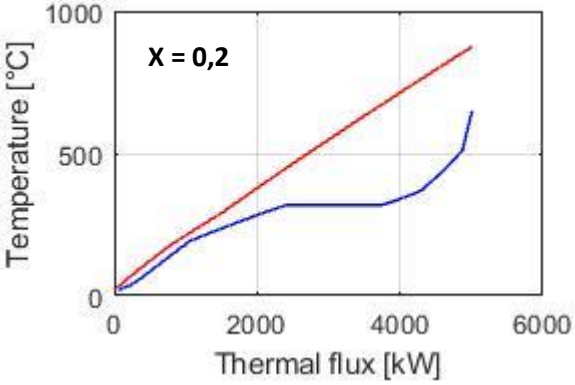

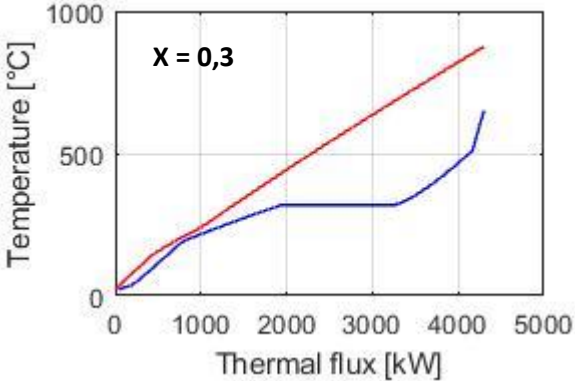

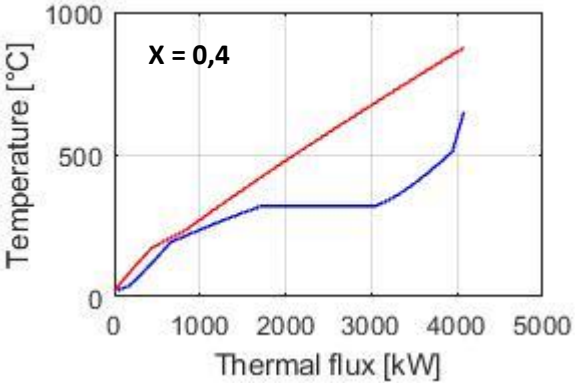

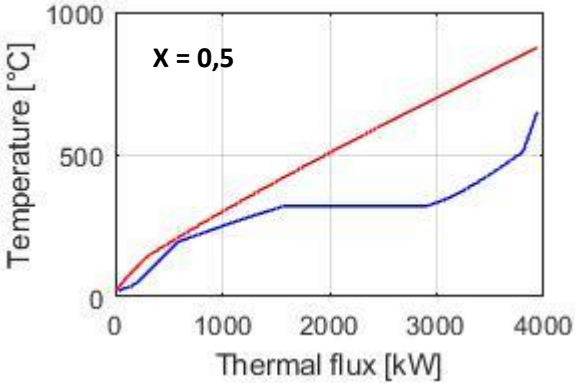

Single reheating layout

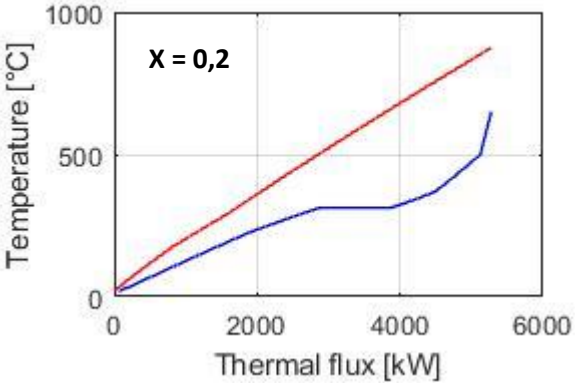

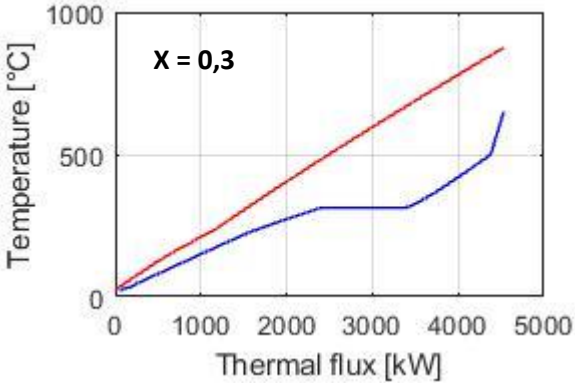

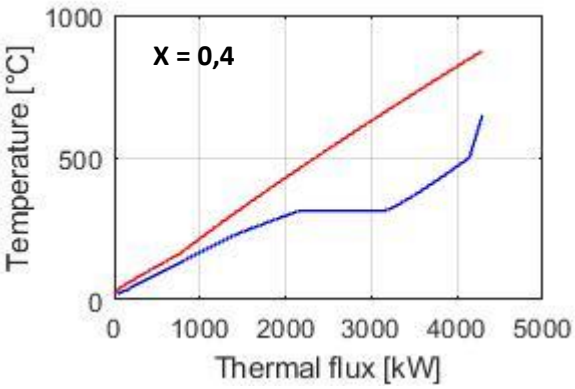

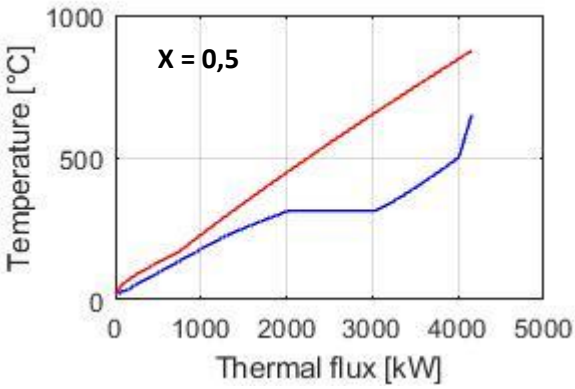

Regeneration + reheating layout

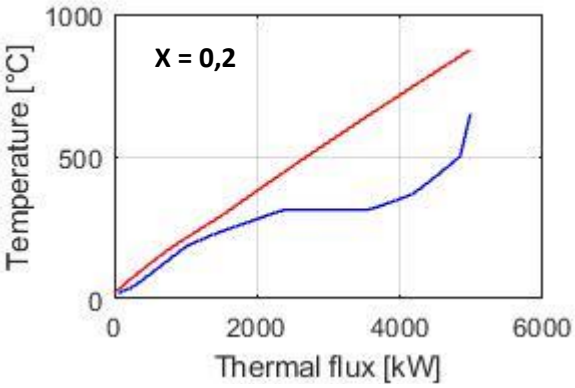

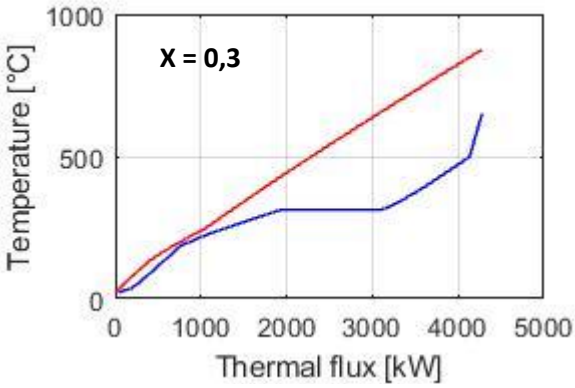

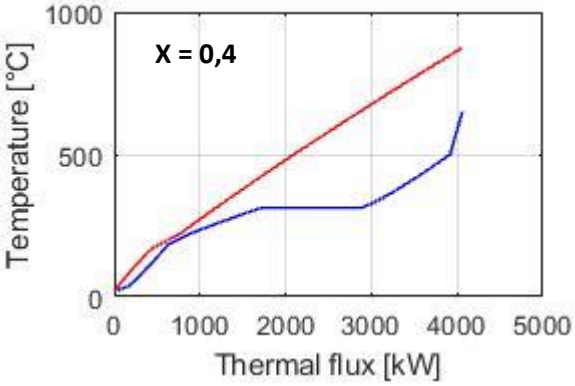

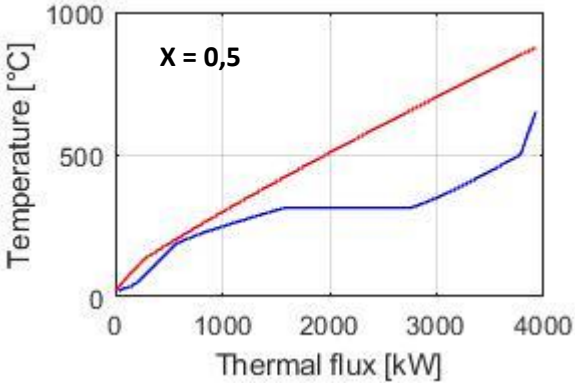

- **Brayton-Joule cycles – SCO_2**

Single inter-cooling layout

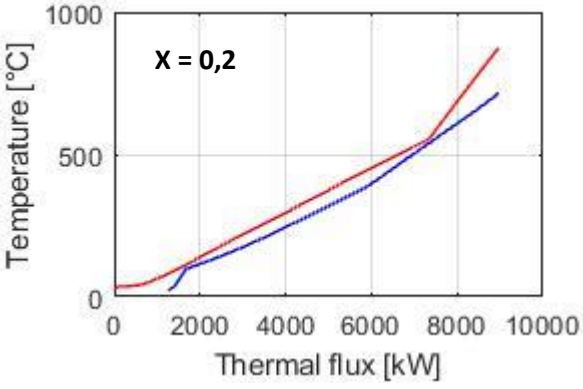

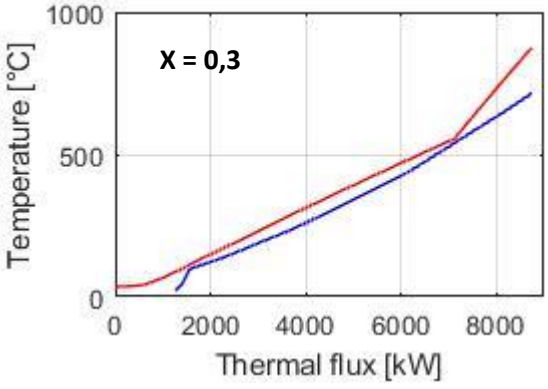

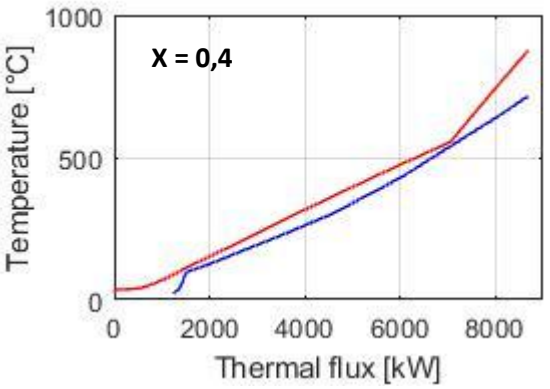

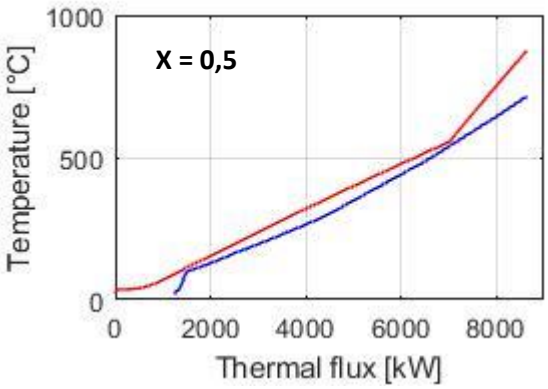

Recompression layout

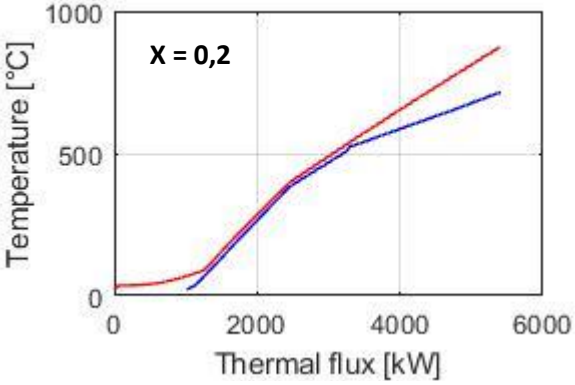

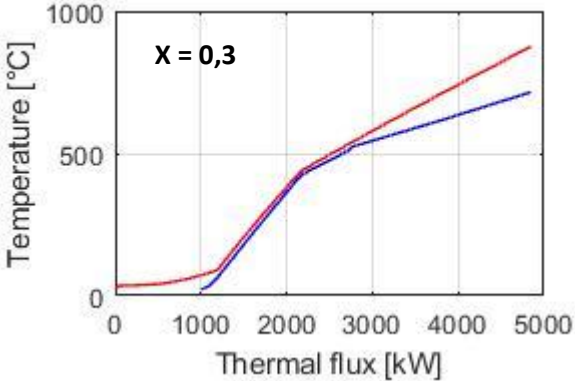

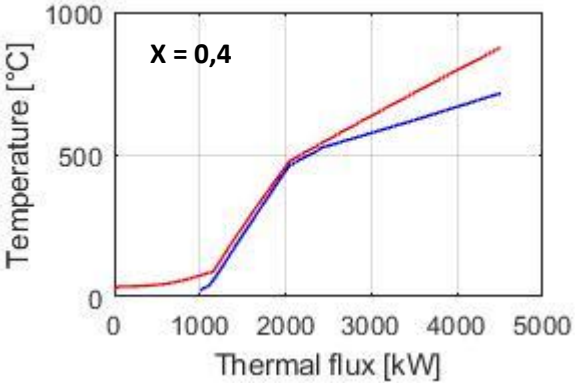

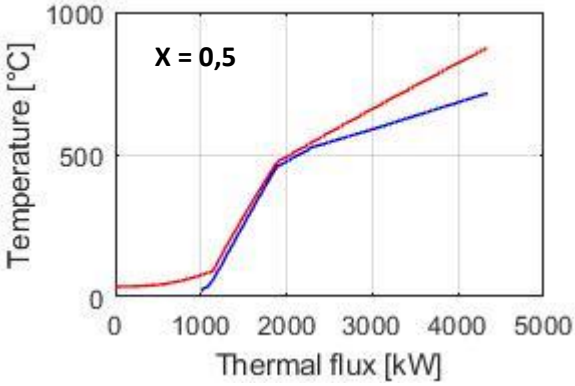

1.8. REFERECES

[1] S. E. B. Edwards and V. Materic, "Calcium looping in solar power generation plants," *Solar Energy,* vol. 86, no. 9, pp. 2494-2503, Sept. 2012.

[2] M. Benitez-Guerrero, J. Valverde, P. E. Sanchez-Jimenez, A. Perejon and L. Perez-Maqueda, "Multicycle activity of natural CaCO3 minerals for thermochemical energy storage in Concentrated Solar Power plants," *Solar Energy,* vol. 153, pp. 188-199, Sept 2017.

[3] C. Ortiz, M. Romano, J. Valverde, M. Binotti and R. Chacartegui, "Process integration of Calcium-Looping thermochemical energy storage system in concentrating solar power plants," *Energy,* pp. 535-551, 15 July 2018.

[4] A. Alovisio, R. Chacartegui, C. Ortiz, J. Valverde and V. Verda, "Optimizing the CSP-Calcium Looping integration for Thermochemical Energy Storage," *Energy Conversion and Management,* vol. 136, pp. 85-98, Mar. 2017.

[5] C. Ortiz, R. Chacartegui, J. Valverde, A. Alovisio and J. Becerra, "Power cycles integration in concentrated solar power plants with energy," *Energy Conversion and Management,* pp. 815-829, Oct. 2017.

[6] A. Alovisio, *Process integration of a thermochemical energy storage system based on Calcium Looping incorporating air/CO2 cycles in CSP power plants,* 2015.

[7] J. Facao and A. Oliveira, "Analysis of Energetic, Design and Operational Criteria When Choosing an Adequate Working Fluid for Small ORC Systems," *ASME 2009 International Mechanical Engineering Congress and Exposition,* vol. 6, pp. 175-180, Nov. 2009.

[8] S. Energy, "Siemens Organic Rankine Cycle Waste Heat Recovery with ORC," Mar. 2014.

[9] J. Bonafin, M. Del Carria, M. Gaia and M. Duvia, "Turboden Geothermal References in Bavaria: Technology, Drivers and Operation," *Proceedings World Geothermal Congress ,* Apr. 2015.

[10] M. Astolfi, S. Lasala and E. Macchi, "Selection Maps For ORC And CO2 Systems For Low-Medium," *IV International Seminar on ORC Power Systems,* 2017.

[11] J. Milewski and J. Krasucki, "Comparison of ORC and Kalina cycles for waste heat recovery in the steel industry," *Journal of Power of Technologies,* vol. 97, no. 4, pp. 302--307, 2017.

[12] Siemens Energy, “Pre-designed Steam Turbines,” 2012.

[13] J. Moore, S. Cich, M. Day, T. Allison, J. Wade and D. Hofer, "Commissioning of a 1 MWe Supercritical CO2 Test Loop," *The 6th International Supercritical CO2 Power Cycles Symposium,* Mar. 2018.

[14] J. D. Osorio, R. Hovsapian and J. C. Ordonez, “Dynamic analysis of concentrated solar supercritical CO2-based power,” *Applied Thermal Engineering,* vol. 93, p. 920–934, Jan. 2016.

2. DEVELOPMENT OF A MULTILEVEL MODEL FOR THE OPTIMIZATION OF BRAYTON-JOULE CYCLES BASED ON SUPERCRITICAL CO_2

2.1. INTRODUCTION

Modelling of multi-component systems is mandatory in order to estimate performances of most of the technical devices. This can be achieved by means of zero-dimensional approaches for all the components, as usually done for power cycles, heat pumps and refrigeration machines. In some other cases, more complex models (such as 1D, 2D or 3D) can be required in order to increase level of detail of the investigation. In other cases, a different level of detail can be required for the various components. This can due to the higher gradient of the thermodynamic quantities or to the different complexity of the phenomena involved in the components. In this last case, a multi-level approach is a solution that can provide various benefits. Multi-level approach consists in combining models with different level of details (0D, 1D, 2D or 3D model), for the various component. Concerning the advantages provided by the multi-level approach, the first consists in better catching the behavior the components that require it, by using a model with a higher level of accuracy. The second is that no useless computational resources are allocated in order to compute with a higher level of accuracy the parts of the systems that do not require a detailed analysis. This makes the computational costs acceptable without losing important information. In this framework, the integration of the CaL process and the power cycle can be done by means of a multi-level approach. This consists in using 1D, 2D or 3D model for the carbonator and integrating it in the zero-dimensional model of the power cycle components. This is done by simulating in detail the reactor (as shown in the figures 20) and evaluating the heat exchanged with the power cycle. This allows a more complete investigation of the carbonator side to achieve detailed results. Results of the carbonator simulation are integrated with zero dimensional models of the other power cycle components.

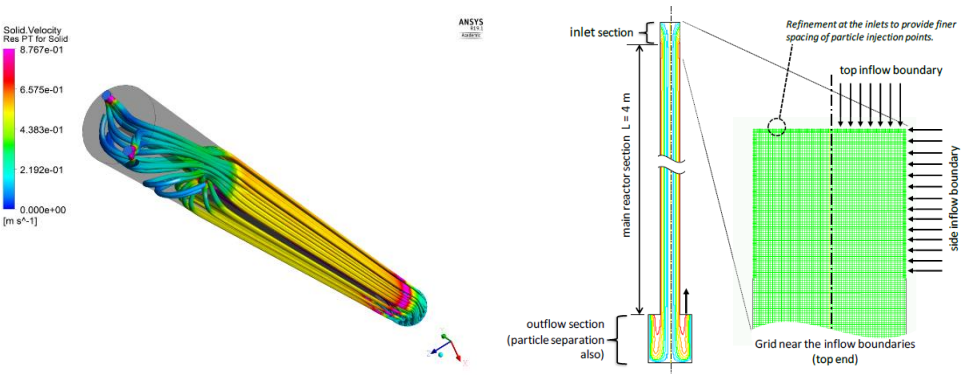

Figure 20 - Carbonator models developed at SOCRATCES (3D and 2D)

The aim of this work is to develop an algorithm able to quickly determine the optimal operating conditions for various types of CO_2 supercritical Brayton cycles, integrating in a 0-D simulation the 1-D and 2-D results obtained in the previous deliverables of the SOCRATCES project (D.2.2 and D.2.3). The condition of brief computational time is requested in order to make a possible implementation of the script in a control and regulation logic inside the power plant itself. Therefore, a compact model has been built for each system configuration that can be used to investigate the system performances varying the design variables.

In the present section, an optimization of various types of supercritical CO2 Brayton cycles is proposed for CSP applications though the CaL process. The analysis has been conducted step-by-step:

a. At first an analysis of the heat exchange in the regenerator is performed because of the variable specific heat of the carbon dioxide in the supercritical region.
b. Secondly, a parametric analysis is performed in order to show which is the effect of a change of each parameter on the cycle performance; this allows obtaining which are the independent variables of an optimization process.
c. An optimization is performed for each cycle. This allows evaluating the best performances for each considered scheme.
d. An economic discussion is performed with the aim of analyzing which is the impact in term of cost of each optimized configuration.
e. For last is executed an estimation of the product between the heat transfer coefficient and the surface (UA [kW/K]) and an estimation of the surface area requested for the heat exchange in correspondence of the carbonator wall.

The study has been performed within the framework of the European project Socratces; the description of the system is performed in section 2.2.

2.2. CASE STUDY

As concern the power cycle selection, various s-CO2 cycles have been considered for the analysis:

a. Classic Brayton supercritical cycle (Base)
b. Bryton cycle with recirculation (Rec)
c. Bryton cycle with recirculation and re-heating (Rec-RH)
d. Bryton cycle with recirculation, re-heating and intercooling (Rec-RH-Int)

The cycles have been schematized in Fig. 21.

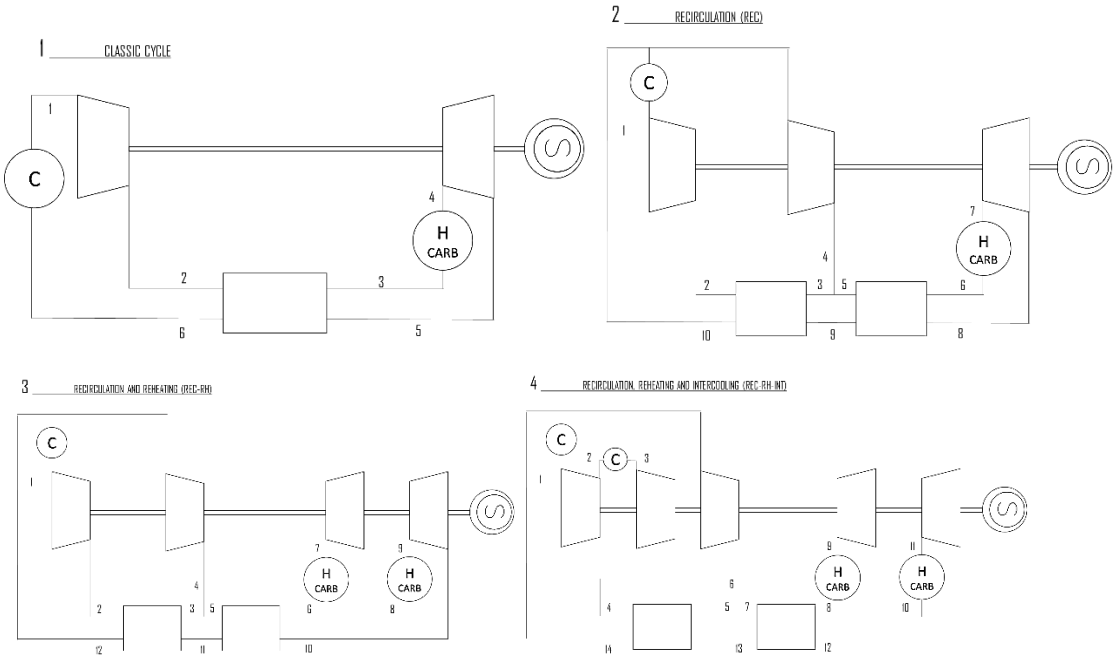

Fig. 21. s-CO2 cycles proposed for the CaL-power cycle integration at large scale

2.3. METHODOLOGY

2.3.1 Specific heat variability

The main aim of the work is to perform and optimization strategy for various sCO2 cycles. The first problem that arise concern the necessity of taking into account the specific heat variability in the operating condition of the cycle. Temperatures are between critical value and the temperature at which the carbonation reaction takes place minus the minimum temperature difference at the heat exchanger (usually between 10°C and 30°C). Pressure are between the critical pressure and a maximum value selected on the basis of the maximum allowed pressure for the various types of technologies.

2.3.2 Evaluation of the independent variables (parametric analysis)

Since the last goal of the work concern the elaboration of an optimization strategy that takes into account only the variables that can be subjected to variation, a parametric analysis is performed. This is done by varying each design variable within a proper range (that takes into account the technical limitation) by keeping all the other variables constant. In particular, the value of each other design variable i, is the mean value between the minimum and the maximum of the range ([xi_mix+xi_max)/2].

The system simulation is performed by means of a model developed in Matlab® with the aim of simulating the behavior of the s-CO2 cycles. The code is structured as follows:

- Proper function for data interpolation and calculation have been built for the evaluation of the thermodynamic properties:
  - specific heat evaluation as a function of temperature and pressure;
  - enthalpy evaluation as a function of temperature and pressure;
  - temperature evaluation as a function of enthalpy and pressure;
  - entropy evaluation as a function of temperature and pressure;

- Blocks for compressor and turbine have been built, as reported in Tab. 33

Turbine block	Compressor block

s2id=s(InTurb);
p(FinTurb)=p(InTurb)/ BetaT;
h2id=h_ps(p(FinTurb),s2id);
h(FinTurb)=h(InTurb)+ rendisT*(h2id-h(InTurb));
s(FinTurb)=s_ph(p(FinTurb),h(FinTurb));
T(FinTurb)=T_ph(p(FinTurb),h(FinTurb));
c(FinTurb)=cp(p(FinTurb),T(FinTurb));
	s2id=s(InCompr);
	p(FinCompr)=p(InCompr).* BetaC;
	h2id=h_ps(p(FinCompr),s2id,Input);
	h(FinCompr)=h(InCompr)+(h2id-h(InCompr))/rendisC;
	T(FinCompr)=T_ph(p(FinCompr),h(FinCompr),);
	s(FinCompr)=s_ph(p(FinCompr),h(FinCompr),);
	c(FinCompr)=cp(p(FinCompr),T(FinCompr);

Tab. 33 Code for turbine and compressor blocks

- The mass flowing the cycle has been evaluated by considering a constant power produced by the *n_t* turbines. It is evaluated as:

$$G = \sum_{i=1}^{n\_t} \frac{Wt_i}{(h_{in\_ti} - h_{out\_ti})} \quad (3)$$

Optimization

Concerning the evaluation of the best configuration the optimization is performed by means of a genetic algorithm. This algorithm has been used in various fields related to energy systems [17-19] with the aim of finding minimum when the objective function is complex and presents various local minima. In this case, this is selected because a) the computational costs to simulate the cycle are very low therefore repeating the simulation several times does not represent a limitation b) this avoid finding local minima. This allows evaluating the set of independent variables that provide maximum performances:

$$\eta = \frac{\sum_{i=1}^{n\_t} Wt - \sum_{i=1}^{n\_c} Wc}{\sum_{i=1}^{n\_h} \Phi_h} \qquad (4)$$

where *n_t*, *n_c* and *n_h* are respectively the number of expansion stages, compression stages and heaters.

Economic analysis

In the end, the optimized configurations are analysed from an economic perspective. This has been done by means of a techno-economic analysis. For each configuration, the total cost of the plant normalised by its expected yearly functioning time [€/s] is evaluated. With the aim, at first the investment cost (C_{inv}) have been calculated for each component of each configuration. This has been done by proper cost functions [20]. The cost functions are related to the kind of equipment, dimensions, material used and operating conditions (temperature and pressures). Once the investment cost is evaluated, the component cost ratio is evaluated for each component as follows.

$$Z = \frac{C_{inv} \cdot f_{amort}}{h_y \, 3600} \quad (5)$$

Where f_{amort} is the amortisazion factor, h_y are the functioning hours per years.

2.4. RESULTS

At first results related to the heat exchange at the regenerators are discussed. This is done since CO2 in supercritical conditions is subjected to large specific heat variation. Fig. 3 shows values of specific heat for the points of the cycle (in Fig.22) (results for the recirculation cycle is considered). Variation up to 400% are registered. This highlights the importance of a check of the heat exchanged at the regenerators in order to avoid non-sense design.

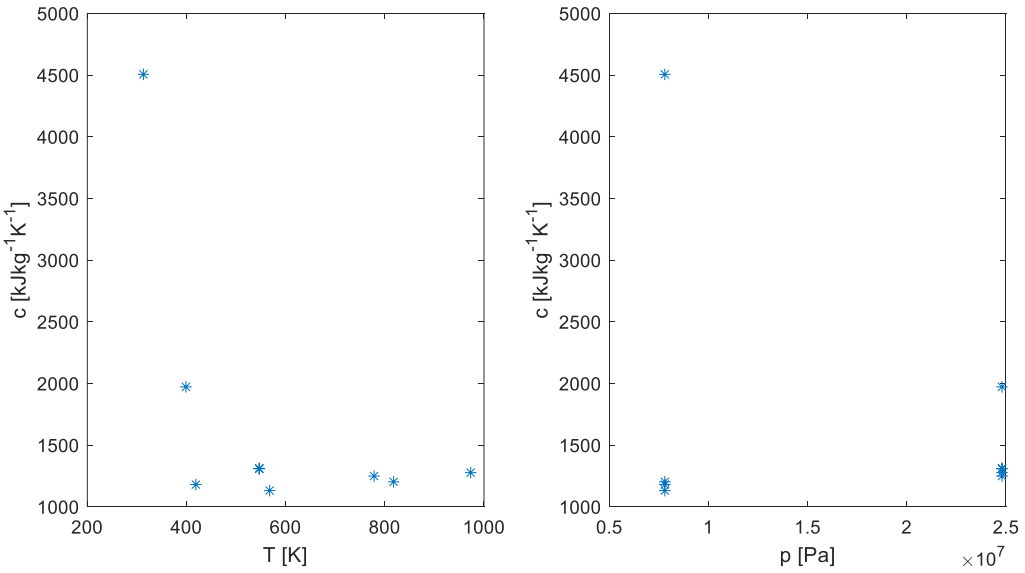

Fig. 22 Specific heat variation with temperature and pressure along the power cycle

For each considered type of cycle, various plots are obtained with the aim of monitoring the heat exchanged at the regenerator. Fig. 23 shows results obtained for s-CO2 in the second cycle (recirculation). In particular, Fig. 23 shows the distribution of the various quantities along the length of the two regenerators; x=0 is the section 2-10 while x=1 is the section 6-8. The dashed red line represents section 3-9. In Fig.23 shows: a) the temperature evolution within the heat exchanger length for the hot and cold mass flow rate, b) the temperature difference c) the specific heat evolution d) the evolution of the product of the mass flow rate times the specific heat (Gc). When no recirculation is required, the same evolution of specific heat and Gc is obtained, since the same mass flow is used in all the heat exchangers. This is what happens in case 1 (classic s-CO2 Brayton cycle). In case 1, Gc of the cold fluid is always higher than Gc of the hot fluid. This means that, if the minimum temperature difference between the two sides is guaranteed at the section 2-6, this is automatically preserved in the entire exchange area.

In case 2, mass flow rate of the cold fluid in the first regenerator (left side of the graph) is lower than the mass flow circulating in all the hot side, and the second regenerator in the cold side. This means that evolution of Gc can be significantly different than that of the specific heat. As can be noticed comparing the two lower plots in Fig. 4 the specific heat largely varies within the heat exchanger length. Therefore in this case, it is not sufficient guarantying the temperature difference in the outlet section of the firs compressor, since Gc of the cold fluid is not always lower than Gc of the hot fluid. In this case, a check in the section between the two regenerators is required.

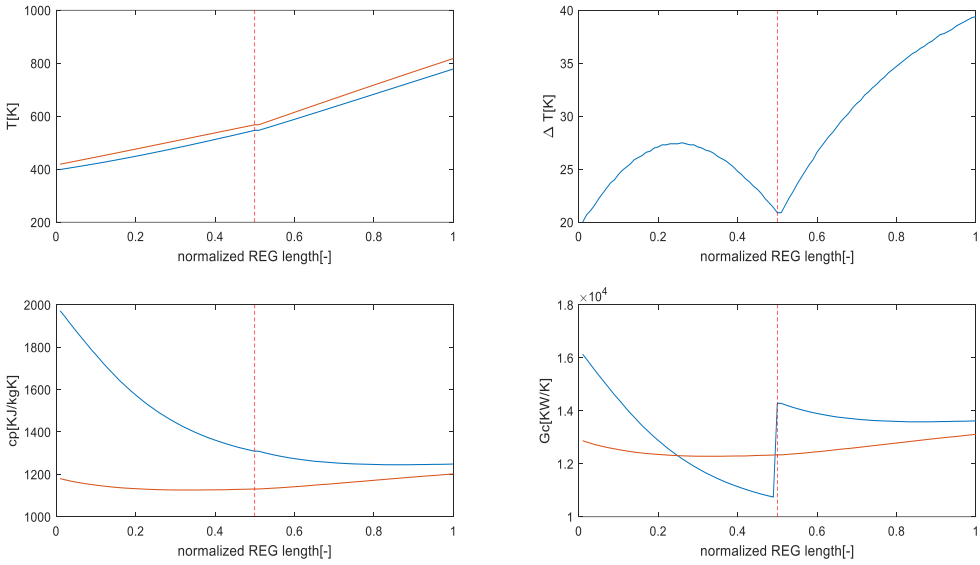

Fig. 23 Regenerator analysis (cycle type 2, REC): a) temperature; b) temperature difference between hot and cold side; c) specific heat; d) mass flow times specific heat

Results of the parametric analysis have been reported in Fig. 24 for all the considered cycles (from (a) to (d)). When classical s-CO2 Brayton cycle is considered (Fig. 5a) all the design variables are considered in the analysis: T1 and p1 (both at the inlet section of the compressor), T4 (at the inlet section of the turbine) and β, the compression ratio. When the other cycle designs are considered (REC, REC-RH, REC-RH-INT), only the design variable that were not considered in the previous analysis have been reported. Therefore the design variables considered in the other cases are:

- recirculation cycle: fraction of recirculated mass flow rate.
- recirculation and reheating cycle: ratio between expansion ratio in the first turbine and the total expansion ratio.

- recirculation, reheating and intercooling cycle: ratio between the two stage of compression.

Concerning the classic cycle (Fig. 23a) T1, p1 and T4 show a monotonic evolution within the considered range. This means that it makes no sense to look for the best value by using an optimization approach, since the best value is on boundary of the considered range. As concern the compression ratio β, the evolution presents a maximum; this means that it is a variable that can be selected properly by means of an optimization approach.

Concerning the recirculation cycle, the variation of the recirculated mass flow allows an increase of the system performance; in particular higher is the mass flow recirculated, higher is the system performance. This means that is should be selected as low as possible taking into account the limitation connected to the minimum temperature difference at the outlet section of the heat exchanger.

The recirculation and reheating cycle analysis shows that the ratio between the expansion stages in the first and in the second turbine presents a maximum within the considered range. This means that the ratio between the two expansion stages can be considered as an optimization variable.

Considering the recirculation-reheating-intercooling cycle, the project variable that is included is the ratio between the two compression stages. This also has a non-monotonic evolution, therefore this can be considered as an optimization variable.

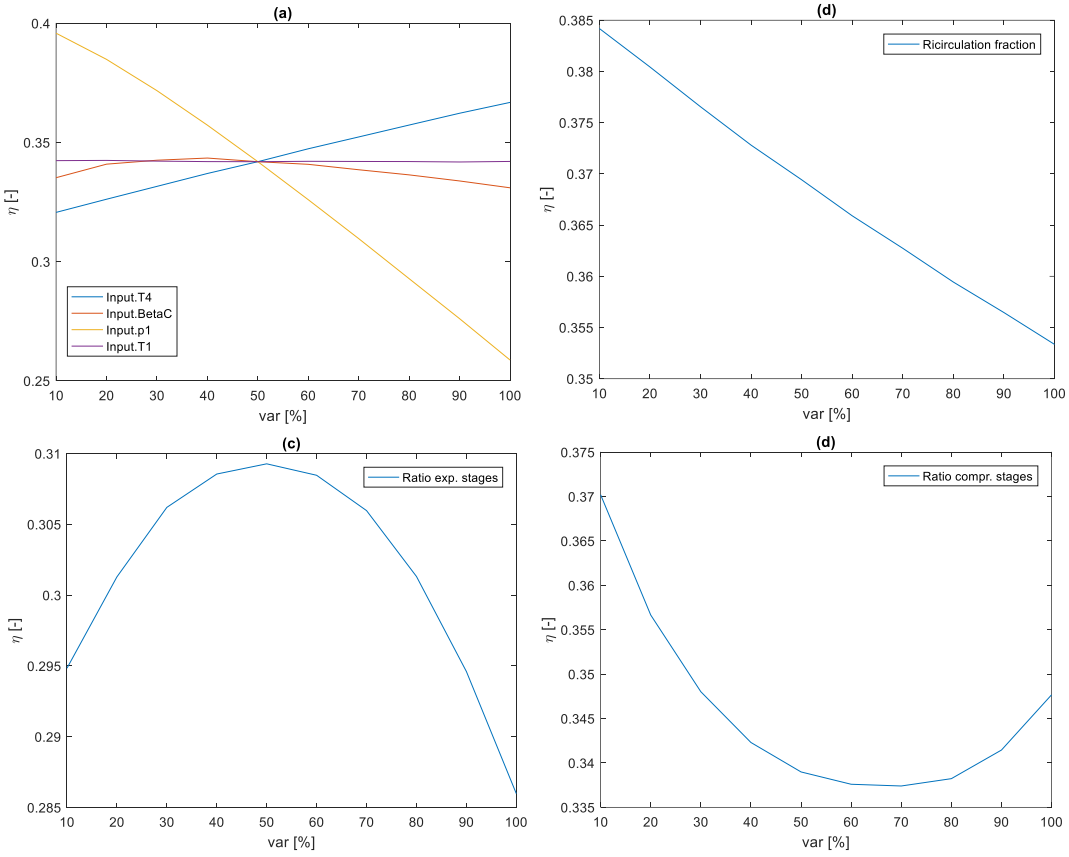

Fig. 24 Parametric analysis. Variation of the power cycle performances by varying the design variables of the various considered schemes: a) classic; b) REC; c) REC-RH; d) REC-RH-INT

In the last part of this section, the optimization results are shown (Fig. 25). The independent variables have been evaluated by the previous analysis (see Fig. 24); these are, for the various cycle types:

- Classic cycle: compression ratio
- Recirculation cycle: compression ratio, flowrate split fraction
- Recirculation-Reheating cycle: compression ratio, and ratio between the expansion stages, flowrate split fraction
- Recirculation-Reheating-Intercooling cycle: compression ratio, ratio between the expansion stages, ratio between the compression stages, flowrate split fraction

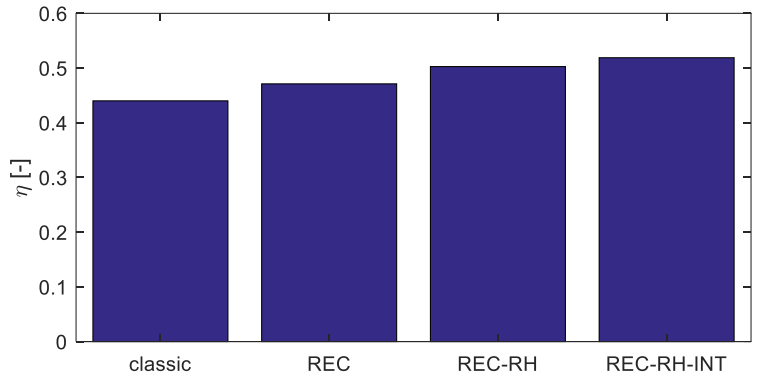

Fig. 25 Best performance obtained for each considered power cycles

The efficiency obtained by means of the optimization process is 0.44 in the case of the basic design, and increases up to 0.52 for the other cycles, particularly for the recirculation recirculation-reheating and recirculation-reheating-Intercooling. An improvement of more than 3% can be achieved by including the recirculation within the process; this provides an important increase in the performances. In order to wisely select the power cycle an economic and thermos-economic analysis should be performed. This is out of the goals of the work but it represent a future work to make the optimization process suitable for design purposes and technology selection.

Concerning the Matlab script developed, in the table below are reported the computational times of the optimization process in relation to the number of elements that compose a single population and the maximum generations number imposed for the genetic algorithm.

		Computational times [s]			
# population	# generation	CLASSIC	REC	REC-RH	REC-RH-INT
50	50	7	9	10	11
75	75	9	15	19	22
100	100	11	17	24	35
125	125	13	23	30	50

Tab. 34 – Energetic optimization computational times for the investigated plant layouts

Taking into account the optimal configuration, an economic analysis has been performed with the aim of achieving which is the additional cost required for increasing the power cycle efficiency. This has been reported n Fig. 26. Considering the investment cost, more than 0.7 M€ are necessary in order to pass from configuration 1 to configuration 2. Further 0.85 M€ are necessary in order to reach configuration 3, since this passage requires the installation of a new turbine. Only further 0.3 M€ are required to have configuration 4. In total, 1.85 M€ are necessary in order to increase the performances of the system of 8%.

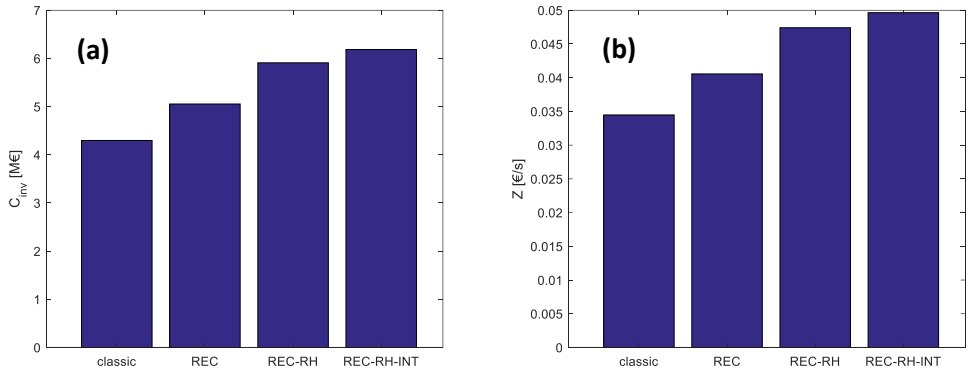

Fig. 26 Economic analysis results a) Investment cost b) Component cost ratio

Concerning the component cost ratio, the evolution is the same since operating hours and amortization factor are the same for the four configurations.

In order to takes decisions that also involve economic aspects, various analyses might be performed. An exergoeconomic analysis could be applied to analyze which are the components that could be improved, in each configuration. Furthermore, it could be possible performing a multi-objective optimization of the system by taking into account both the performances and the economic aspects.

Now, the last analysis performed consists in an estimation of the UA coefficient for the case of thermal exchange with the power block executed directly on the carbonator wall in correspondence of different wall temperature (which is assumed as uniform on the entire surface). Then, with this result obtained it's possible to make another estimation: the surface involved by the thermal exchange for different values of the coefficient of heat exchange. These values have been extracted from the previous deliverables published in relation to the SOCRATCES project and had been adopted in the development of the 1-D and 2-D carbonator models. So, integrating this information inside a 0-D optimization allows to make a multilevel power plant simulation, in accordance with the effort to execute the most complete and consistent analysis as possible.

The trend presented by the two parameters investigated confirms the expectations, since their variation in correspondence of higher carbonator wall temperatures consists in a nonlinear decreasing (Fig. 27). The nominal value of the coefficient of heat exchange at the reactor wall should be equal to 15 W/(m^{2}K) (in accordance with the analysis performed for the carbonator prototipe in the SOCRATCES deliverable D.2.3), anyway the estimation has been made for two other values: 5 W/(m^{2}K) for the possible case of only natural convection and an average value of 10 W/(m^{2}K) for an eventual functioning under intermediate conditions. Of course these assumptions are referred to the prototype scale, but it has been chosen to adopt them anyway since they are the only available data at the state of the art, taking into account that the scale-up operating conditions shouldn't be extremely different.

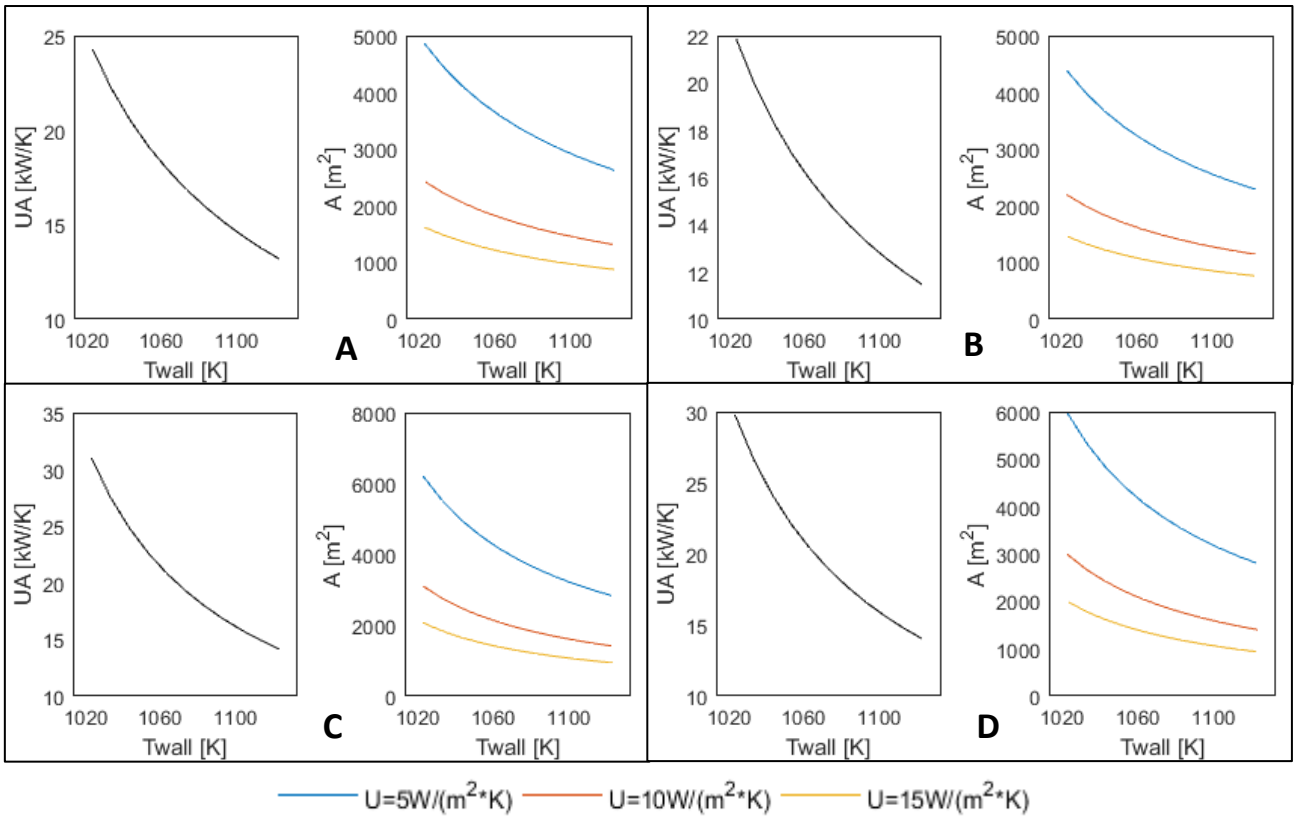

Fig. 27 - UA and exchange area estimation for different values of carbonator wall temperature. A) classic; B) REC; C) REC-RH; D) REC-RH-INT

Concerning the graphs above, the surface required for the heat transfer decreases when it's passing from the classic to the REC layout simply because, being more efficient, the REC configuration requires a lower thermal flux to the carbonator. This is not anymore true for the REC-RH and the REC-RH-INT layouts because it must be considered another aspect related to the heat exchange: in fact, although the heating need decreases with respect to the two previous cases, the introduction of a reheating stage determines an increasing of the temperatures of the thermodynamic cycle at which it must be provided the thermal flux. As a consequence, the temperature difference between the carbonator wall and the working fluid is reduced, determining an increase of the heat transfer area necessary to satisfy the power block demand.

2.5. REFERENCES

[1] Pramanik, S., & Ravikrishna, R. V. (2017). A review of concentrated solar power hybrid technologies. *Applied Thermal Engineering*, *127*, 602-637.

[2] Dowling, A. W., Zheng, T., & Zavala, V. M. (2017). Economic assessment of concentrated solar power technologies: a review. *Renewable and Sustainable Energy Reviews*, *72*, 1019-1032.

[3] Kumar, A., Prakash, O., & Dube, A. (2017). A review on progress of concentrated solar power in India. *Renewable and Sustainable Energy Reviews*, *79*, 304-307.

[4] Verda, V., Guelpa, E., Kona, A., & Russo, S. L. (2012). Reduction of primary energy needs in urban areas trough optimal planning of district heating and heat pump installations. *Energy*, *48*(1), 40-46.

[5] Sciacovelli, A., Guelpa, E., & Verda, V. (2014). Multi-scale modeling of the environmental impact and energy performance of open-loop groundwater heat pumps in urban areas. *Applied Thermal Engineering*, *71*(2), 780-789.

[6] Guelpa, E., Mutani, G., Todeschi, V., & Verda, V. (2018). Reduction of CO2 emissions in urban areas through optimal expansion of existing district heating networks. *Journal of Cleaner Production*, *204*, 117-129.

[7] Alberini, A., Bigano, A., Ščasný, M., & Zvěřinová, I. (2018). Preferences for energy efficiency vs. renewables: what is the willingness to pay to reduce CO2 emissions?. *Ecological Economics*, *144*, 171-185.

[8] Xu, B., Li, P., & Chan, C. (2015). Application of phase change materials for thermal energy storage in concentrated solar thermal power plants: a review to recent developments. *Applied Energy*, *160*, 286-307.

[9] Prieto, C., Cooper, P., Fernández, A. I., & Cabeza, L. F. (2016). Review of technology: thermochemical energy storage for concentrated solar power plants. *Renewable and Sustainable Energy Reviews*, *60*, 909-929.

[10] Ortiz, C., Chacartegui, R., Valverde, J. M., Alovisio, A., Becerra, J. A. (2017). Power cycles integration in concentrated solar power plants with energy storage based on calcium looping. Energy Conversion and Management, 149, 815-829.

[11] Turchi, C. S., Ma, Z., Dyreby, J. (2009, April). Supercritical CO2 for application in concentrating solar power systems. In SCCO2 Power Cycle Symposium, RPI, Troy, NY (pp. 1-5).

[12] Iverson, B. D., Conboy, T. M., Pasch, J. J., Kruizenga, A. M., *Supercritical CO2 Brayton cycles for solar-thermal energy. Applied Energy, 111, 957-970.*,

[13] …. Zhao, Y., Li, P., & Jin, H. (2017). Heat Transfer Performance Comparisons of Supercritical Carbon Dioxide and NaCl–KCl–ZnCl2 Eutectic Salts for Solar s-CO2 Brayton Cycle. *Energy Procedia*, *142*, 680-687.

[14] Ma, Y., Zhang, X., Liu, M., Yan, J., & Liu, J. (2018). Proposal and assessment of a novel supercritical CO2 Brayton cycle integrated with LiBr absorption chiller for concentrated solar power applications. *Energy*, *148*, 839-854.

[15] Padilla, R. V., Too, Y. C. S., Benito, R., Stein, W. (2015). Exergetic analysis of supercritical CO2 Brayton cycles integrated with solar central receivers. Applied Energy, 148, 348-365.,

[16] Wang, J., Sun, Z., Dai, Y., & Ma, S. (2010). Parametric optimization design for supercritical CO2 power cycle using genetic algorithm and artificial neural network. Applied Energy, 87(4), 1317-1324.

[17] Guelpa, E., Sciacovelli, A., Verda, V., & Ascoli, D. (2016). Faster prediction of wildfire behaviour by physical models through application of proper orthogonal decomposition. *International Journal of Wildland Fire*, *25*(11), 1181-1192.

[18] Yu, H., Fang, H., Yao, P., & Yuan, Y. (2000). A combined genetic algorithm/simulated annealing algorithm for large scale system energy integration. *Computers & Chemical Engineering*, *24*(8), 2023-2035.

[19] Sciacovelli, A., Guelpa, E., & Verda, V. (2013, November). Pumping cost minimization in an existing district heating network. In *ASME 2013 International Mechanical Engineering Congress and Exposition* (pp. V06AT07A066-V06AT07A066). American Society of Mechanical Engineers.

[20] Turton R., Bailie R.C., Whiting W.B., Shaeiwitz J.A. Analysis, Synthesis and Design of Chemical Processes (3rd ed.). Upper Saddle River (N.J.) : Prentice Hall, 2009

3. CONCLUSIONS

Concerning the work exposed in the first section, it's proposed an analysis and its relative developing methodology for the power generation inside the field in which the future SOCRATCES plant is expected to operate. The aim of this study is to investigate the different alternatives for the integration of a Calcium-Looping in the CSP environment for a pilot plant and therefore to suggest a possible strategy for the choice of its layout. The closed-loop direct integration and the indirect integration are the two main configurations analyzed and, concerning this last one, the thermodynamic cycles investigated are the Organic Rankine, the steam Rankine and the Brayton-Joule with supercritical CO_2.
In order to make a reasonable comparison, for all the various alternatives is executed an energetic optimization such that the plant configurations are compared with their maximum achievable efficiencies. The optimization process, which is the real core of this work, consists in a genetic algorithm based on the pinch analysis; the most important constraint imposed to the algorithm is that the configuration obtained must have a null external heating requirement, such that the use of fossil fuels is avoided. Of course it must be noticed that, at the end of this process, the heat exchanger network must be designed (in accordance to the pinch analysis) if the detailed plant layout is requested.
The performances are calculated for different values of calcium oxide activity and carbonator operating temperature in order to provide a sensitivity analysis for two of the most important plant parameters. The best results are obtained for the maximum values of X and T_{carb}, with carbonator side efficiencies slightly higher than 49% in case of direct integration and indirect integration with SCO_2.
Finally, a restricted analysis for the case of indirect integration with power block directly fed by the carbonator wall is exposed with the aim to discuss the possible convenience of a different heat recovery.

Concerning the work exposed in the second section, an optimization approach is proposed for achieving high performances in supercritical CO_2 Brayton cycle for solar concentration applications. Various types of cycles have been considered. The analysis has been conducted by paying attention to the heat exchange in the regenerators. This is done because carbon dioxide in the supercritical region presents significant variation of the specific heat. A parametric analysis has been performed, by varying, one by one, all the design variables. This allows achieving which variables provide maximum performances by maximizing or minimizing their value in the acceptable range. When the variation of a variable provides a non-monotonic evaluation (with a maximum or minimum), this is considered an independent variable for the optimization. In the end, the optimization is performed by means of a genetic algorithm.

The process has been developed with a particular attention to the computational time in order to obtain an algorithm suitable for the implementation in a control logic for the regulation of the power plant. In this way, for any possible situation in which the thermodynamic cycle may operate, the optimal functioning conditions are obtained nearly instantaneously, allowing to maximize the plant efficiency.

Results show that the in case two regenerators are used (when recirculation is performed), is not sufficient setting the minimum temperature difference at the outlet section of the heat exchange. In this case proper attention should be paid in the cold section, between the two regenerators (in case more than one recirculation is performed this should be check in all the points between the regenerators). The parametric analysis shows that compression ratio, ratio between the expansion stages and ratio between the compression stages are the variables that should be investigated in an optimization analysis. The optimization analysis shows that

performances are over 44% for each cycle and these can reach the 52%. In particular, a significant gap (more than 3%) can be achieved by using the recirculation; this provides an important improvement in the performances.
Considering the economic aspects, an economic analysis is performed with the aim of showing the investment cost required for all the configurations. Resuls shows that an extra 1. 85 M€ of investment cost is required to increase the performances of the system of 8%.

Finally, the UA coefficient and the surface for the heat exchange directly performed on the carbonator wall are calculated as a function of the reactor wall temperature. The REC layout appears as the less demanding configuration in terms of exchange area, while the REC-RH and the REC-RH-INT layouts adoption determine an increase comprised between the 16% (high T_{wall}) and the 36% (low T_{wall}).